The Therapeutic Potential of Thiocyanate Administration In Influenza Lung Infection

by

NUHA MILAD ASHTIWI

(Under the Direction of Balázs Rada)

ABSTRACT

Influenza viruses causes acute respiratory infections which may lead to annual seasonal epidemics. In the 20th century, three major pandemics occurred in 1918-1919,1957 and 1968. Influenza infection causes more than 90% of deaths among people over 65 years of age. The CDC recommends the antiviral drugs baloxavir marboxil (Xofluza), oseltamivir (Tamiflu) and zanamivir (Relenza) for both influenza prevention and treatment.

Thiocyanate (SCN^-) is a natural compound in the human body. SCN^- plays an important role in the innate immune system as a precursor of the antimicrobial hypothiocyanous acid (HOSCN). HOSCN is generated from SCN^- by peroxidases using H_2O_2. HOSCN has antimicrobial activities against various viruses and bacteria *in vitro*. Our group has shown that HOSCN effectively inactivates several respiratory pathogens *in vitro* and *in vivo*, including influenza A and B viruses. We hypothesized that *in vivo* administration of SCN^-, the substrate for HOSCN, helps the immune system of the airways to fight influenza infections.

Our results revealed that oral administration of 400 µg/kg/day NaSCN between 2–7 days post-infection (dpi) reduced mortality in C57BL/6J mice by more than 90% when infected with one of the following influenza virus strains: A/PR8/1934 (H1N1), A/Hong Kong/1968 (H3N2) or B/Lee/1940 (repeated two times). This beneficial therapeutic effect of oral SCN^- was entirely independent of the Duox1 gene as Duox1-deficient animals were rescued by SCN^- to the same extent as wild-type mice. SCN^- acted in a dose-dependent manner as 100% mortality observed in A/PR8/34-infected animals was entirely prevented by 200 or 400 µg/kg/day NaSCN treatment (2-7 dpi). C57BL/6J mice infected with a lethal dose of B/Florida/04/2006 were also largely rescued from mortality when treated with oral SCN^- in the same way. Lung histology performed at 5 dpi demonstrates robust lung disease in A/PR8/34 or B/Florida/04/2006 infected mice that were mainly prevented by oral SCN^- treatment (400 µg/kg/day, 2-7 dpi). Influenza lung viral titers were also drastically reduced in SCN^-- treated mice at 4 dpi, compared to untreated animals following A/PR8/34 or B/Florida/04/2006 challenges.

INDEX WORDS: Influenza, SCN^-, $OSCN^-$, DUOX1, HOSCN.

The Therapeutic Potential of Thiocyanate Administration In Influenza Lung Infection

By

NUHA MILAD ASHTIWI

MD, University of Tripoli, 2006

MHS, Quinnipiac University, 2014

A Dissertation Submitted to the Graduate Faculty of the University of Georgia in Partial Fulfillment of the Requirements for the Degree

DOCTOR OF PHILOSOPHY

ATHENS, GEORGIA

2024

The Therapeutic Potential of Thiocyanate Administration In Influenza Lung Infection

By

`

NUHA MILAD ASHTIWI

Major Professor:	Balázs Rada
Committee:	Jeff Hogan
	Wendy Watford
	Jarrod Mousa
	Ralph Tripp

Electronic Version Approved:

Ron Walcott
Interim Dean of the Graduate School
The University of Georgia
May 2024

DEDICATION

This thesis is dedicated to my parents, family and children who have supported me throughout my education.

ACKNOWLEDGEMENTS

I am thankful to my thesis mentor, Dr. Balázs Rada, for his constant support and patience throughout the entire process of researching and writing. Without his guidance, this work would not be completed. I would also like to thank my committee members, Drs. Tripp, Hogan, Watford and Mousa for valuable comments and suggestions on my work, which assisted me to construct and produce this thesis.

My sincere appreciation goes also to the present and past members of the Rada lab, Tripp lab and Tompkins lab at UGA for their support and encouragement throughout my PhD period.

Finally, I would like to express my deepest gratitude to my five children, Aram, Aleen, Maysam and Aseel and Hashim Younis, without your love and care, this work would not have been possible.

TABLE OF CONTENTS

Page

ACKNOWLEDGEMENTS v

LIST OF FIGURES ix

CHAPTER

1. INTRODUCTION 1

Specific Aims 3

2. LITERATURE REVIEW……4

2.1 DUOX1 IN MAMMALIAN DISEASE PATHOPHYSIOLOGY……4

Abstract……5

Structural features and discovery of DUOX1……..7

Physiological role of DUOX1……..8

DUOX1 and its maturation factor DUOX1A……10

DUOX1 in the skin……12

DUOX1 in the respiratory system……14

DUOX1 in allergy and asthma……14

DUOX1 in nasal polyposis……15

DUOX1 in chronic obstructive pulmonary disease (COPD)……17

DUOX1 in lung fibrosis……..19

DUOX1 in cancer……..……21

DUOX1 in other diseases……..……..24

Concluding Remarks……..……26

2.2 THE THERAPEUTIC POTENTIAL OF THIOCYANATE AND HYPOTHIOCYANOUS ACID AGAINST PULMONARY INFECTIONS……..……..29

Abstract……....30

Introduction……..31

Antiviral activity of HOSCN……...34

Antibacterial activity of HOSCN……..…….36

Antifungal activity of HOSCN……....37

Molecular and cellular targets of HOSCN in pathogens……38

Defense mechanisms of pathogens against HOSCN……41

SCN^-/HOSCN therapy to combat infections……...44

Conclusions……46

3. THE HYPOTHIOCYANITE AND AMANTADINE COMBINATION TREATMENT PREVENTS LETHAL INFLUENZA A VIRUS INFECTION IN MICE……53

Abstract……54

Introduction……55

Materials and Methods……57

Results……65

Discussion……..……72

Figures and Legends……..……..…....78

4. THIOCYANATE TREATMENT REDUCES MORTALITY IN MICE IN MICE INFECTED WITH INFLUENZA VIRUSES……94

Abstract……95

Introduction……...96

Materials and Methods……99

Results……103

Discussion……...109

Figures and legends……...113

5 CONCLUSIONS……..……122

REFERENCES……129

LIST OF FIGURES

Page

Figure 2.1 Conditions associated with either high or low expression of the NADPH oxidase DUOX1……..28

Figure 2.2 The origin and function of SCN^- and HOSCN in the airways……48

Figure 2.3 Proposed therapeutic benefits of SCN^- in respiratory infections……..48

Table 1. Molecular and cellular targets of the antimicrobial action of HOSCN……51

Table 2. Defense mechanisms of bacteria against HOSCN……..52

Figure 3.1 The AMT+$OSCN^-$ combination treatment significantly reduces the replication of several influenza A virus strains *in vitro*……..79

Figure 3.2 The AMT+$OSCN^-$ combination treatment reduces influenza virus uptake into host cells. ……...81

Figure 3.3 The AMT+$OSCN^-$ combination treatment reduces influenza virus uncoating in host cells. ……83

Figure 3.4 The AMT+$OSCN^-$ combination treatment reduces nucleoprotein expression of influenza virus in host cells. …….85

Figure 3.5 The AMT+$OSCN^-$ combination treatment restricts influenza virus replication in primary human bronchial epithelial cells…….86

Figure 3.6 A triple combination therapy including AMT, $OSCN^-$, and OSL, is superior to dual and single drug regimens against amantadine-sensitive and amantadine-resistant influenza A strains *in vitro*……..……89

Figure 3.7 The AMT+$OSCN^-$ combination treatment cured mice from lethal H1N1 influenza A virus infection……..91

Figure 3.8 The AMT+$OSCN^-$ combination treatment cured mice of lethal H3N2 influenza A virus challenge……93

Figure 4.1: Oral administration of different doses ranging 100- 1000 μg/kg/day of SCN^- treatment cured mice from lethal H1N1 influenza A virus infection……..……..…113

Figure 4.2: Oral administration of 400 μg/kg/day 2-7 dpi rescued mice from mortality after lethal B/Florida/04/06 infection……114

Figure 4.3: Oral SCN^- treatment was started different days post infection (48hrs, 72hrs, 96 hrs and 120 hrs post infection……115

Figure 4.4: All Oral SCN^- treatment was continued for the duration of 2, 3, 4, 5 days after mice were infected with lethal dose of B/Florida 04/2006…….……..116

Figure 4.5: Intravenous administration of 200 μg/kg/day SCN^- (1-3 dpi) prevents mortality in C57BL/6J mice infected with lethal doses of A/PR8/34 (A and B), B/Florida 04/06 (C and D)……117

Figure 4.6: Lung histology performed at 5 dpi demonstrates robust lung pathology in A/PR8/34 and B/Florida- infected mice that was mainly prevented by oral SCN^- treatment (400 μg/kg/day, 2-7 dpi)……119

Figure 4.7: Oral SCN^- and $OSCN^-$ provided similar therapeutic efficacy regardless of DUOX1 presence……..120

Figure 4.8: Nebulization of 400 μg/kg/day SCN^- (1-5 dpi), twice a day, prevents mortality in C57BL/6J mice infected with lethal doses of B/Florida 04/06 (A and B)……121

CHAPTER 1

INTRODUCTION

A serious economic burden can be caused by influenza worldwide epidemics[1]. Acute respiratory infection can be caused by influenza virus, and it can lead to high morbidity and mortality among patients[2]. In the United States, influenza infection causes around 200,000 hospitalizations and 36,000 deaths among patients with co-morbidities in a typical endemic season[2]. Most influenza vaccines might only prevent the infection if the epidemic strain matches the vaccine strain antigenically[3]. Moreover, seasonal influenza vaccine cannot provide prophylactic effect against antigenically pandemic influenza strain[3]. The FDA-approved antiviral drugs for influenza treatment are adamantanes and neuraminidase inhibitors[4]. Adamantanes are M2 inhibitors that include amantadine and rimantadine. Adamantanes were active against influenza A viruses but not influenza B viruses[5]. In hospitals and outpatient clinics, adamantanes are not used to treat patients due to the widespread drug resistance[5, 6]. Neuraminidase inhibitors (NI) are oseltamivir (Tamiflu) for oral route, zanamivir (Relenza) for inhalation route and peramivir for intravenous route[7, 8]. In October 2018, a cap-dependent endonuclease inhibitor, baloxavir marboxil was approved by FDA as antiviral drug for influenza [9]. Oseltamivir is only effective when it is administered within 48 hours of infection[10]. Oseltamivir blocks the enzymatic activity of NA proteins. Some mutations such as “H275Y” mutation can lead to oseltamivir resistance[11]. Resistance against FDA-approved anti-influenza drugs is

increasing, thus new treatment can provide a promising therapeutic option against influenza.

The airway epithelial lining is the first line of defense during respiratory airway infections[12]. The airway surface liquid contains lactoperoxidase (LPO). The role of LPO is to catalyze the reaction between H_2O_2 and thiocyanate (SCN^-) producing hypothiocyanite ($OSCN^-$) in the airway surface liquid (ASL)[13]. Dual oxidase 1 (DUOX1) is a member of NADPH oxidases, and it is the main source of H_2O_2 in the airway[14]. DUOX1 is mainly expressed in the apical membrane of respiratory epithelial cells[14]. DUOX1 is upregulated in airway epithelial cells during influenza infection[15]. SCN^- ion is a natural compound in human body fluids such as saliva, milk, urine and plasma[16]. SCN^- is crucial for H_2O_2-Thiocyanate Peroxidase-System, an important part of the immune response[17, 18]. SCN^- and $OSCN^-$ served as broad spectrum antimicrobial agents as they showed their efficacy against various viruses, bacteria, fungi and protozoa[19, 20, 21, 22, 23, 24, 25]. SCN^- treatment alleviated inflammatory processes in several ischemic and hypertensive conditions in non-infectious conditions[26, 27, 28]. SCN^- can modulate the myeloperoxidase activity to reduce the hypochlorous acid (HOCl) production and increase the hypothiocyanous acid (HOSCN)[29]. Surprisingly, the therapeutic efficacy of SCN^- as a single or combined therapy against lethal influenza infection in murine model had not been studied. We intended first to determine the appropriate therapeutic dose, route, and duration for SCN^- treatment. Moreover, we explored the therapeutic efficacy of SCN^- versus $OSCN^-$ in C57BL/6J (wild type) and Duox1-deficient mice.

Specific Aims

The main hypothesis of the proposed research is that SCN^- can be used as a single or combined treatment to prevent mortality from lethal influenza infection in a murine model.

Specific Aim 1. Explore the therapeutic efficacy of SCN^- using different timing, dosing, and route.

1A. Use different doses to determine which can provide the best efficacy and less toxicity.

1B. Determine the effective start point to decrease viral replication.

1C. Use different routes (Intravenous, orally and nebulization).

Specific Aim 2: Evaluate the therapeutic efficacy of combining $OSCN^-$ and FDA-approved drugs (amantadine and oseltamivir) on influenza A strains *in vitro* and *in vivo.*

Specific Aim 3. Determine the end point therapeutic effect of $OSCN^-$ versus SCN^- on disease mortality and morbidity in C57BL/6J and Duox1-deficient mice infected with A/PR8/34 (H1N1), A/HK/68 (H3N2) and B/Lee/40.

CHAPTER 2

DUOX1 IN MAMMALIAN DISEASE PATHOPHYSIOLOGY[14]

Ashtiwi Nuha, Accepted by *Journal of Molecular Medicine*. Reprinted here with permission of the publisher. March 11, 2021.

ABSTRACT

Dual oxidase 1 (DUOX1) is a member of the protein family of Nicotinamide Adenine Dinucleotide Phosphate (NADPH) oxidases. DUOX1 has several normal physiological, immunological, and biochemical functions in different body locations. Dysregulated oxidative metabolism interferes with various disease pathologies, and numerous therapeutic options are based on targeting cellular redox pathways. DUOX1 forms an important enzymatic source of biological oxidants, and DUOX1 expression is frequently dysregulated in various diseases. While this review shortly addresses the biochemical and cellular properties and proposed physiological roles of DUOX1, its main purpose is to summarize the current knowledge with respect to the potential role of DUOX1 enzyme in disease pathology, especially in mammalian organisms. Although DUOX1 is normally prominently expressed in epithelial lineages, it is frequently silenced in epithelial-derived cancers by epigenetic mechanisms. While abundant information is available on DUOX1 transcription in different diseases, an increasing number of mechanistic studies indicate a causative relationship between DUOX1 function and disease pathophysiology. Specific functions of the DUOX1 maturation factor, DUOXA1, will also be addressed. Lastly, urgent and outstanding questions on the field of DUOX1 that could provide valuable new diagnostic tools and novel therapeutic options will be discussed.

Keywords

Dual oxidase 1; DUOX1; NADPH oxidase; pathophysiology

INTRODUCTION

The family of NADPH oxidases consists of seven members, NOX 1–5 and Dual oxidases 1 and 2 (DUOX1, DUOX2), and represent enzymes that mediate regulated cellular production of reactive oxygen species (ROS). These enzymes play various functional roles in biological processes that include innate immunity, oxidative signal transduction, and biochemical reactions, e.g., biosynthesis of the thyroid hormones[30]. ROS can, however, damage various molecules including nucleic acids, proteins, carbohydrates and lipids. Excessive exposure to ROS results in oxidative stress and could lead, for instance, to genetic mutations. ROS has been correlated with the pathophysiology of many diseases that tend to occur late in life, including atherosclerosis, hypertension, diabetic nephropathy, lung fibrosis, cancer, and Alzheimer's disease. Insufficient DUOX2 activity in rodent models leads to hypothyroidism, and DUOX2 mutations have been associated with this disease in humans[30]. Human DUOX1 is highly expressed in the lung, pancreas, placenta, prostate, testis, and salivary gland[31]. It was suggested that DUOX1 has a crucial role in innate host defense[32]. Previous studies over the past years have, however, highlighted associations of DUOX1 gene expression with numerous diseases. While several, excellent, prior reviews focused on both DUOX enzymes, on their physiological roles in all living organisms, the specific goal of this review is to summarize scientific literature linking DUOX1 gene expression to human and murine pathophysiology.

STRUCTURE FEATURES AND DISCOVERY OF DUOX1

DUOX enzymes were initially described as thyroid oxidases because they were first identified in the thyroid gland and linked to calcium sensitive H_2O_2 generation[33, 34]. Edens et al. explained the cloning of homologous sequences from *Caenorhabditis elegans* and suggested the DUOX nomenclature according to the structural features of the proteins[31]. The location of *DUOX1* and *DUOX2* is on human chromosome 15, and both genes are arranged in a head-to-head configuration[31]. The two *DUOX* genes are separated by a 16 kb region[35]. The length of the *DUOX1* gene is 36 kb, containing 35 exons[31]. The human DUOX1 protein comprises 1,551 amino acids and shows 83% sequence similarity with the human DUOX2 amino acid sequence[31]. In addition to its NADPH oxidase portion, the unique N-terminal peroxidase homology domain shows high sequence similarity to peroxidases[31, 36]. While peroxidases contain heme molecules[31, 36], the peroxidase homology domains of DUOX proteins do not bind heme because they lack key amino acid residues[36] (that are crucial for heme binding and are present in highly conserved positions in all peroxidases)[37]. Calcium ions regulate the enzymatic activity of DUOX proteins (H_2O_2 production) due to two EF hand motifs between the peroxidase homology domain and the NADPH oxidase portion[37]. The DUOXA (maturation factor) proteins are essential for full maturation of the DUOX proteins and coordinate their localization to the plasma membrane. However, immature DUOX proteins within the endoplasmic reticulum (ER) have also been shown to possess catalytic activity [38, 39, 40]. *DUOXA1* is arranged in a head-to-head configuration and is co-expressed with *DUOX1* [40]. DUOXA1 co-expression enables DUOX1 transition from ER to the Golgi complex, maturation, and translocation to the plasma membrane[40]. *DUOXA1* mRNA was

first shown to be expressed in the thyroid gland and, at a lower level, in the esophagus [40]. Two transcripts of ~2.9 and ~3.5 kb sizes were detected, compatible with alternative splicing of the 5'-untranslated exons and using alternative 3'-polyadenylation signals[40]. The *DUOXA1* open reading frame was confirmed by sequencing from human thyroid cDNA[40]. The splicing sites are conserved at the single codon level[40]. Transcriptional modes of regulation of *DUOX1* and its corresponding maturation factor is not completely characterized yet[41]. Multiple studies detected the expression of *DUOX1* in a variety of cell types: keratinocytes[42], urothelial cells[43], primary respiratory epithelial cells, and non-epithelial cells such as T cells[43], innate lymphoid cells[44], and alveolar macrophages[45, 46]. This reported expression pattern determines the proposed physiological roles of DUOX1.

PHYSIOLOGICAL ROLE OF DUOX1

DUOX1 has a crucial role in ROS generation. ROS are important in various physiological processes including host defense, mitogenesis, hormone biosynthesis, apoptosis and fertilization[13]. ROS-producing systems, for instance, play an important function in phagocytic cells where ROS generated during phagocytosis in a partnership by the NOX2-based NADPH oxidase and myeloperoxidase contributes to microbial killing and host defense[47]. A ROS-based, antimicrobial system analogous to this phagocytic system has been proposed in the airway epithelium. Respiratory epithelial cells were proposed to orchestrate a fast and potent, oxidative, extracellular, antimicrobial system consisting of the protein lactoperoxidase (LPO), the thiocyanate anion (SCN^-), and H_2O_2[48 49, 50, 51]. Antimicrobial LPO is present in large amounts in mammalian airways, and its inhibition leads to weakened microbial clearance *in vivo* [32, 48, 49, 51]. LPO is mainly

secreted by submucosal glands in the respiratory mucosa [32, 48]. SCN^- is abundant in the airway surface liquid to support LPO function[48, 50]. SCN^- is not produced by the airway epithelium itself, it is transported from the blood into tissues through the epithelium and concentrated in the airway surface liquid by several epithelial transporters[52, 53]. LPO oxidizes SCN^- using H_2O_2 into antimicrobial hypothiocyanite ($OSCN^-$) in the airway surface liquid[54]. It has been suggested that DUOX1, a Ca^{2+}-regulated NADPH oxidase highly expressed in the apical membrane of the respiratory epithelium producing large amounts of extracellular H_2O_2, works in partnership with LPO to produce antimicrobial $OSCN^-$ [34, 36, 55]. As discussed earlier, the main *in vivo* function of DUOX2 is the production of H_2O_2 for thyroid hormone biosynthesis since both *DUOX2*-deficient human patients and *DUOX2*-deficient mice suffer only from hypothyroidism, and no other, reported conditions [56, 57, 58]. The *in vivo* role of DUOX1 remains largely unknown. *DUOX1*-deficient human patients have not been identified yet. DUOX1 is the dominant NADPH oxidase expressed and the main H_2O_2 source in the respiratory epithelium[36, 59, 60, 61, 62]. DUOX1 is expressed in well-differentiated, polarized, ciliated, air-liquid interface cultures of primary respiratory epithelial cells of several mammalian species (human, rat, mouse) but not in most cell lines used as *in vitro* models of the respiratory epithelium[36, 59, 60].

In addition, DUOX1-generated H_2O_2 plays an essential role as a chemoattractant for the immune system. In zebrafish, the tissue-scale gradient of H_2O_2 induces recruitment of leukocytes to the location of injury, and *DUOX1* knockdown decreases immune cell recruitment[63]. The murine respiratory epithelium and cultured tracheal epithelial cells isolated from mice express *DUOX1*[44, 64]. Ongoing studies are focusing on the DUOX1/H_2O_2/LPO/SCN^- system as an effective, broad-spectrum antimicrobial

system exploring the antimicrobial role of LPO in mammalian experimental models[32]. Moreover, DUOX1 has been proposed to have an important function in the normal wound healing process due to its ability to activate the transition of fibroblasts to myofibroblasts and subsequent deposition of the collagen matrix[65]. Several, recent reviews summarize the proposed physiological roles of DUOX1[32, 66, 67, 68]. This review article aims to provide an updated summary on the recent knowledge associated with DUOX1-generated H_2O_2 and various diseases such as allergic conditions, pulmonary diseases and cancer[44, 65, 69, 70].

DUOX1 AND ITS MATURATION FACTOR DUOXA1

The *DUOX1* gene is normally expressed in a coordinated manner with its maturation factor or activator, *DUOXA1*. The DUOXA1 protein consists of five alpha helical transmembrane regions, with extracellular loops and an intracellular tail, and associates with immature DUOX1 within the endoplasmic reticulum to promote its proper folding, glycosylation and transport to the plasma membrane to generate a mature, fully functional enzyme[40, 71, 72]. Though, immature DUOX1 still shows intrinsic catalytic activity, as well[39]. Several studies show that DUOX1-DUOXA1 protein interactions potentially include intramolecular disulfide bonds between their extracellular parts[73, 74]. Moreover, it was recently observed that the specificity of produced ROS, $O2^-$ as an intermediate or H_2O_2 as its end product, is determined by sequences in the extracellular A loop of the DUOX proteins, which bind to the N-termini of DUOXA proteins[75]. DUOXA1 has numerous splice variants whose physiological roles remain still unclear[71]. It has been previously shown that specific splice variants of DUOXA1 can also combine with DUOX2,

which allows H_2O_2 generation at almost the exact levels as that of the matching DUOX2-DUOXA2 heterodimers; that was, however, not true for mispairing DUOX1 with DUOXA2 [71, 75]. Beyond being associated with corresponding DUOX proteins, the DUOXA1 protein might also have a role independent of DUOX1. DUOXA1 was first recognized in *Drosophila melanogaster*, as a complimentary part to a master regulator of the Notch cell differentiation pathway, Numb, and was then named Numb Interacting Protein (NIP)[40, 76, 77]. The characteristics of sequence in the NIP proteins indicated that they are membrane-associated proteins, and it was suggested that NIP regulates the subcellular localization of Numb by sequestering Numb to the plasma membrane during asymmetric cell division[76]. DUOX-dependent ROS production is regulated by mammalian NIP proteins and hence were known as DUOX activators, DUOXA1 and DUOXA2[40, 76]. Knowing the essential function of the Notch signaling pathway as a main controller of cellular differentiation, changing the expression of the *DUOXA1* gene could have obvious downstream impacts on the Notch pathway, thus causing abnormalities in cell differentiation and/or tumor progression. Additionally, aberrant Notch signaling was reported in various types of cancers, with its signaling or expression is either pro- or anti-tumorigenic, which highly relies on the tissue and cellular context [78, 79, 80]. Surprisingly, Notch signaling and oncogenic EGFR signaling have been considered correlative[35], which could be linked to a main function for DUOX1/DUOXA1 on these processes. Further than its function as a maturation factor for DUOX1 or in controlling the notch pathway, DUOXA1 might also have other independent functional roles. For example, recent studies indicated that DUOXA1 has a role in cellular differentiation in muscle satellite cells[81] and neuronal cells[78, 82], which include interactions with p53, promoting its

functions in tumor suppressor, cell cycle stages, and differentiation[78]. Additionally, DUOXA1 was proposed to possess other, DUOX1-independent roles in different tissues including the brain and breast [78, 82, 83]. Overall, DUOX1 expression requires a functional DUOXA1 protein and was reported to be associated with numerous diseases in several tissues.

DUOX1 IN THE SKIN

In a previous study, using a DNA microarray, it was shown that of the seven NOX/DUOX family members expressed in normal human epidermal keratinocytes (NHEK), IL-4/IL-13 treatment only induced gene expression of *DUOX1* [42]. Moreover, this induced *DUOX1* expression was associated with high H_2O_2 production that was significantly inhibited by diphenyleneiodonium, an inhibitor of NADPH oxidases, and by small interfering RNA against *DUOX1* [42]. Lastly, the elevated level of DUOX1 in IL-4/IL-13-treated NHEKs induced STAT6 phosphorylation through oxidative inactivation of the protein tyrosine phosphatase 1B. This study discovered a new function of IL-4/IL-13-induced *DUOX1* gene expression in creating a positive feedback loop for IL-4/IL-13 signaling in keratinocytes[42]. Previous studies in nonmammalian organisms indicated that DUOX1 is involved in innate cutaneous host defense to infectious triggers and epidermal wound responses[63, 84, 85]. In another study assessing the effects of cytokines on *DUOX1* gene expression in cultured NHEK cells, DUOX1 levels were found to be 50-fold higher compared to DUOX2 levels. *DUOX1 gene* expression was augmented by IL-4 and IFN-γ[86]. On the other hand, in the human bronchial epithelial cell line HBE1, IL-4 upregulated only *DUOX1*, while IFN-γ enhanced only *DUOX2*, not *DUOX1*, gene

expression[86]. These studies demonstrate that epithelial *DUOX1* gene expression in different tissues can vary in cytokine regulation[86].

DUOX1 has been associated with Ca^{2+}-dependent keratinocyte differentiation [87]. DUOX1 represents the predominant DUOX isoform in human keratinocytes, the major epidermal cell type in the skin (>90%) [63]. DUOX1 is also present in nonepithelial cells such as macrophages and innate lymphoid cells that reside in the skin. DUOX1 plays a proposed role in innate lymphoid cells and macrophage polarization[46, 63]. Atopic and allergic contact dermatitis are caused by exaggerated immune responses to allergic stimuli characterized by high levels of IgE antibodies [88]. Atopic dermatitis can be followed by food allergy, allergic rhinitis and/or allergic asthma, in a process named atopic march[88]. DUOX1 can also play a role in the pathogenesis of atopic dermatitis as it is induced by type 2 cytokines, and it is present in epidermal keratinocytes[42, 89, 90]. The local generation of DUOX1-derived H_2O_2 by *TNF*-deficient keratinocytes in the skin activates the transcription factor NF-κB, enhancing the induction of genes encoding pro-inflammatory molecules[91]. Moreover, complete pharmacological inhibition of DUOX1 eliminated skin inflammation. DUOX1 is highly expressed in the skin tissues of psoriasis and lichen planus patients [91]. These studies suggest that pharmacologic and genetic approaches targeting *DUOX1* could provide innovative methods to treat atopic dermatitis, psoriasis, lichen planus, and other chronic inflammatory diseases[42, 91].

DUOX1 IN THE RESPIRATORY SYSTEM

1. DUOX1 in allergy and asthma

DUOX1 gene is expressed in airway epithelial cells and plays a proposed role in innate airway epithelial responses to infection or injury [92]. *DUOX1* is highly expressed in the nasal mucosa of patients with chronic sinusitis [93]. Elevated *DUOX1* expression was reported in cultured nasal or bronchial epithelial cells from patients with allergic asthma[44]. The *in vivo* role of DUOX1 is best understood in allergic inflammation[44]. Using *Duox1*-deficient mice and siRNA-mediated *DUOX1* down-regulation, Habibovic et al. showed the essential role of DUOX1 in the induction of type 2 inflammatory responses, mucus metaplasia, subepithelial remodeling, and airway hyperresponsiveness to methacholine[44]. In previous studies, DUOX1 was shown to interfere with neutrophilic rather than eosinophilic inflammation in severe exacerbations of asthma[94]. Severe exacerbation of asthma is usually dominated by neutrophilic inflammation, and it is more resistant to current treatments than other types of asthma[94]. DUOX1 inhibition might offer a novel therapeutic option for patients with allergic asthma. DUOX1 enhances the activation of Src and EGFR that can cause mucosal hyperplasia and allergic airway inflammation[44]. IL-4 or IL-13 induces *DUOX1* gene expression in the epithelium of the respiratory tract. These cytokines enhance the Th2 response and antibody production, thus stimulating various types of allergies[95]. In a previous study, *DUOX1* was shown to regulate the expression of 50% of the genes induced upon IL-4/IL-13 stimulation by combining DNA microarray analysis and *DUOX1* siRNA knockdown. These studies suggested that DUOX1 might regulate the function of some transcription factors, and induces STAT1, 3 and 6 phosphorylation[41]. Elevated *DUOX1* gene expression is associated with multiple

allergic conditions. Thus, selective inhibition of DUOX1 might be an attractive alternative to treating severe allergic asthma. DUOX1-induced H_2O_2 production could also induce cellular proliferation and mucosal hyperplasia due to its ability to recruit inflammatory cells and activate Src and EGFR signaling[44]. This might contribute to the pathogenesis of chronic rhinosinusitis in patients with nasal polyps[96]. Until recently, the regulation of *DUOX1* by proinflammatory cytokines has remained ambiguous. In a previous study, *DUOX1* expression was enhanced in primary respiratory tracheobronchial epithelial cells grown on air-liquid interface cultures for one week and treated for 24 hours with various types of cytokines. *DUOX1* expression was induced by Th2 cytokines such as IL-4 (4.5-fold elevation) and IL-13 (4.4-fold elevation). *DUOX1* gene expression increased in a time- and dose-dependent manner [97]. DUOX1 is the main DUOX isoform in the respiratory epithelium[94]. Maximal *DUOX1* expression can be reached at low levels of Th2 cytokines. *DUOX1* expression is persistent and takes a long time to disappear. DUOX1 may be an essential component of IL-4, IL-13 signaling leading to mucus secretion[97], bronchial smooth muscle hyperplasia and hypertrophy. Abnormal expression of IL-13 can augment *DUOX1* gene expression, subsequently lead to mucus hypersecretion[97] and muscular hyperplasia which exacerbate the disease and associate with poor outcomes[98, 99]. High *DUOX1* expression in asthmatic patients is correlated with severe symptoms and poor prognosis[92, 94].

2. DUOX1 in nasal polyposis

Nasal polyps are painless, smooth, noncancerous projections on the interior surface of the nasal canals or sinuses. Polyps projects like teardrops or grapes. Polyps

are caused by chronic inflammation linked to asthma, persistent infection, allergies, drug sensitivity and some immune diseases[100]. A previous study compared DUOX1 expression in nasal mucosal tissues from patients with chronic rhinosinusitis with or without polyps to that of non-inflamed control nasal tissues. *DUOX1* was upregulated in nasal tissues from patients with chronic rhinosinusitis with polyps in comparison to the controls. The level of DUOX1 in specimens from patients with chronic nasal sinusitis without polyps was like the controls[101]. DUOX1 generates H_2O_2 into the extracellular space[102]. H_2O_2 levels were elevated in patients with chronic sinusitis without polyps in nasal secretions. Furthermore, in patients with chronic rhinosinusitis with polyps, H_2O_2 levels were three-fold higher than the control levels. These results suggest the link between the presence of H_2O_2 in nasal secretions and *DUOX1* expression in nasal tissues[101]. H_2O_2 is produced in the airway mucosa and is normally exhaled during expiration. Various experiments showed that individuals with inflammatory lung diseases exhale higher levels of H_2O_2 than healthy, control individuals[102]. The extent of inflammation and the white blood cell count are linked positively with exhaled H_2O_2, which is proved to be generated both by the epithelium and by activated white blood cells during airway inflammation[103]. Measurements of H_2O_2 in nasal fluids cannot differentiate between the H_2O_2 generated by the epithelium or by mucosal white blood cells. Thus, it is complicated to quantify the fraction of DUOX1- vs. phagocyte (NOX2)-mediated H_2O_2 production. In previous studies, it has been proven that DUOX-generated H_2O_2 attracts leukocytes[93]. In one study, it was observed that the level of inflammatory cytokines such as eotaxin, monokine induced by gamma interferon, and TNF-α were prominently escalated in patients with chronic rhinosinusitis with polyps

and their amount in nasal fluids was closely linked with *DUOX1* gene expression[93]. *DUOX1* is upregulated in patients with chronic rhinosinusitis. Close correlations between *DUOX1* expression and H_2O_2 release, and correlation between key inflammatory cytokines and *DUOX1* expression, indicate a role of DUOX1 in the inflammatory response in chronic rhinosinusitis[93].

3. DUOX1 in chronic obstructive pulmonary disease (COPD)

Cigarette smoking is considered a predisposing factor for various chronic respiratory illnesses involving chronic obstructive pulmonary diseases (COPD) and asthma[104]. COPD involves emphysema and chronic bronchitis. COPD is the fourth leading cause of mortality in the United States[68], and it comes in the third place as a cause of death in 2020[69]. COPD symptoms are caused by constant airflow constriction that is often progressive and linked to various predisposing factors, leading to the exacerbation of the disease. COPD is characterized by constant inflammation and damage of the airways and the lung parenchyma. Exposure to smoking has been linked to enhanced oxidative stress and interferes with multiple biological mechanisms, including carcinogenesis and inflammation[105, 106]. The COPD pathophysiology is characterized by chronic inflammation and damage to the small airways and the lung parenchyma[65]. It is believed that oxidative stress is increased in patients with COPD due to chronic exposure to cigarette smoke, a main risk factor, which contains a high concentration of oxidants [67]. Exposure to cigarette smoke augments cell calcium trafficking, induces mRNA and protein expression of *DUOX1* in murine lungs and human cells. Furthermore, DUOX1 generates H_2O_2 that activates protein kinase C, leads to secretion of proinflammatory

cytokines and blocks A2A adenosine receptor-stimulated wound repair[107]. A previous study has used the human bronchial epithelial cell line Nuli-1 and C57BL/6 mice. It has shown that silencing the expression of *DUOX1* partially enhanced the resistance of epithelial cells to the negative effects of cigarette smoke on wound healing after injury [107]. Cigarette exposure regulates *DUOX1* expression in the lower respiratory tract. These studies indicate that airway expression of *DUOX1* is diversely associated with smoking and COPD[100]. Acute cigarette smoke exposure promotes intracellular calcium mobilization to activate *DUOX1*. It is still not well understood how *DUOX1* is regulated in smoking patients with COPD. In one study, epithelial *DUOX1* expression was investigated in the airways of smokers, and the association between this expression and COPD in the early stages of the disease. First, bronchoscopy was used to brush the tracheal and bronchial epithelium from patients who have never smoked and are current smokers[100]. *DUOX1* gene expression in harvested tracheal and bronchial epithelium was significantly downregulated in current smokers as compared to cases with no history of smoking. Furthermore, laser capture microdissection and microscope-assisted manual dissection were used in surgically resected lung tissues to harvest bronchiolar epithelium and alveolar septa[100]. Smoker patients with mild/moderate COPD had lower bronchiolar *DUOX1* expression than subjects who have never smoked, while a difference between former smokers, with and without COPD, was observed only for DUOX1. The expression of *DUOX1* in the alveoli was low and was similar between the groups. These results imply that the airway expression of *DUOX1* and *DUOX2* is diversely associated with smoking and COPD[100]. A recent study reported that downregulation of epithelial *DUOX1* gene in COPD contributes to disease pathogenesis[108]. DUOX1 levels

in the small airways were decreased in advanced COPD and correlated with lung function loss and emphysema markers and remodeling markers. *DUOX1* gene downregulation was also correlated with extracellular matrix remodeling observed in a genetic model of COPD[108]. DUOX1 deficiency exacerbated both, the development of subepithelial airway fibrosis in acrolein-exposed mice, and alveolar emphysema in elastase-administered animals. These studies further highlight that *DUOX1* downregulation contributes to COPD pathogenesis.

4. DUOX1 in lung fibrosis

Several factors and diseases can cause lung fibrosis including cytotoxic drugs, inflammation, allergic diseases, connective tissue diseases such as sarcoidosis, autoimmune diseases including rheumatoid arthritis and systemic lupus erythamtosis, and inhalation of organic materials such as asbestos[109]. Excessive production and deposition of extracellular matrix in pulmonary fibrosis cause lung tissue damage, which leads to the impairment of pulmonary function[109]. *DUOX1* is expressed in fibroblasts in response to lung tissue damage. DUOX1-generated H_2O_2 enhances the TGF-β1 signaling pathway in fibroblasts by inhibiting phospho-Smad3 degradation[65]. *DUOX1* is highly expressed in primary lung fibroblasts from patients with idiopathic pulmonary fibrosis (IPF). This elevation was accompanied by an escalation in the expression of α-SMA (smooth muscle actin), a marker of myofibroblasts[65]. Induction of lung damage by bleomycin or radiation enhanced the expression of *DUOX1* and *DUOXA1*. This elevation was linked to high mRNA expression of fibrosis markers including collagen (*Col1a1*), α *smooth muscle actin* (*ACTA2)* and the profibrotic factor *Tgf-β*[65]. *Duox1*-deficient mice

were used to examine tissue damage due to bleomycin and radiation, and it was found that these mice had less radiation-induced lung damage indicating that Duox1 is involved in the process of fibrosis formation[65]. After bleomycin treatment, *Duox1*-deficient mice showed elevation in TGF-β1 in the lung tissue. In addition, elastase, which is released from activated neutrophils, was significantly lower in *Duox1*-deficient mice compared to control animals[65]. The expressions of both *DUOX1* and *DUOXA1* mRNAs were stimulated by TGF-β1 in a dose- and time-dependent manner in wild-type fibroblasts. DUOX1 also inhibited the expression of α-SMA and collagen I mRNAs[65]. Extracellular H_2O_2 enhances phosphorylation of Smad2/3 and elimination of DUOX1 enhanced the reduction of phosphorylated Smad2/3 levels[65]. Phosphorylation of Smad2/3 was inhibited by catalase, indicating that this step was H_2O_2-sensitive[65]. Knockdown of *DUOX1* in IPF-derived cells using RNAi caused a significant decrease in extracellular H_2O_2 generation, which led to decreased TGF-β1-dependent accumulation of phospho-Smad3[65]. This study mechanistically proves that DUOX1-derived H_2O_2 determines the strength and duration of Smad signaling in the TGF-β1 pathway[65]. NEDD4L is the main ubiquitin ligase that selectively interacts with activated Smad2/3 for destruction. The effect of NEED4L depletion on TGF-β1-induced Smad3 phosphorylation was evaluated by RNAi-mediated knockdown[65]. *NEDD4L* knockdown inhibited the decline in phospho-Smad3 accumulation in *DUOX1*-deficient fibroblasts, indicating that the absence of DUOX1 enhances the action of NEDD4L to enhance TGF-β1 signaling[65]. The NEDD4L oligomeric state is crucial for polyubiquitin chain assembly. Moreover, the enzyme catalytic site has a cysteine portion, essential for its activity[110]. The oligomeric state of NEDD4L and its activity could be affected by H_2O_2-mediated oxidation [65]. Selective DUOX1 inhibitors

could, therefore, represent a novel therapeutic option against pulmonary fibrosis. IPF was shown to be linked to a high risk of pulmonary malignancy due to the appearance of unusual or dysplastic epithelial changes in fibrosis which develop into invasive malignancy[111].

DUOX1 in cancer

DUOX1 can promote or attenuate cancer growth according to its tissue expression and the type of malignancy. Although DUOX1-generated H2O2 can induce cellular proliferation, migration and angiogenesis in some types of cancers, DUOX1-mediated immune cell recruitment can restrict tumor growth and metastasis[112] and promotes tumor cell clearance[91]. The fraction of innate immune cells, including NK cells, monocytes, dendritic cells, and mast cells, was elevated in patients with high DUOX1 levels[89]. The mechanism by which ROS are produced by tumor cells remained incompletely understood until the discovery over the last 15 years of the family of NADPH oxidases[113]. *DUOX1* was reported to act as a selective tumor-suppressor gene during tumor initiation and progression[33]. The G2/M phase of the cell cycle acts as a cycle checkpoint and inhibits the entry into mitosis[114]. It plays an important role in controlling and maintaining tissue homeostasis, when tumor growth is induced by DNA damage [88]. In various types of malignancies, restoring *DUOX1* expression in cancer cells with low *DUOX1* expression significantly inhibited the growth of cancer cells by arresting the G2/M phase of the cell cycle and enhancing ROS production[33]. A study found an association between intracellular ROS accumulation and tumor suppression[81]. ROS can cause a specific type of cell death, termed anoikis, in normal cells. Although anoikis is a

barrier to abnormal growth and metastasis, cancer cells have often acquired increased threshold for anoikis and thus elevated metastatic potential. Moreover, elevated *DUOX1* expression was associated with enhanced immune pathways related to interferon (IFN)-alpha, IFN-gamma, and natural killer (NK) cell signaling. Malignancies such as lung cancer, hepatocellular carcinoma, follicular thyroid carcinoma, and breast cancer have low *DUOX1* expression[70, 115, 116, 117, 118], others including pancreatic ductal adenocarcinoma, gastric carcinoma, and cervical carcinoma have high reported *DUOX1* expression[119, 120, 121, 122]. Subsequently, ROS might enhance anti-apoptotic, proliferative, metastatic and angiogenic signaling, on the other hand, ROS may also contribute to cytotoxic and proapoptotic effects that constrain malignant progression and carcinogenesis according to the tissue location and type of cancer[112]. *DUOX1* gene expression is silenced in lung and hepatocellular carcinomas compared to surrounding normal tissues. It was proposed to be silenced due to *DUOX1* promoter hypermethylation since both directions of the promotor regions of *DUOX1* and *DUOX1A* are rich in CpG islands[115]. Similarly to *DUOX1, DUOXA1* was downregulated in different cancers as shown by TCGA data analysis of *DUOXA1* mRNA expression[112]. Surprisingly, recent research in lung malignant cells proved that the overexpression of *DUOX1*, but not *DUOXA1*, could reestablish epithelial characteristics and decrease invasive and migratory properties[69]. A previous study has shown that *DUOX1* expression was significantly lower in most cell lines of liver cancer and primary hepatocellular carcinoma tissues compared to non-tumor tissues[70]. The prognosis of hepatocellular carcinoma after hepatectomy can be predicted by the level of *DUOX1* expression[70]. Individuals with elevated *DUOX1* mRNA levels have prolonged disease-free and overall survival

compared to those with low *DUOX1* mRNA expression. The level of *DUOX1* mRNA expression was an independent prognostic factor for overall survival in hepatocellular carcinoma patients[83]. *DUOX1* could work as a tumor suppressor gene in the initiation of hepatic carcinoma and could be considered a novel biomarker for prognosis and therapy in liver cancer[83]. In follicular thyroid carcinoma with poor differentiation, elevated *DUOX1* expression is linked to low mortality rate[117], however, data from TCGA analysis indicate *DUOXA1*mRNA expression is enhanced in other thyroid cancers[112]. Thus, *DUOX1* and *DUOX1A* might work independently in thyroid malignancies. Additionally, *DUOX1* gene expression was proven to be decreased in breast cancer cell lines and in breast cancers when compared to their non-tumor counterparts[93]. This led to increased cell proliferation rates and adhesion properties, which are typical features of transformed cells[93]. Moreover, some studies in breast cancer cells examined the functional significance of *DUOXA1* downregulation and showed decreased *DUOXA1* expression in metastatic cell lines, altered cell adhesion, and susceptibility to doxorubicin after transient overexpression of *DUOXA1*[83]. Pancreatic inflammation due to ROS production and cytokine release have been linked to repeated inflammation in pancreatic tissues and to the development and progression of pancreatic ductal adenocarcinoma[119, 120, 121, 122, 123]. *DUOX1* mRNA and protein levels were 57.9-fold higher in patients with cervical carcinoma than in normal controls[120]. *DUOX1* mRNA levels were prominently increased in patients diagnosed with human papilloma virus HPV 16 compared to patients diagnosed with human papilloma virus HPV 18 and human papilloma virus HPV 45[120]. Chronic infection with human papillomavirus develops cervical carcinoma and is a leading cause of death among women worldwide and in the United

States[122]. Patients who are diagnosed with cervical squamous cell carcinoma have higher *DUOX1* expression than those with endocervical adenocarcinoma[120]. Furthermore, high *DUOX1* gene expression is a poor prognostic sign in gastric carcinoma[121]. Compared to common silencing of *DUOX1* that happens in various malignancies according to both TCGA data and immunohistochemical data in the Human Protein Atlas, these data often show positive DUOXA1 protein expression in various cancer tissues (e.g. neuroendocrine, head and neck, testicular cancers) as well as mixed immunostaining in multiple other cancers[112]. Overall, these studies indicate that *DUOX1* and *DUOXA1* might function independently, and changes of *DUOXA1* expression in malignancies might impact tumor pathology by DUOX1-independent mechanisms, associated with p53 or Numb/Notch pathways, in addition to regulating the actions of DUOX1. Further studies are needed using *DUOX1* and *DUOXA1* knockout animal models (global or conditional) to explore the potential mechanisms by which *DUOX1* and *DUOXA1* suppress or promote tumor growth. Understanding these mechanisms may provide valuable new diagnostic insights and novel therapeutic opportunities in cancer research. Likewise, it would be interesting to assess whether *DUOX1* and *DUOX1A* gene mutations are associated with or protect from any form of cancer.

DUOX1 IN OTHER DISEASES

DUOX1 plays an important role in H_2O_2 production, which might act as predisposing factor for several diseases including irradiation mediated heart damage[124, 125, 126]. Irradiation-induced fibrogenesis is a predisposing factor for several cardiac diseases such as coronary and carotid artery fibrosis, hypertrophy, ischemia and

pericarditis[76]. A study indicated that DUOX1 is important in stimulating the Smad-dependent TGF-β1 signaling pathway, which promotes irradiation-mediated pulmonary fibrogenesis after inflammation[75]. Radiation-induced heart disease (RIHD) is a common side effect of radiation therapy for the management of multiple malignancies, and RIHD increases the mortality rate among patients under radiotherapy[127]. Histological studies have shown that the recruitment of inflammatory cells such as neutrophils via DUOX1 plays an important function in chronic oxidative damage, inflammation and fibrosis, causing cardiac tissue structure alterations and elevating the risk of cardiac attack[77, 78]. In addition, DUOX1-mediated neutrophil recruitment could contribute to fibrosis due to elastase production[65]. *Duox1*-deficient mice have lower neutrophil elastase levels[75]. A function for H_2O_2-mediated pulmonary fibrosis was previously proven by the protective effect of catalase, an enzyme that degrades H_2O_2[80]. TGF-β1-mediated myofibroblast differentiation was previously proven to be linked to extracellular H_2O_2 production, which could damage the heart[75]. In a study using rats, metformin attenuated the upregulation of *Duox1* after irradiation exposure and lowered the recruitment of inflammatory cells[128]. Metformin is an oral diabetes type 2 medicine that helps control blood glucose levels[129]. Lowering *Duox1* gene expression via metformin could potentially play an important role in protecting against irradiation's toxic effects on the heart[128]. In another study also using rats, melatonin was used to attenuate *Duox1* expression and lower irradiation-mediated lung injury[130]. Subsequently, these studies reveal the potential importance of *DUOX1* expression in promoting fibrotic changes. Selective DUOX1 inhibitors could improve the outcome of these diseases. Since DUOX1 is mostly expressed in the respiratory system, DUOX1 might also have a role in the pathogenesis of cystic fibrosis[131]. Cystic fibrosis (CF)

is an autosomal recessive disorder that mostly occurs in Caucasians. It is due to mutations in a single gene on the long arm of chromosome 7 that encodes the cystic fibrosis transmembrane conductance regulator protein. Pathology of CF is mainly caused by abnormal Na^+ and Cl^- ion transport in various tissues such as the lungs, pancreas, gastrointestinal tract, liver, sweat glands, and male reproductive system. Patients with CF have high morbidity and mortality due to progressive pulmonary disease. DUOX1-mediated recruitment of immune cells such as neutrophils and macrophages to the respiratory epithelial surface might contribute to the oxidative and proteolytic stress implicated in the pathogenesis of CF[131]. The function of DUOX1 enzyme in the molecular mechanisms of these diseases need to be explored in more detail.

CONCLUDING REMARKS

High level of *DUOX1* expression has been linked to many disease pathologies. It has been successfully marked as a good prognostic factor in patients with hepatocellular carcinoma[116] (Fig. 1). Recent research showed a correlative association between low *DUOX1* expression and epithelial-to-mesenchymal transition (EMT), cancer stem cell characteristics and resistance of epidermal growth factor receptor-targeted therapy[69]. Most of the data proposing a link between DUOX1 and disease conditions remain, however, correlative, rely on mRNA analyses and do not provide a causative relationship. While results obtained on human clinical samples are essential to establish the potential clinical relevance of DUOX1, mechanistic studies using animal models or *in vitro* experimental systems are needed to understand better whether and how DUOX1 promotes or attenuates the pathogenesis of a variety of diseases. While these tools such

as Duox1-deficient mice are available, most of the correlative data between DUOX1 and diseases has not been confirmed in mechanistic studies. Generating mouse models with tissue-specific deficiencies in *Duox1* is highly desired to understand its role in different diseases better. Creating *Duox1*-deficient animals in mammalian species other than the mouse would solve problems and limitations related to using mice as an experimental model. *Duox1* overexpression in mice could also provide a new, independent approach to help better understand the potential role of *DUOX1* overexpression in certain pathophysiology.

Another important chapter in this field is the absence of information regarding existing *DUOX1* single nucleotide polymorphisms (SNPs) and their correlation with different diseases. While several studies have linked *DUOX2* SNPs to hypothyroidism [132, 133], and numerous studies indicate that the development of hypothyroidism is a predisposing factor for the onset of thyroid cancer[134, 135, 136], little is known about *DUOX1* SNPs. Only one study reported two *DUOX1* SNPs on exons 27 and 28 without any link to disease pathology[137].

Appropriate progress in the field is also delayed by the lack of DUOX1-specific antibodies. Specific detection of DUOX1 on the protein level, and its distinction from DUOX2, is very important and highly desired but remain largely problematic. Most antibodies used in the field detect both isoforms. While several companies sell antibodies claimed to be specific to DUOX1, they fail to characterize their specificities and to provide experimental evidence for it. Testing these antibodies on *Duox1*-deficient murine tissues/cells or on human cell lines overexpressing DUOX1 and DUOXA1 should be a routine and mandatory exercise before product launch to the market. DUOX1 functions

in a complex with DUOXA1. While recent studies have emerged studying this protein-protein interaction in detail, more work is needed to better understand the subcellular localization and molecular interaction of DUOX1 and DUOXA1, especially in the complex situation of an *in vivo* organism.

In summary, *DUOX1* gene expression has been linked to a range of clinical conditions and the contribution of DUOX1 to airway diseases has been started to be explored in murine models, several challenges remain though in the field that need to be addressed in the future.

Figures and legends

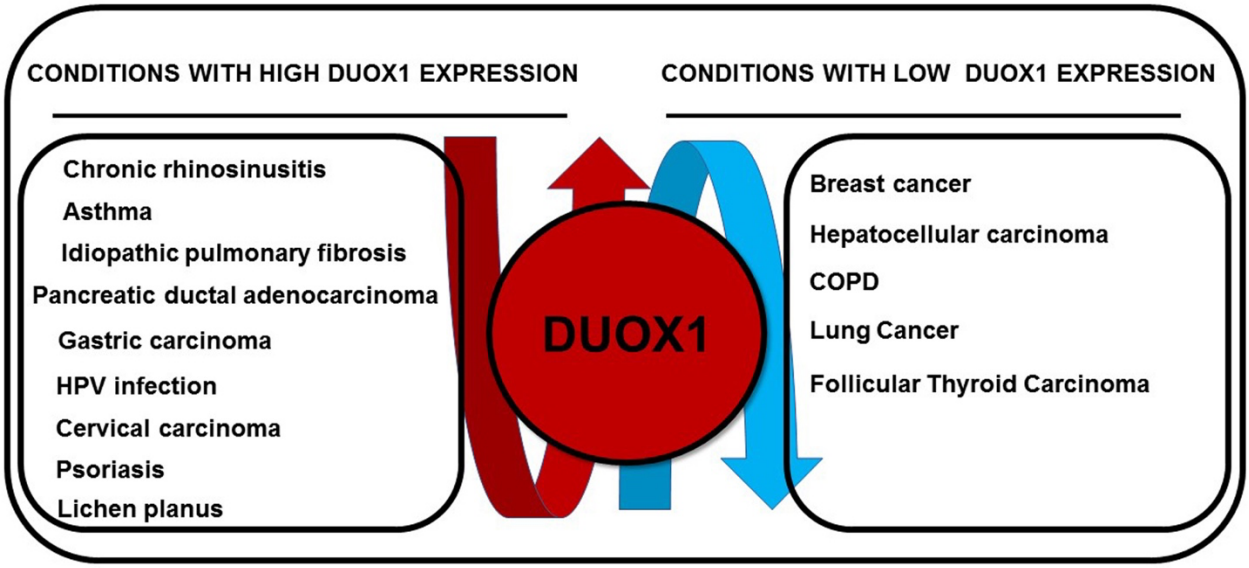

Figure 2.1 Conditions associated with either high or low expression of the NADPH oxidase DUOX1.

THE THERAPEUTIC POTENTIAL OF THIOCYANATE AND HYPOTHIOCYANOUS ACID AGAINST PULMONARY INFECTIONS

Ashtiwi, Nuha. Submitted to *Free Radical Biology and Medicine*, March 18, 2024.

ABSTRACT

Hypothiocyanous acid (HOSCN) is an endogenous oxidant produced by peroxidase oxidation of thiocyanate (SCN^-), a ubiquitous sulfur-containing pseudohalide synthesized from cyanide. HOSCN is a potent microbicidal agent against pathogenic bacteria, viruses, and fungi, functioning through thiol-targeting mechanisms independent of currently approved antimicrobials. Additionally, SCN^- reacts with hypochlorous acid (HOCl), a highly reactive oxidant produced by myeloperoxidase (MPO) at sites of inflammation, also producing HOSCN. This imparts both antioxidant and antimicrobial potential to SCN^-. In this review, we discuss the roles of HOSCN/SCN^- in immunity and potential therapeutic implications for combating infections.

Keywords

Thiocyanate, hypothiocyanous acid, infections, redox, peroxidase

Abbreviations

Duox, dual oxidase; EPO, eosinophil peroxidase; HOBr, hypobromous acid; HOCl, hypochlorous acid; HOSCN, hypothiocyanous acid; HSV-1, herpes simplex virus 1; H_2O_2, hydrogen peroxide; LF, lactoferrin; LPO, lactoperoxidase; MPO, myeloperoxidase; NIS, sodium iodide symporter; NOX, NADPH Oxidase; $OSCN^-$, hypothiocyanite; PTC, papillary thyroid cancer; PXN, peroxidasin; RSV, respiratory syncytial virus; SCN^-, thiocyanate; TPO, thyroid peroxidase; TrxR, thioredoxin reductase.

SCN^-/HOSCN to treat lung infections

Introduction

Acute respiratory infections (ARIs) are a major global health concern, leading to significant hospitalizations and mortality. ARIs have consistently ranked among the primary causes of death, resulting in an annual global loss of up to 3 million lives between 2010 and 2019, as reported by WHO [138]. ARIs consistently represent approximately 5% of the total annual global deaths, as highlighted in WHO reports for 2010 and 2019 [139]. In low-income countries, ARIs are a prominent cause of death, accounting for an estimated 10-25% of all deaths among children under 5 [139, 140, 141] (WHO 2014b). Furthermore, in resource-poor settings, ARIs contribute significantly to avoidable deaths (WHO 2007). ARIs were the leading cause of disease burden worldwide, as measured by disability-adjusted life years (WHO 2004).

ARIs are caused by a variety of viruses and bacteria [139, 142]. Despite the availability of therapies that can mitigate infection severity and reduce mortality, many respiratory infections remain refractory to treatment due to the absence of effective drugs [143]. Vaccines are accessible for certain respiratory pathogens such as influenza virus, SARS-CoV-2, or *Streptococcus pneumoniae*, but their efficacy is limited by antigenic drift. Notably, low-income countries often lack access to working medications [144, 145, 146], and available antiviral drugs exhibit efficacy primarily during early disease stages [147]. Antibiotic resistance is another growing global concern[148]. Several bacterial pathogens causing respiratory infections, including *Pseudomonas aeruginosa* (priority 1), *Staphylococcus aureus* (priority 2) and *S. pneumoniae* (priority 3) are listed by WHO in 2017 as global

antibiotic-resistant priority pathogens for which new antibiotics are urgently needed [149]. Hypothiocyanous acid (HOSCN) and its precursor thiocyanate (SCN^-) represent promising candidates, which is the subject of this review.

Thiocyanate (SCN^-) and hypothiocyanous acid (HOSCN)

Thiocyanate (SCN^-), a pseudohalide anion carrying a single negative charge localized at the sulfur atom, is present in various human secretions such as saliva, milk, airway lining fluid, and blood plasma [150, 151]. Human plasma typically contains SCN^- levels ranging from 10 to 300 μM [21, 152, 153], whereas its concentrations in saliva can reach mM levels, 10-fold higher than serum values [21 154 51, 155]. SCN^- is derived from cyanide by sulfurtransferases, including mitochondrial rhodanese and cytosolic mercaptopyruvate sulfurtransferase, and does not possess direct antimicrobial properties (**Figure 1**) [23]. Effective transport of SCN^- across airway epithelial cells and its concentration in the airway surface liquid relies on the basolateral sodium-iodide-symporter (NIS), while CFTR, TMEM16A, and pendrin can transport SCN^- apically into the airway lumen [53, 154]. In air-liquid cultures of respiratory epithelial cells, SCN^- is predominately transported through the transcellular route rather than the paracellular route [154]. This transport can be reversibly inhibited by competitive inhibitors of NIS in the basolateral compartment and CFTR inhibitors in the apical compartment [154].

SCN^- serves an essential role in the innate immune system as the precursor of the antimicrobial HOSCN (**Figure 1**) [156]. HOSCN, with a pK_a of 4.85, predominantly exists as ionized $OSCN^-$ under physiological conditions [157]. The oxygen in $OSCN^-$ becomes protonated at a lower pH. Protonated $OSCN^-$ reacts rapidly with thiol groups, which are abundant in cells [158]. Thus, HOSCN likely does not diffuse far from its generation site in

most physiological environs. This localizes HOSCN nearby the chordata peroxidases chiefly responsible for its production: lactoperoxidase (LPO), myeloperoxidase (MPO), eosinophil peroxidase (EPO), thyroid peroxidase (TPO), and peroxidasins (PXNs).

LPO is a 78.5 kDa monomeric protein consisting of a single polypeptide chain. After reducing H_2O_2 to water and forming compound I, LPO accepts two SCN electrons to produce HOSCN/$OSCN^-$ (**Figure 1**) [159, 160].

By generating HOSCN, LPO exerts bacteriostatic and bactericidal activities [161]. Other chordata peroxidases and peroxidasins catalyze the formation of HOSCN efficiently under physiological conditions using a similar mechanism to that of LPO (**Figure 1**) [162] [162, 163, 164]. MPO can catalyze the formation of hypochlorous (HOCl) and hypobromous acid (HOBr) from chloride or bromide, respectively [165]. MPO production of HOCl has been associated with irreversible tissue damage, e.g. production of chlorotyrosine in proteins [165, 166]. HOCl and HOBr are stronger oxidants than HOSCN, capable of generating irreversible oxidative products of biomolecules [167, 168, 169]. SCN^- can decrease HOCl and HOBr concentrations by outcompeting chloride and bromide substrates, leading to the generation of HOSCN, and by non-enzymatically scavenging HOCl and HOBr, thereby producing HOSCN [168, 169, 170]. Reactivity of SCN^- with HOCl/HOBr and prevention of their formation, in both cases yielding HOSCN, confers antioxidant and cytoprotective properties to SCN^- which have been extensively rviewed elswher[16, 21, 171, 172]. Importantly, the dose makes the poison: these reviews include review of potential toxicity of either thiocyanate or HOSCN, when concentrations of either are too high.

HOSCN production requires a source of H_2O_2, typically an NADPH oxidase such as dual oxidases (DUOXs) [173, 174, 175, 176]. Both DUOX1 and DUOX2 can provide H_2O_2 for

the LPO system [47]. DUOX1 is expressed mainly in the upper airway epithelium [97], while DUOX2 is expressed mainly in the salivary glands [177]. We have shown that in mice Duox1 supports the immune response during influenza A lung infection, [178] but is dispensable during lung infection with *Mycobacterium tuberculosis* [179]. As Duox1 is linked to HOSCN production, one interpretation of these results is that DUOX-peroxidase-mediated production of HOSCN is critical to immunity against certain respiratory pathogens, like influenza A virus.

The remainder of this review emphasizes the therapeutic potential of SCN^- and HOSCN in infections. It is not within the scope of this review to provide a comprehensive list of all *in vitro* studies on the antimicrobial actions of HOSCN; this topic has been reviewed elsewhere [32, 180]. Instead, this report specifically addresses *in vitro* research that contributes to a better understanding of *in vivo* observations reported in the literature. This discussion encompasses both the *in vivo* antimicrobial and anti-inflammatory benefits of SCN^- and HOSCN, as well as limitations and future research directions required to make SCN^-/HOSCN therapy a reality for fighting human infections.

Antiviral activity of HOSCN

HOSCN exhibits virucidal activity against several pathogenic viruses, including herpes simplex virus 1 (HSV-1), respiratory syncytial virus (RSV), echovirus 11, and influenza viruses [20, 32, 181]. HOSCN oxidizes thiol moieties of protein cysteines important for virion function, such as host cell binding [178]. Thus, HOSCN's antiviral effects are likely mediated by extracellular interactions with virions, though the possibility of additional intracellular mechanisms remains.

Salivary HOSCN, among the most concentrated in the body, likely has a role in salivary antiviral immunity by complementing serum-derived antibodies, especially IgG and IgM, to neutralize HSV [182]. Activation of salivary peroxidase activity has been associated with 70-80% reduction in the incidence of aphthous ulcers, which are linked to HSV and varicella zoster infections [183, 184, 185]. HOSCN exhibits its highest effectiveness in HSV control under acidic pH conditions, favoring its protonated state and showing the importance of salivary pH [19]. Radiotherapy for head and neck cancer may lead to latent HSV-1 reactivation due to impaired peroxidase function in the saliva, decreasing the steady-state concentration of HOSCN to levels insufficient for herpes virus control [186, 187, 188].

Our work has demonstrated the inhibitory effect of HOSCN against diverse strains of influenza virus *in vitro* [13, 189, 190, 191]. Recent findings underscore the *in vivo* significance of the HOSCN-generating antiviral system, revealing its direct targeting of influenza virus and impairment of its attachment and entry into host cells, resulting in reduced infection severity *in vivo* in a murine model of influenza lung infection [178]. Additionally, *in vivo* oral administration of HOSCN in combination with the drug amantadine (currently restricted by the FDA due to emerging drug resistance) demonstrated efficacy against lethal A/PR8 (H1N1) and A/HK/68 (H3N2) influenza A virus lung infections in mice [20]. Similarly, *in vitro* treatment with HOSCN, either alone or combined with amantadine or oseltamivir, was effective against various influenza strains [13, 20, 189].

HOSCN, in combination with lactoferrin, has been evaluated against SARS-CoV-2, the causative agent of the COVID-19 pandemic [192]. In this study, 100 μM HOSCN demonstrated the ability to inhibit at least 50% of SARS-CoV-2 replication *in vitro* [192].

Coronavirus spike proteins contain cysteine-rich regions, and the spike protein of SARS-CoV-2 possesses the most cysteine-rich cytoplasmic tail among related pathogenic coronaviruses, rendering it susceptible to oxidation by HOSCN. Given that S-acylation of cysteine residues has been identified as crucial for infectivity of SARS-CoV-2 *in vitro*, it is plausible that HOSCN inhibits the S-acylation of critical cysteines [193].

Antibacterial activity of HOSCN

Similar to viral pathogens, numerous bacterial species have been identified as susceptible to HOSCN *in vitro* [32, 180]. More recently, clinical isolates of *P. aeruginosa* and *Staphylococcus aureus* from cystic fibrosis (CF) patients were shown to be killed by HOSCN *in vitro*, arguably with some isolates exhibiting varying levels of susceptibility [22]. Both nonencapsulated and encapsulated *Streptococcus pneumoniae* strains were also susceptible to HOSCN, independent of the bacterial capsule, suggesting that HOSCN may penetrate the capsule to react with intracellular targets within the bacterium [148, 194, 195]. However, *S. pneumoniae* has also been shown to resist HOSCN via specific oxidoreductases [196]. More research is needed to resolve these contrasting observations.

HOSCN may be a more potent antimicrobial in combination with other agents. Inhaled HOSCN and lactoferrin (LF) in combination with antibiotics such as aztreonam or tobramycin reduced the biofilm formation of *Pseudomonas aeruginosa* and was not cytotoxic to airway epithelial cells [197]. HOSCN/lactoferrin also decreased levels of four strains of *P. aeruginosa* below detection limits and reduced the microbial load in sputum from patients with CF[198]. SCN^- analogs also hold therapeutic potential. The SCN^- analog selenocyanate demonstrated greater potency *in vitro* than SCN^- itself in killing CF

pathogens including *P. aeruginosa*, *Burkholderia multivorans* and methicillin-resistant *Staphylococcus aureus* [22, 199].

Antifungal activity of HOSCN

SCN^- exhibits *in vitro* antifungal properties against several species. Early exploratory reports indicated the susceptibilities of several fungal species to HOSCN including *Aspergillus niger*, *Pencillium chrysogeum*, *Aspergillus flaws*, *Alternaria* sp., *Trichoderma* sp., *Corynespora cassiicola*, *Phytopthora meadii*, *Claviceps* sp., and *Corticium salmonicolor* [200, 201]. *Candida albicans is also susceptible to LPO-generated HOSCN in vitro* [202]. Normal saliva contains LF and LPO, which provide a modest candidacidal effect [203, 204]. The combination of HOSCN with LF showed a fungicidal effect against *C. albicans*. HOSCN can inhibit fungal functions, including amino acid and sugar transport, respiration, and glycolysis [205]. Alterations in the fungal membrane can enhance the efficacy of HOSCN by exposing vital cellular components [206].

HOSCN and LF synergistically exert their antifungal action, with lactoferrin altering the fungal membrane and enhancing HOSCN uptake by fungal cells [207]. HOSCN has been found effective in inhibiting the growth of *Saccharomyces cerevisiae, Aspergillus niger, Rhodutorula rubra*, *Byssochlamys fulva, and Mucor rouxii in apple juice* [208]. *In addition to HOSCN, LPO can directly degrade certain fungal toxins, including aflatoxin B1 and G1, with* aflatoxin G1 being inactivated 1.5 times more effectively than aflatoxin B1 [209]. The LPO system can also oxidize alpha-amanitin, a potent hepatotoxin produced by the *Amanita phalloides* fungus [210, 211].

Molecular and cellular targets of HOSCN in pathogens

Although the antimicrobial properties of HOSCN have been reported for various microorganisms [32], the precise molecular mechanisms and targets underlying its antimicrobial action remain incompletely understood. Clarifying the microbicidal mechanism of action of HOSCN is relevant for its potential future use in HOSCN/SCN^- therapy. These mechanisms will likely vary across different pathogens due to the broad reactivity of oxidants with diverse molecules. Early studies reported key cellular processes targeted by HOSCN in bacteria, primarily of the *Streptococcus* genus (**Table 1**). For example, HOSCN reversibly inhibited glucose transport in *Streptococcus agalactiae*. HOSCN modified thiol groups in the bacterial cell membrane, which led to glucose transport blockage [212]. Another study showed that glucose uptake was impaired in bacteria when cows were prophylactically treated with HOSCN and immunized with colostral proteins from *S. sobrinus* or *S. mutants* [213]. HOSCN was generated at pH 5.5 or 6.5, by bovine milk LPO, KSCN and H_2O_2 [213]. In the saliva, the growth of *Streptococcus mitis* was inhibited when treated with HOSCN due to valine uptake inhibition [214]. After HOSCN treatment, the growth of *Streptococcus cremoris* was inhibited reversibly due to the inhibition of oxygen uptake and glycolysis [215]. HOSCN treatment targeted glyceraldehyde 3-phosphate dehydrogenase (GAPDH) in the glycolytic pathway in the following bacterial strains *Streptococcus sanguis, S. mitis, S. mutans, and S. salivarius* (**Table 1**) [216]. In *E. coli*, HOSCN reversibly blocked bacterial growth due to oxidation of bacterial thiol groups [217]. Moreover, HOSCN can inhibit the urease activity of *H. pylori*, an activity required for the bacterium to withstand the stomach's acidic environment [218]. In *Streptococcus pneumoniae,* two genes have been identified in a mutant screen that make

the bacterium sensitive to HOSCN: *hrcA* and *ctsR* [219] (**Table 1**). Both genes are heat shock protein repressors [220, 221] and their activation by HOSCN could lead to reduced expression of heat shock proteins yielding a weaker shield against HOSCN-mediated oxidative stress and damage. The activity of *hrcA* has been reported to be redox-sensitive and mediated by reduction-induced oligomerization via cysteine residues [222].

While more is known about the antibacterial mechanism of action of HOSCN, it has remained largely unknown how HOSCN inactivates viruses. We have shown that the binding of influenza A and B viruses to the host airway epithelium is the step in the viral infection cycle inhibited by HOSCN *in vitro* [178]. When several influenza virus strains were exposed to HOSCN *in vitro*, subsequent steps of the viral replication cycle were inhibited: virus binding, endosomal uptake, viral RNA synthesis, and overall virus replication [178]. HOSCN did not affect the virions' neuraminidase activity or the ability of the host cells to protect themselves against influenza infection [178]. The molecular basis for this action of HOSCN remains to be explored but modifications of cysteine residues in hemagglutinin, the viral surface protein responsible for virus binding to host cells [223], is the primary suspect mechanism [178].

In general, HOSCN's oxidizing potential targeting cysteines in proteins key to microbial metabolism, protection and survival is suspected to form the molecular basis of its broad-ranging antimicrobial activity [32, 158]. HOSCN readily reacts with numerous biomolecules containing thiols and selenols, including glutathione (GSH), GAPDH, and thioredoxin reductase (TrxR) [158, 224, 225, 226]. Oxidoreductases like TrxR and GSH reductase can repair HOSCN oxidation products by donating electrons from NADPH, a product of the pentose phosphate pathway, linking redox state to glucose metabolism [225].

The initial products of HOSCN's reaction with thiol groups are thiosulfenyl thiocyanates (RS-SCN), which can further undergo hydrolysis to sulfenic acid intermediates or reduction by thiols to form disulfides, depending on steric constraints [227, 228, 229]. These intermediates may also form heterodimeric disulfides, such as S-glutathionylated cysteine residues [227, 228, 229]. Whether HOSCN plays a crucial role in specific glutathionylation events that regulate cellular signaling remains unclear [230]. Lower pH can enhance the rate of oxidation by HOSCN, depending on the thiol [226]. Under physiological pH, $OSCN^-$ predominates over HOSCN, limiting its reactivity [157]. At high concentrations, HOSCN can also modify residues lacking thiols, such as tryptophan (Trp), histidine and tyrosine [231]. While HOSCN can oxidize Trp to 2-hydroxytryptophan on proteins *in vitro*, it cannot oxidize free Trp or Trp-containing peptides [228], It is uncertain whether Trp oxidation by HOSCN occurs under physiological conditions [232].

Currently, there is not a specific biomarker for HOSCN. Increased HOSCN levels correlate with thiol oxidation, but this can result from many other processes [233]. HOBr and HOCl rapidly react with multiple functional groups in biological molecules [234, 235, 236], whereas HOSCN selectively targets thiols (RSH, cysteine), selenols and selenoethers [157, 226, 237]. As thiol oxidation by HOSCN yields reducible products, HOSCN decreases damage to biological targets caused by HOCl or HOBr [238]. Interestingly, HOSCN or a related radical species (possibly $SCN^{\bullet}$, $OSCN^{-\bullet}$, or $(SCN)_2^{-\bullet}$) formed by MPO can induce peroxidation of plasma lipids and isolated LDL, which can be blocked by ascorbate [236, 239, 240]. However, there is no evidence of HOSCN reactivity with lipid double bonds [235, 236], and the reactivity of HOSCN with lipids in the presence of thiols remains uncertain. Furthermore, HOSCN does not react with isolated nucleosides, isolated DNA, or DNA

within intact cellular systems [237, 238]. Thus, it is plausible that most of HOSCN's antimicrobial activity is thiol-mediated. However, it remains important for organism-specific reactions to become elucidated.

Defense mechanisms of pathogens against HOSCN

In 2018, when we published a long, comprehensive review of all the reports up until then demonstrating the antimicrobial action of HOSCN against viruses, bacteria, fungi, and parasites [32], tolerance mechanisms against HOSCN remained largely undiscovered. Since then, however, a growing body of evidence suggests that bacteria possess mechanisms to reduce the damage by HOSCN (summarized in Table 2). The most information on HOSCN tolerance mechanisms has been reported for *Streptococcus pneumoniae*. We have observed that HOSCN can kill *S. pneumoniae in vitro* at physiologically relevant concentrations of SCN^- (400 μM) [194]. In contrast, Shearer et al. reported that *S. pneumoniae* is resistant to HOSCN *in vitro* and HOCl in the presence of NETs [196]. Differences in HOSCN sensitivity may, in part, result from different exposure durations: 4-6 hours of exposure in the study demonstrating killing [194], and 30 minutes in the study showing resistance [196]. Nevertheless, we did observe that *spxB*, a pyruvate oxidase and the main bacterial H_2O_2 source [241], can protect *S. pneumoniae* from HOSCN [194], a finding later confirmed[219]. Thus, *spxB* increases the tolerance of *S. pneumoniae* towards HOSCN (Table 2). Additionally, glutathione utilization has been shown to protect *S. pneumoniae* against HOSCN produced by LPO *in vitro* [242]. Bacterial growth in the presence of HOSCN was significantly decreased in the case of mutants unable to import glutathione or to recycle oxidized glutathione [242]. Furthermore, a new flavoprotein

disulfide reductase has been discovered in *S. pneumoniae* that was named Har (hypothiocyanous acid reductase) [243]. Bacterial growth was unaffected by Har deficiency but was inhibited when Har deletion was combined with disruption of glutathione import or recycling, proposing a role of Har in combination with glutathione utilization to protect *S. pneumoniae* from HOSCN [243]. In a genome-wide screen, 37 genes associated with HOSCN tolerance have been identified in *S. pneumoniae* [219]. Bacterial mutants deficient in these genes were significantly inhibited in their growth in the presence of HOSCN [219]. Generation of mutants with single-gene deletions of genes involved in redox homeostasis (trxA, sodA, and spxB) in *S. pneumoniae* validated the results of the mutant screen [219]. TrxA is an oxidoreductase involved in the thioredoxin/thioredoxin reductase system [244]. SodA is manganese-containing superoxide dismutase converting superoxide to H_2O_2 and protecting bacteria from superoxide-mediated damage [245]. As discussed earlier, spxB is a pyruvate oxidase generating bacterial H_2O_2 in *S. pneumoniae*. Several other hits (*manY, manA, relA, thiN, ktrB*) of the mutant screen that have not been confirmed with single gene deletion mutants in reports yet could also represent additional mechanisms of HOSCN tolerance of *S. pneumonaie* [219]. In *Staphylococcus aureus*, merA has been identified as an HOSCN reductase, safeguarding bacterial cells [246].

In Gram-negative bacteria, a recent study identified the flavoprotein RclA in Escherichia coli that reduces HOSCN to SCN^- and protects the bacterium against HOSCN toxicity *in vitro* [247]. RclA has previously been implicated in reactive chlorine resistance and is conserved in various epithelium-colonizing bacteria, hinting at the potential significance of its HOSCN-reducing activity in host-microbe interactions [247]. *E. coli* mutants lacking *rclA* display susceptibility to direct HOSCN exposure in a minimal

glucose medium [248]. RclA homologs from *S. aureus*, *S. pneumoniae,* and *Bacteroides thetaiotaomicron* have also demonstrated protective effects against HOSCN when expressed in *E. coli* [247]. In *E. coli*, the LPO-SCN^- system was shown to induce the upregulation of genes like *corA* and *mgtA* that encode metal ion transporter, *cysJ* (encoding the alpha subunit of sulfite reductase), *tcyP* (encoding a cysteine transporter), and *fruB* (encoding a fructose transport protein). However, the precise contributions of these genes to HOSCN response remain ambiguous [249].

In response to HOSCN, *P. aeruginosa* upregulates the expression of RclX, a predicted peroxiredoxin [250]. Transcriptional changes in *P. aeruginosa* PA14 in response to HOSCN and HOCl have been reported [250]. Additionally, treatment of *P. aeruginosa* PA14 with a bolus exposure of HOSCN in a minimal glucose medium leads to protein aggregation, triggering the heat shock response and causing membrane damage [251]. *P. aeruginosa* produces high levels of polyphosphate, a conserved polymer that binds unfolded proteins, thereby preventing protein aggregation resulting from HOSCN-induced protein unfolding [251]. Two independent studies investigating the whole genome transcriptomic responses in *P. aeruginosa* to HOSCN reported significant overlap in their findings. The responses included the induction of protein-stabilizing chaperons, RclR and MexT, regulons and sulfur-containing amino acid metabolism [250, 251]. Additionally, HOSCN reductase activity has been observed in chronic colonizing strains of *P. aeruginosa* from cystic fibrosis patients [225].

There are additional proposed mechanisms through which microbes could potentially undermine HOSCN's antimicrobial activities of HOSCN. Rather than directly targeting HOSCN, bacteria might inhibit the function or the expression of proteins involved

in HOSCN generation. For instance, our research has demonstrated that pyocyanin, a redox-active secreted toxin of *P. aeruginosa* known for its proinflammatory effects on the host [252, 253], can inhibit Duox-mediated H_2O_2 production, Duox1 protein expression, and HOSCN-mediated killing of *P. aeruginosa* and *Burkholderia cepacia* in human respiratory epithelial cell cultures [59, 254].

These emerging findings suggest the existence of 'redox warfare' between the innate immune system and inhaled pathogens in the lung. Subsequent investigations are necessary to delve deeper into the responses of various microorganisms to HOSCN across diverse experimental conditions. Such endeavors will contribute to a more comprehensive understanding of the mechanisms underlying HOSCN resistance and facilitate the development of inhibitors targeting these mechanisms to enhance HOSCN-based innate immune responses.

SCN^-/HOSCN therapy to combat infections

Given the substantial body of literature demonstrating the *in vitro* antimicrobial effects of HOSCN generated by peroxidases from SCN^- and H_2O_2, a pertinent question arises: could this innate immune mechanism be therapeutically enhanced to improve clinical outcomes in infections?

While evidence regarding this system's *in vivo* significance and efficacy in eliminating microbes in mammalian organisms remains limited, it is steadily accumulating. For example, our study revealed that mice deficient in Duox1 are more susceptible to influenza A virus lung infection than their wild-type counterparts [178]. Conversely, we also found that Duox1 deficiency does not influence the susceptibility of mice to lung infections

caused by another pathogen, *Mycobacterium tuberculosis* [179]. Studies have shown a correlation between SCN^- concentrations in airway surface liquid and improved lung function in individuals with cystic fibrosis [255]. Furthermore, excess iodide exposure in humans leads to increased salivary levels of iodide and antimicrobial hypoiodous acid [256]. These findings agree with the notion that peroxidase substrates (SCN^-, I^-) are enriched in mucosal secretions in humans, namely saliva and airway lining fluid [16].

This underscores the potential for oral or intravenous administration of peroxidase substrates to enhance airway defenses against respiratory pathogens in humans.

There is precedence for using peroxidase substrates in animal models to protect against acute infections. For instance, potassium iodide administration improved outcomes in sheep infected with respiratory syncytial virus [257]. In our studies, we demonstrated that nebulized SCN^- improves outcomes in mice with *P. aeruginosa* lung infection [23, 258]. Additionally, we found that HOSCN administration improved the outcomes of lethal influenza infection in mice by potentiating the effects of anti-influenza drugs [20]. This suggests that SCN^-/HOSCN could be employed as part of combination therapies. HOSCN production *in vivo* could not only be enhanced by pharmacological administration of SCN^-, but also by increasing H_2O_2 production generated by Duox1/2 or Nox2. This possibility should also be explored in the future in detail.

The accumulating data suggest that SCN^-/HOSCN-based therapies could be developed and used to target infections. Given HOSCN's reactivity and short half-life, direct administration to sites of infection is logical, whereas SCN^- functions more as a prodrug and scavenger of stronger oxidants (HOCl, HOBr). Thus, SCN^- may prove effective when either administered locally [23, 258] or systemically to combat infections.

Conclusions

SCN^- and HOSCN have been studied as antimicrobial agents *in vitro* and *in vivo* against a wide range of pathogens. They have also been explored as potential treatments for respiratory, gastrointestinal, neurological and cardiovascular diseases, with a history of use as an antihypertensive[152, 259, 260, 261, 262, 263, 264]. Emerging evidence suggests the safety and efficacy of SCN^- and HOSCN in combatting pathogenic infections and inflammation, particularly in short-term lung applications.

By reacting with thiols in protein cysteines important to the function of the pathogen, HOSCN interrupts important steps in mechanisms of pathogen survival including metabolism and host cell entry. Additionally, HOSCN could potentially overcome pathogen resistance to existing antimicrobial drugs. Agents targeting anti-HOSCN pathogen mechanisms represent an entirely new avenue of study that may empower innate immune function against specific organisms.

Ultimately, SCN^- and HOSCN hold clear promise for therapy in human lung infections. By limiting HOCl, SCN^- has the potential to serve as an antioxidant in inflammatory diseases that feature neutrophilic involvement. HOSCN is expected to control pathogens by reacting with critical protein cysteins. While there are clear reports of potassium SCN^- toxicity from the early 20^{th} century, when this drug was utilized in large doses to be tested as an antihypertensive, far lower doses of SCN^- are anticipated to be sufficient for antimicrobial and anti-inflammatory therapy. However, additional studies are needed to confirm both safety and benefit of SCN- and HOSCN in controlling infections, as both molecules have potential for toxicity in sufficiently high doses. The molecular mechanisms of pathogen control reviwed here can guid further HOSCN rsearch into

pathogen control. Adjunctive therapies targeting anti-HOSCN resistance mechanisms may also become important, or complementary therapies of SCN^- and other anti-pathogn drugs.

Figures and legends

Figure 2.2 The origin and function of SCN^- and HOSCN in the airways.

A) Several peroxidases are present in the respiratory tract: myeloperoxidase (MPO, neutrophils), lactoperoxidase (LPO, airway epithelium), eosinophil peroxidase (EPO, eosinophils) and peroxidasin (PXN, extracellular matrix). These are each capable of producing HOSCN, whil MPO alone is capable of producing HOCl **B)** In neutrophils, the NADPH oxidase enzyme complex generates superoxide anions ($O_2^{\cdot -}$) in the phagosome or the extracellular space. Superoxide dismutates to form H_2O_2, and epithelial enzymes such as dual oxidase (DUOX) 1/2 also contribute directly to H_2O_2 formation from NADPH and oxygen. Extracellular MPO, released from neutrophils by exocytosis or NETosis, generates HOCl from H_2O_2 and Cl^-. SCN^- reacts with HOCl, replacing the oxidant with HOSCN. SCN^- is also able to directly react with Compound I of MPO, directly forming HOSCN and preventing HOCl formation. HOSCN has antimicrobial potential for bacteria, viruses and fungi, outlined in this review. **C)** The formation of SCN^- from CN^- is mediated by mercaptopyruvate sulfurtransferases in the cytosol and by rhodanese, via the thiosulfate sulfur donor, in mitochondria.

Figure 2.3 Proposed therapeutic benefits of SCN^- in respiratory infections.

SCN^- administration promotes the *in vivo* generation of antimicrobial HOSCN by LPO in airway infections caused by viral and bacterial pathogens. MPO released from neutrophils recruited to the airways upon infection generates HOCl that damages lung tissues. SCN^- reduces HOCl generation by two proposed mechanisms: 1) MPO also converts SCN^- into

antimicrobial HOSCN and 2) SCN^- degrades already generated HOCl by forming antimicrobial HOSCN. Overall, SCN^- administration could have clinical benefits in airway infections as results of its combined effects on promoting microbial clearance and reducing inflammation-associated, oxidative tissue damage.

Figure. 2.2.

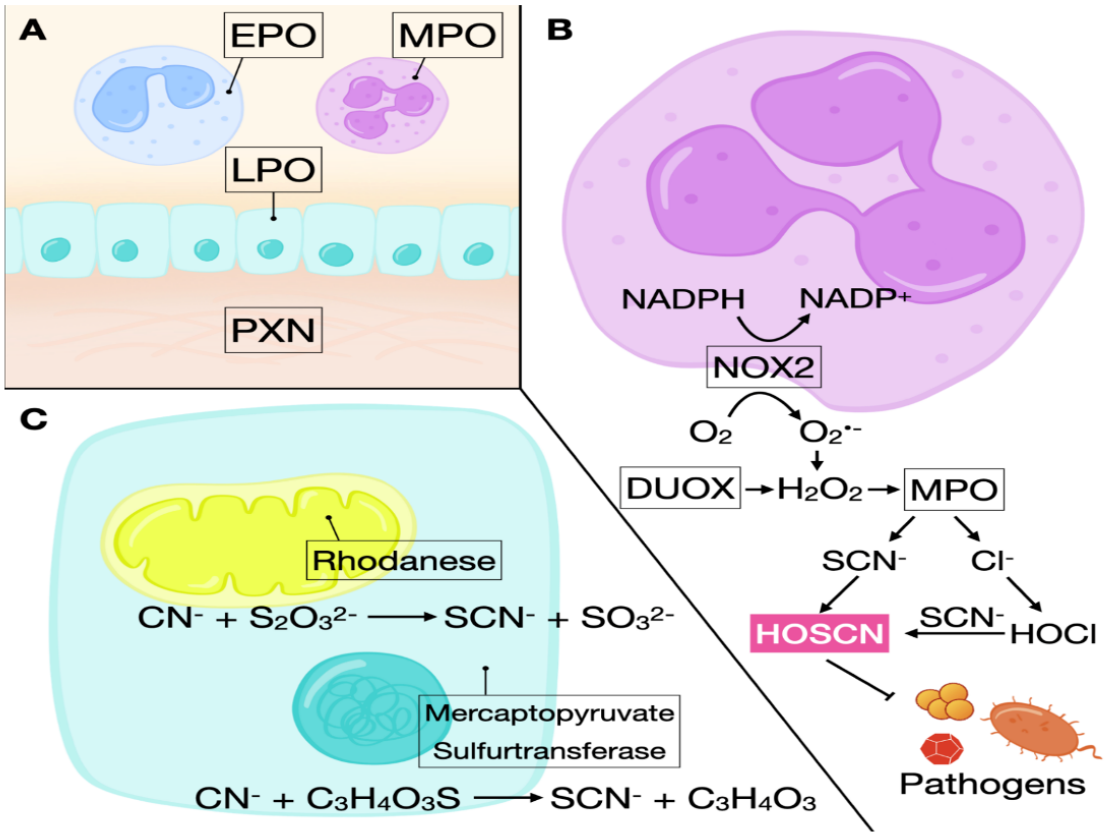

Figure. 2.3.

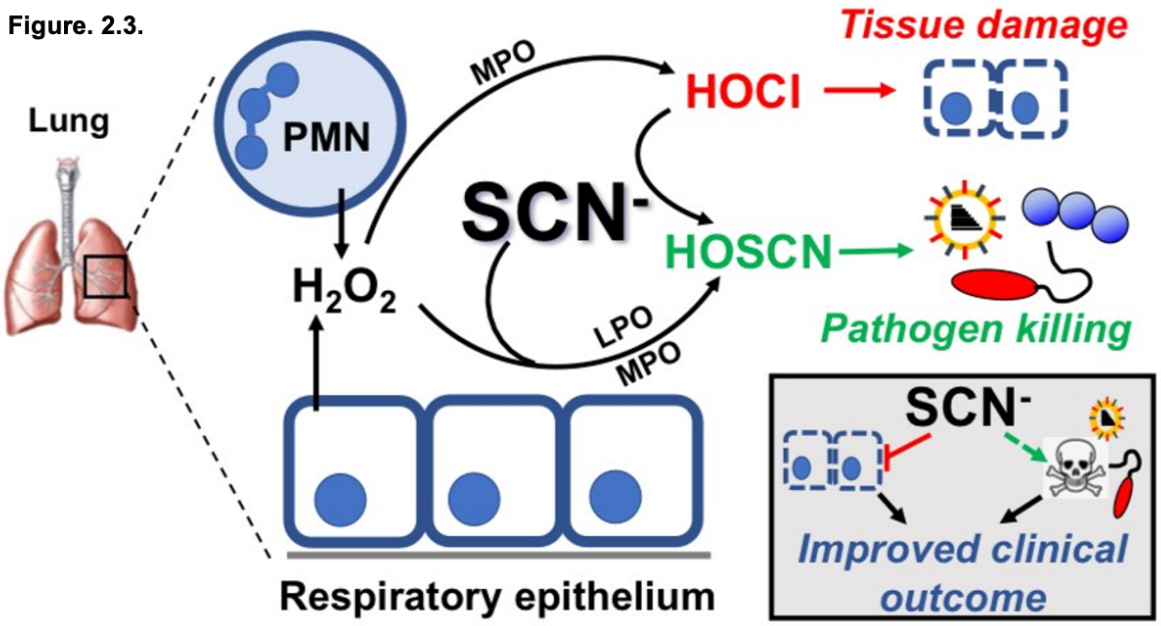

Tables

Table 1. Molecular and cellular targets of the antimicrobial action of HOSCN.

HOSCN effect	Species	Refs.
Bacteria		
Inhibition of glycolysis (hexokinase, GAPDH, and 6- phosphogluconate dehydrogenase and aldolase) and glucose uptake	*S. agalactiae, S. cremoris, S. pyogenes, S. sangius, S. mitis, S. mutans, S. salavarius, S. sobrinus*	25, 212, 213, 214, 215, 216
Inhibition of oxygen uptake (electrochemical proton gradient and respiratory dehydrogenase)	*E. coli*	25, 217
Inactivation of urease that compromises the ability of the bacterium to adapt to low pH	*H. pylori*	218
Viruses		

Inhibition of virus binding to the airway epithelium (possible target: cysteines in hemagglutinin)	Influenza A and B viruses	[178]

Table 2. Defense mechanisms of bacteria against HOSCN.

Bacterial species	References
Streptococcus pneumoniae	
spxB, pyruvate oxidase	[194, 265]
glutathione utilization	[242]
Har, HOSCN reductase	[243]
trxA, oxidoreductase in Trx system	[265]
sodA, superoxide dismutase	[265]
Additional genes to be confirmed (*manY, manA, relA, thiN, ktrB*)	[265]
Staphylococcus aureus	
MerA, flavoprotein disulfide reductase	[246]
Escherichia coli	
RclA, highly active HOSCN reductase	[247]
increased expression of *corA, mgtA, tcyP, fruB*	[249]
Pseudomonas aeruginosa	
rclX, predicted peroxidasin	[250]
polyphosphate preventing protein aggregation	[251]
Induction of *RclR* and *MexT*	[250, 251]

Pyocyanin inhibiting Duox	59, 254

CHAPTER 3

THE HYPOTHIOCYANITE AND AMANTADINE COMBINATION TREATMENT PREVENTS LETHAL INFLUENZA A VIRUS INFECTION IN MICE[20]

Ashtiwi Nuha, Accepted by *Front Immunol*. Reprinted here with permission of the publisher. May 18, 2022.

Abstract

The influenza virus has a large clinical burden and is associated with significant mortality and morbidity. The development of effective drugs for the treatment or prevention of influenza is important in order to reduce its impact. Adamantanes and neuraminidase inhibitors are two classes of anti-influenza drugs in which resistance has developed; thus, there is an urgent need to explore new therapeutic options. Boosting antiviral innate immune mechanisms in the airways represents an attractive approach. Hypothiocyanite ($OSCN^-$) is produced by the airway epithelium and is effective in reducing the replication of several influenza A virus strains *in vitro*. It remains, however, largely unexplored whether $OSCN^-$ has such an antiviral effect *in vivo*. Here we determined the therapeutic potential of $OSCN^-$, alone or in combination with amantadine (AMT), in preventing lethal influenza A virus replication in mice and *in vitro*. Mice intranasally infected with a lethal dose of A/Puerto Rico/8/1934 (H1N1) or A/Hong Kong/8/1968 (H3N2) were cured by the combination treatment of $OSCN^-$ and AMT. Monotherapy with $OSCN^-$ or AMT alone did not substantially improve survival outcomes. However, AMT+$OSCN^-$ treatment significantly inhibited viral replication, and *in vitro* treatment inhibited viral entry and nuclear transport of different influenza A virus strains (H1N1 and H3N2) including the AMT-resistant strain A/WSN/33 (H1N1). A triple combination treatment consisting of AMT, oseltamivir, and $OSCN^-$ was also tested and further inhibited *in vitro* viral replication of the AMT-resistant A/WSN/33 strain. These results suggest that $OSCN^-$ is a promising anti-influenza treatment option when combined with other antiviral drugs.

Introduction

The influenza virus can cause some mortality and high morbidity rates, especially in immunocompromised patients and those with comorbidities such as diabetes, chronic renal failure, malignancies, or immune system disorders[266, 267, 268, 269]. Four types of anti-influenza drugs having different mechanisms of action are available. Amantadine (AMT) and rimantadine are viral M2 channel inhibitors, and oseltamivir (OSL) and zanamivir are neuraminidase inhibitors (NAIs). The NAIs are only effective if the medication is administered within 48 h of symptom onset, and delayed treatment can result in high morbidity and mortality rates and a reduction in therapeutic efficacy[270, 271]. Insufficient inhibition of the viral replication leads to the emergence of drug resistance, which is associated with prolonged disease duration[272, 273]. Early published results showed that some 2009 H1N1 virus strains are AMT-resistant, which is associated with an S31N mutation in the M2 proton channel, but they remain susceptible to NAIs, i.e., OSL and zanamivir[274]. It has been reported that many H1N1 isolates tested in the United States are resistant to OSL[274, 275]. As almost all seasonal H3N2 and H1N1 viruses are resistant to AMT, and currently the majority of H1N1 strains from clinical isolates are also resistant to OSL, there is a strong rationale for developing new, combination therapies.

A previous study showed that therapeutic treatment with AMT, ribavirin, and/or OSL against a panel of influenza A viruses (IAVs) in triple combination had greater effects than any of the double combinations[276]. A triple combination of anti-influenza drugs (TCAD) was shown to be effective against several AMT-resistant and OSL-resistant influenza viruses[276]. AMT and OSL were combined at doses that were clinically approved, and these concentrations had less therapeutic efficacy when administered as a

monotherapy[276]. In addition, other studies also showed the clinical efficacy of TCAD therapy in mice and that TCAD therapy increased the survival rate and lowered the body weight loss of mice infected with susceptible and AMT-resistant A/H1N1 viruses[276]. These results suggested that the combined treatment is an effective, anti-influenza approach to overcome drug resistance issues.

Recently, we have reported that Dual oxidase 1 (Duox1), an NADPH oxidase family member highly expressed in the respiratory epithelium, promotes antiviral innate immunity in IAV-infected mice[178]. *Duox1*$^{-/-}$ mice infected with IAV had enhanced mortality and morbidity and impaired lung viral clearance[178]. These data support a previously proposed model[36] where Duox1 generates intraluminal H_2O_2 that is used by LPO to convert its main substrate SCN^- to antimicrobial $OSCN^-$[178]. We have shown that several influenza A or B strains are inactivated *in vitro* by $OSCN^-$ generated by LPO, SCN^-, and H_2O_2 [13, 178, 190]. H_2O_2 is derived from an enzymatic reaction in a cell-free system or by Duox1 present in normal human bronchial epithelial (NHBE) cells[13, 178, 190]. We also showed that $OSCN^-$diminished influenza replication and viral RNA synthesis in host cells inhibited by the H_2O_2 scavenger, catalase[178]. The binding of influenza viruses to host cells and viral entry were significantly reduced by $OSCN^-$ in an H_2O_2-dependent manner *in vitro*[178]. Overall, this novel *in vivo* antiviral function of $OSCN^-$ and Duox1 proposes that enhancing this mechanism could have therapeutic potential in treating influenza infections.

In this study, we evaluated the therapeutic potential of $OSCN^-$ single treatment and the $OSCN^-$+AMT combination treatment on lethal influenza infection in a mouse model. We also studied the effects of these treatments on viral uptake and replication in host cells. Our data show that combination therapy of $OSCN^-$+AMT prevents mortality in lethal

IAV infection *in vivo* by significantly reducing viral replication in host cells. Our data present an innovative approach to treating severe influenza infection that combines a traditional antiviral drug with a natural product of the innate immune system and achieves synergistic effects in viral clearance and prevention of influenza-related morbidity and mortality.

Materials and Methods

Influenza Virus Propagation.

IAVs were purchased from BEI Resources (managed by the American Type Culture Collection [ATCC]), NIH. The following IAVs were used in this study: A/California/04/2009 (H1N1; NR-13663), A/Puerto Rico/8/1934 (H1N1; NR-3169), A/turkey/Kansas/4880/1980 (H1N1; NR-3473), A/WSN/1933 (H1N1;(NR-3688), A/Aichi/2/1968 (H3H2; NR-3177), A/Wisconsin/67/2005 (H3N2; NR-41800), and A/Hong Kong/8/1968 (H3N2; NR-346). A/Texas/50/2012 (H3N2) was received through the Center for Research on Influenza Pathogenesis (CRIP). IAVs were propagated in Madin–Darby canine kidney (MDCK) cells as described[178]. Briefly, viruses were cultured in MDCK cells (ATCC, CCL034) using an infection medium (DMEM/F-12 supplemented with 1 mM of l-glutamine with 1 μg/ml of tosylsulfonyl phenylalanyl chloromethyl ketone-treated trypsin). Viruses were harvested 48 h post-infection (hpi). A/Puerto Rico/8/1934 (H1N1) was grown in the allantoic cavity of 9-10-day-old specific pathogen-free embryonated chicken eggs at 37°C. Viral titers were determined by plaque-forming unit (PFU) assay and hemagglutination (HA) assay[178]. The AMT-resistant influenza A/WSN/1933 virus was first passaged in MDCK cells, then grown in 10-day-old embryonated chicken eggs for 2 days

and titrated by plaque assay. The mouse-adapted A/Hong Kong/8/1968 H3N2 virus was passaged in MDCK cells. A/California/04/2009 (H1N1), A/Aichi/02/1968 (H3N2), A/Texas/50/2012 H3N2, and A/Wisconsin/67/2005 H3N2 were passaged in MDCK cells once before *in vitro* assays.

Animal Experiments.

All mouse procedures were approved by the Animal Care and Use Committee at the University of Georgia (UGA; protocol ID: A2017 07-010-Y2-A1). Six-week-old C57BL/6 mice from Jackson laboratories were anesthetized by intraperitoneal injection of 2,2-tribromoethanol (Avertin) at the dose of 200 mg/kg. Mice were infected intranasally with a 50-µl suspension of 150 PFU of A/Puerto Rico/8/1934 influenza virus and 3,000 PFU of A/Hong Kong/8/1968 influenza virus. Each mouse received an infectious dose of 2 × LD_{50} to achieve 100% lethality. Influenza virus lethal dose 50 (LD_{50}) lung titers were determined using the method of Reed and Muench[277]: $\log_{10}$ 50% endpoint dilution = $\log_{10}$ of dilution showing mortality next above 50% − (difference of logarithms × logarithm of the dilution factor). For all experiments, treatments were begun 48 h after infection and administered twice a day by oral gavage without anesthesia. A 5-day treatment of either monotherapy or a combined drug regimen was administered to mice given a lethal A/PR/8/1934 or A/Hong Kong/8/1968 infection in two independent experiments. Mice receiving a lethal infection of A/Hong Kong/8/1968 were also treated for 10 days. For all studies, AMT 46 mg/kg/day and OSL 25 mg/kg/day were administered alone or in combination. The projected pharmacokinetic parameters were expected to yield plasma levels in mice similar to those in humans[278]. Following infection and during the treatment

period, mice were monitored daily for 21 days for survival and weight loss. Mice with severe symptoms having a body weight loss of ≥30% were euthanized. For endpoint studies, mice were euthanized, and their lungs were removed at indicated times for lung histology and bronchoalveolar lavage fluid (BALF) studies. BAL samples were collected by injecting 1 ml of sterile PBS into the lung as previously described [178]. Collected BALF was separated by centrifugation (400*g*, 10 min) into BAL cells (pellet) and cell-free BAL supernatants. BAL cells were used to measure influenza mRNA levels by qPCR, while BAL supernatants were used to determine viral titers by plaque assays.

Antiviral Compounds.

AMT and OSL phosphate were obtained from Sigma-Aldrich (St. Louis, MO, USA). All drugs were dissolved in sterile water as previously reported [278, 279]. Drugs were administered in sterile water *via* oral gavage. Double and triple combinations were co-formulated and administered as a single solution. The placebo (sterile water) was administered in parallel with antiviral treatments in the same volume (100 µl).

$OSCN^-$ Production and Administration.

To generate $OSCN^-$ *in vitro*, components of the LPO-based antiviral system were used as previously reported[178, 190]. Physiologically relevant concentrations were used, i.e., 6.5 µg/ml of LPO, 400 µM of SCN^-, 0.005 M of glucose, and 0.01 U/ml of glucose oxidase [13, 178]. The entire solution containing freshly produced $OSCN^-$ was administered alone or in combination with AMT or OSL twice daily by oral gavage (100 µl) according to the experimental protocols.

Histopathology.

Murine lungs and tracheas after 5 days post-infection (dpi) (3 days after treatment) with A/PR/8/34 or A/HK/8/68 were inflated with 1 ml of 10% neutral buffered formalin and harvested as described[178]. All collected tissues were consistently fixed overnight in neutral formalin. Tissue samples were processed, and sections were prepared by the Histology Laboratory at the College of Veterinary Medicine at UGA. Sections were either left unstained for subsequent experiments (immunofluorescence) or stained with H&E as described [178].

Cytotoxicity Assays.

The potential cytotoxicity of the tested antiviral compounds was evaluated using the MTT Cell Proliferation Kit (OZ Biosciences, Catalog # MT01000). Briefly, 100,000 MDCK cells in DMEM media were seeded per well of 96-well cell culture plates using eight wells for each compound. Twenty-four hours later, the growth medium was removed, washed at 37°C, and preheated, with sterile phosphate-buffered saline (PBS) and then 200 µl of fresh DMEM [no fetal bovine serum (FBS)] medium containing the compounds. The compounds were tested at concentrations used throughout the manuscript of viral infection studies, i.e., OSL phosphate at 5 µg/ml and AMT at 15 µg/ml. Untreated, influenza virus-infected cells were used as a positive control for cell damage, and uninfected, untreated cells were used as a negative control. The virus-infected, untreated cells exhibited 100% cytopathology at 3 dpi. For single and double combination treatments, each drug was tested at the same concentrations in eight replicates per experiment. The cytotoxicity of single and double drug combinations was determined

using the same experimental protocol in three separate experiments and using the same concentration ranges 3 days after drug addition. The MTT Cell Proliferation kit is a colorimetric assay measuring the mitochondrial reductase activity in living cells that reduces MTT to formazan dyes, giving a blue/purple color. It is based on the cleavage of the membrane-permeable yellow tetrazolium salt MTT to formazan crystals by metabolically active cells. A solubilization solution is then added to dissolve formazan into a colored solution. Quantification of cell viability was determined by absorbance at 570 nm using spectrophotometry and expressed as a percentage of 100% cytotoxicity.

Cell Cultures.

MDCK (CCL34™) cells were maintained under humidity at 37°C with 5% CO_2 in Dulbecco's modified Eagle's medium/Nutrient mixture F-12 Ham (DMEM/F-12) (MilliporeSigma, St. Louis, MO, USA) supplemented with 10% heat-inactivated FBS (Gemini Bio-Products, West Sacramento, CA, USA; Catalog # 100-106). Primary NHBE cells were purchased from Lonza (Walkersville, MD, USA). To seed NHBE cells, 24-well polyester (0.4-μm pore) membrane transwells (Costar) were used at a density of 5×10^4 cells/well. When the NHBE cells reached confluency, the B-ALI™ growth medium in the upper chamber was removed, and the B-ALI™ growth medium in the lower chamber was replaced with the B-ALI™ differentiation medium (Lonza, Walkersville, MD, USA). Cells were kept on the air–liquid interface (ALI) for 4 weeks by feeding every other day with an ALI differentiation medium (the surface of ALI cultures was washed with sterile Hanks' Balanced Salt Solution (HBSS) every other day). Antibiotics (penicillin and streptomycin; Life Technologies, Grand Island, NY, USA) were added to the media up to

4 days before experiments, as previously described[59, 190]. NHBE cells were washed three times with PBS to remove excess mucus on the apical surface prior to infection. Viruses added to the apical side of NHBE cells were allowed to adsorb for 1 h at 37°C. Unbound viruses were removed by aspiration, and NHBE cells were washed again with PBS 3 sequential times. NHBE cells were incubated for the indicated times post-infection at 37°C. Viruses released apically were harvested by the apical addition, and a collection of 300 µl of 0.05% BSA-BEBM that was allowed to equilibrate at 37°C for 30 min. Samples were stored at −80°C until assayed.

Plaque assays were performed as described[13, 178, 190]. Briefly, A/Puerto Rico/8/1934, A/California/04/2009, A/WSN/1933, A/Aichi/02/1968, A/Texas/50/2012, A/Hong Kong/8/1968, or A/Wisconsin/67/2005 were used to infect MDCK cells or NHBE cells in the presence or absence of treatment compounds to evaluate their antiviral activity. A confluent monolayer of MDCK or NHBE cells was inoculated with 100 multiplicity of infection (MOI) viruses in DMEM with 10% bovine serum albumin for 1 hour at 4°C and then 37°C for 1 h. The cells were washed with PBS after inoculum removal. The cells were then overlaid with DMEM containing 1.2% Avicel and *N*-acetyl trypsin (2.0 µg/ml). To observe the effect of the compounds on plaque formation, the overlay media were supplemented with compounds at testing concentrations. The monolayers were fixed and stained with crystal violet dye solution (0.2% crystal violet and 20% methanol) to count plaques. Viral titers were calculated using 10-fold serial dilutions as before[13, 178, 190]. The sizes of representative plaques were determined by measuring the average diameter of

the plaques in two directions that are perpendicular to each other. Plaque size is expressed in mm.

Influenza Virus Entry Assays.

Indirect immunofluorescence techniques were performed to detect the effect of different treatments at different steps of the influenza virus replication cycle using a Zeiss confocal microscope. MDCK cells were propagated as described[178] at 37°C for 24 h and infected at MOI = 100 at 4°C for 1 h for evaluating nucleoprotein (NP) expression as described[178]. Unbound virus was removed by washing three times with cold Dulbecco's PBS (DPBS). Cells were re-fed with OPTI-PRO serum-free medium, then treated with treatments or 0.5% dimethyl sulfoxide (DMSO), and incubated at 37°C. To monitor NP expression, infection was stopped with 4% paraformaldehyde (PFA) at different time points. At 6 hpi, cells were fixed, and NP expression was determined at 24 hpi.

Immunofluorescence Assays.

Detection of influenza viral NP, M1, and M2 proteins in MDCK cells under different treatment conditions was performed as described[178]. Viral entry was determined in MDCK cells at 24 hpi for cells infected with the following H1N1 and H3N2 influenza strains (MOI of 100) at 4°C for 1 h: A/California/04/2009, A/Puerto Rico/8/1934, A/Aichi/2/1968, A/Texas/50/2012, A/Wisconsin/67/2005, and A/Hong Kong/8/1968. Unbound viruses were removed by washing host cells three times with cold PBS. Cells were refed with MDCK media and incubated at 37°C. Cells were stained for the viral M1, M2, and NP proteins as described[178]. Cells were treated with AMT and/or OSL at 15 and/or 5 μg/ml,

respectively. To monitor the uncoating and nuclear import processes, infection was stopped with 4% PFA at 3 and 6 hpi, respectively. Immunofluorescence assays (IFAs) were conducted using influenza M1- and M2-specific monoclonal antibodies as described [178]. Briefly, cells were incubated with anti-IAV NP antibody (AA5H, Abcam, Waltham, MA, USA), influenza A M1 monoclonal antibody (GA2B) (MA1-80736), and influenza A M2 monoclonal antibody (14C2) (MA1-082) for 12 h at 4°. Then cells were incubated for 1 h with an Alexa 488-conjugated goat anti-mouse IgG (H + L) secondary antibody (A32723) and counterstained with 4′,6-diamidino-2-phenylindole nuclear stain (DAPI). The images were acquired at ×60 magnification using a confocal microscope. The immunofluorescence was quantified using Fiji software (NIH, Bethesda, MA, USA) for each fluorescent channel. The fluorescent intensities of studied viral markers (M1, M2, and NP) were normalized on the DNA of MDCK cells and are expressed as M1/DNA, M2/DNA, or NP/DNA ratios.

Quantitative Real-Time PCR.

RNA extraction from treated MDCK, mouse BAL cells, or NHBE cells was performed using TRIzol (Catalog # 15596018; Invitrogen/Thermo Fisher Scientific, Carlsbad, CA, USA). cDNA was synthesized from 2 μg of total RNA using the High-capacity Reverse Transcriptase cDNA kit (Catalog # 4368814; Applied Biosystems/Thermo Fisher Scientific, Carlsbad, CA, USA). Each cDNA sample was diluted 10-fold, and real-time PCR was performed using SYBR Green PCR Master Mix (Catalog # 4309155; Applied Biosystems/Thermo Fisher Scientific, Carlsbad, CA, USA). The primer sequences used for gene amplification are listed as follows: β-actin forward:

5′-CCAACCGCGAGAAGATGA-3′, β-actin reverse: 5′- CCAGAGGCGTACAGGGATAG-3′. The forward NR-15594 and reverse NR-15595 16 primers used to amplify H1N1 and H3N2 transcripts were from the NR-15592 kit (Influenza Virus Real-Time RT-PCR Assay, BEI Resources, ATCC, NIH).

Statistics.

The data are presented as mean ± SEM or mean ± SD, as indicated in the figure legends. Statistical significance between experimental groups was determined using chi-Square, two-tailed Student's t-test, or Mann–Whitney U-test. Significance between multiple groups was assessed using either one-way or two-way ANOVA with Kruskal–Wallis followed by Dunn's multiple comparisons. For each test, $p < 0.05$ was considered significant.

Results

The $OSCN^-$/AMT Combination Treatment Reduces Influenza A Virus Replication *In Vitro.*

We have previously shown that $OSCN^-$ inhibits influenza virus replication *in vitro* [13, 178, 190]. We sought to determine whether combining $OSCN^-$ with AMT drug treatment would further increase antiviral efficacy. Six influenza A virus strains were tested *in vitro* on MDCK cells at a high MOI of 100 to demonstrate the robust nature of the antiviral action of the combined treatment: two H1N1 [A/PR/8/1934 and A/California/04/2009] and four H3N2 strains [A/Aichi/02/1968, A/Wisconsin/67/2005, A/Texas/50/2012, and A/Hong Kong/8/1968]. AMT treatment resulted in decreases in viral titers (Figure 3.1A) in the case

of all strains and decreases in viral gene expression, which were significant in the case of only two out of six IAV strains (Figure 3.1B). OSL treatment had robust and significant reductions in IAV proliferation as measured by PFU assay (Figure 3.1A) and viral RNA synthesis (Figure 3.1B). $OSCN^-$ treatment alone led to diminished viral replication and viral gene expression that reached the levels of significance in case of some strains but remained non-significant in case of others (Figures 3.1A, B). When $OSCN^-$ and AMT were combined, viral titers were significantly reduced compared to untreated, AMT-treated, or $OSCN^-$-treated samples (Figure 3.1A), and viral gene expression levels also showed similar significant differences (Figure 3.1B). No substantial differences in viral replication were found between the combined treatment ($OSCN^-$+AMT) and OSL (Figure 3.1A). The applied treatment conditions alone were not cytotoxic to uninfected MDCK cells as was shown by using the cell cytotoxicity MTT assay (Figure 3.1C). Overall, these results suggest that the concerted action of $OSCN^-$ and AMT leads to significant improvement in inhibiting viral RNA synthesis and proliferation in MDCK cells as compared to single treatments or no treatment.

$OSCN^-$ and AMT Combination Treatment Inhibits IAV Uncoating and Nuclear Import in Host Cells.

To further explore whether the combination of AMT and $OSCN^-$affects viral entry, the same six IAV strains were allowed to adhere to MDCK cells for 1 hour at 4°C. Unbound virions were washed away, and cells with virions bound to their surface were exposed to the indicated treatment conditions post-binding as described previously[178] under the conditions of Figure 3.1. Cells were fixed 3 h later and stained for the viral M2 ion channel

(Figure 3.2) or M1 matrix protein (Figure 3.3), indicative of viral uncoating as before[178]. The combined treatment of AMT+OSCN$^-$ or OSL alone significantly reduced the M2 immunofluorescent signal (M2/DAPI ratio) as compared to the infected but untreated controls in MDCK cells infected by each of the six IAV strains (Figures 3.2A, B). Similar trends could be observed when the localization of M1 matrix protein as a sign of viral uncoating inside host cells was investigated by immunofluorescence (Figure 3.3). The combined treatment significantly diminished IAV uncoating (M1/DAPI signal ratio) in the case of all IAV strains except A/Wisconsin/67/2005, which had a non-significant reduction (Figures 3.3A, B). Uncoating of the virion content is followed by the translocation of the viral RNA to the host cell's nucleus and by the synthesis of new viral proteins[280]. NP is released upon entry and uncoating into the cytosol and then subsequently translocates to the nucleus (nuclear import), where it participates in the formation of viral ribonucleoproteins that will be transported from the nucleus back to the cytosol[281, 282]. Therefore, NP immunofluorescence can be detected in both the cytosol and the nucleus and indicates later stages of the viral life cycle[281]. The NP immunofluorescent signal (NP/DAPI ratio) was also significantly reduced by the combined treatment in comparison to untreated cells in the case of all six IAV strains tested (Figures 3.4A, B). The combined treatment also showed a significant reduction of the NP signal compared to the single treatments (AMT and OSCN$^-$) in the case of five strains (Figure 3.4). Thus, the combined AMT+OSCN$^-$ treatment targets the early steps of influenza replication *in vitro*.

OSCN$^-$ and AMT Combination Treatment Inhibits IAV Replication in Primary Human Bronchial Epithelial Cells.

To confirm the inhibitory action of the combination therapy on IAV replication in physiologically relevant cells, ALI cultures of NHBE cells were infected with only one IAV strain, A/California/04/2009, in the presence of the same treatment conditions as tested before. NHBE cells represent a suitable *in vitro* model of the human respiratory epithelium and, when infected with influenza viruses, express Duox1, produce H_2O_2, and generate $OSCN^-$ when LPO and SCN^- are added exogenously[36, 59, 60, 178, 194]. We have previously shown that the A/California/04/2009 virus strain infects NHBE cells and $OSCN^-$, reducing its proliferation in an NHBE-generated H_2O_2-dependent manner[178]. The combination of AMT and $OSCN^-$ led to significantly reduced viral RNA synthesis (Figure 3.5A) and IAV replication (Figure 3.5B) in NHBE cells as compared to untreated cells or single treatments. Single treatments did not show significant efficacy (Figure 3.5). These data show that the combination treatment inhibits IAV replication in both MDCK cells and NHBE cells.

The AMT+$OSCN^-$ or $OSCN^-$+AMT+OSL Treatments Inhibit the Replication of AMT-Resistant IAV Strains.

We next aimed to investigate whether $OSCN^-$ alone or in combination with AMT or AMT+OSL is efficient in preventing the replication of an AMT-resistant IAV strain. Since all six IAV strains tested showed various levels of susceptibility to AMT treatment *in vitro* (Figures 3.1-3.4), we evaluated A/WSN/33, which is a strain with well-documented AMT resistance, which has been linked to molecular changes associated with resistance identified as single-nucleotide changes leading to corresponding amino acid substitutions in one of four critical sites, amino acids 26, 27, 30, and 31, in the transmembrane region

of the M2 protein[283]. We confirmed the AMT resistance of the A/WSN/1933 (H1N1) strain by plaque size measurements (Figure 3.6A), viral RNA synthesis, and proliferation (Figure 3.6D). In contrast, the A/turkey/Kansas/4880/1980 (H1N1) virus strain, which was shown to be susceptible to $OSCN^-$ in our prior report[13], is highly susceptible to AMT as also assessed by PFU titers and sizes (Figure 3.6B). Both strains are susceptible to OSL (Figures 3.6A, C). After having characterized the drug resistance of these two strains, next, we evaluated the effect of the AMT+$OSCN^-$double treatment and the triple combination of AMT, $OSCN^-$, and OSL on viral gene expression and proliferation using quantitative PCR and plaque formation using MDCK cells. We observed pronounced therapeutic effects of both the double and triple treatment combinations in the case of both strains as compared to the single-agent therapies or the “no treatment” control (Figures 3.6D, E). However, the combined effect of the TCAD regiment was greater than that of any double combination tested. These results demonstrate that combining OSL with the dual combination provides additional synergy.

$OSCN^-$+AMT Combination Treatment Protects Mice Against Lethal Infection by an H1N1 IAV Strain

To demonstrate the therapeutic efficacy of the combination of AMT and $OSCN^-$ on airway infection elicited by an H1N1 IAV strain, C57BL/6 mice were intranasally infected with a lethal dose (150 PFU) of the A/PR/8/1934 virus strain. All drugs were administered in equally divided doses (twice a day) by oral gavage for 5 days in a row starting 2 days after IAV infection (Figure 3.7A). All drug concentrations investigated were clinically relevant doses and were used for murine efficacy studies[279, 284]. Five treatment conditions

were used; OSL was administered at a daily dose of 25 mg/kg and AMT at a dose of 46 mg/kg. $OSCN^-$ was generated *in vitro* in a cell-free system as described previously [279, 284], the same way as in the *in vitro* assays (Figures 3.1-3.6). Mice infected with IAV but only treated with solvent (placebo group) all succumbed to the infection at 6 dpi (Figure 3.7B). AMT treatment delayed the disease progression, but all AMT-treated mice died at 10 dpi (Figure 3.7B). When $OSCN^-$ was used alone, it rescued some animals from death at 21 dpi (Figure 3.7B). Impressively, the combined (AMT+$OSCN^-$) and OSL treatments provided 100% protection and resulted in complete survival of all the animals at 21 dpi (Figure 3.7B). Untreated or AMT-treated mice suffered significant weight losses due to disease progression (Figure 3.7C). $OSCN^-$-treated mice demonstrated some temporary weight loss, while animals treated with OSL or the AMT+$OSCN^-$combination did not lose weight (Figure 3.7C). Treatment efficacy on viral replication was also tested by using BAL samples from different treatment groups by performing viral plaque assay on the BAL supernatants and viral qPCR in BAL cells. Both the AMT+$OSCN^-$and OSL-treated groups showed significantly lower viral titers and gene expression levels as compared to the placebo (untreated) group at 5 dpi (Figure 3.7D, E). (Histopathological evaluation of the lung in the placebo, AMT, $OSCN^-$, and OSL monotherapy groups at 5 dpi (3 days posttreatment) showed congestion and destruction of the bronchial/bronchiolar epithelium and alveolar cells and associated mixed inflammatory infiltrate and hemorrhage. The bronchiolar epithelium was often hyperplastic, indicating bronchiolar epithelial regeneration (Figure 3.7F). However, the combined AMT+$OSCN^-$treatment revealed fewer pathological effects resembling a healthy lung (Figure 3.7F). Thus, we

conclude that the combined treatment of $OSCN^-$ and AMT is effective against the lethal infection by an H1N1 IAV strain (A/PR/8/1934) in this murine model.

$OSCN^-$+AMT Combination Treatment Protects Mice Against a Lethal Infection by an H3N2 IAV Strain

As the AMT+$OSCN^-$ combination treatment was successful at rescuing mice from lethal infection (Figure 3.7), we explored whether this effect would also occur in mice lethally infected with an H3N2 IAV strain that also causes seasonal epidemics and infects immunocompromised patients in hospitals[285, 286, 287, 288]. Mice were intranasally infected with a lethal dose of the A/Hong Kong/8/1968 IAV strain that is also susceptible to $OSCN^-$ [13], AMT, and OSL (Figures 3.1- 3.4). Mice were infected on day 0 and subjected to the same five treatment conditions 2–7 dpi (Figure 3.8A) as PR8 was before (Figure 3.7). As expected, all mice succumbed to the infection at 6 dpi but were unaffected by AMT treatment (Figure 3.8B). While $OSCN^-$treatment slightly delayed this response, all animals expired at 10 dpi (Figure 3.8B), similar to mice infected with the H1N1 IAV strain (Figure 3.7B). Interestingly, the AMT+$OSCN^-$ combination treatment or the OSL monotherapy did not prevent the occurrence of mortality but only delayed its onset (Figure 3.8B). All the animals succumbed to the infection at 14 dpi despite the 5-day-long OSL treatment, and only one animal remained alive at 21 dpi in the combination treatment group (Figure 3.8B). This contrasts with the results obtained using the H1N1 strain (Figure 3.7B). All animals experienced significant weight loss before succumbing to the infection (Figure 3.8C). Interestingly, the differences seen in mortality and weight loss between

the treatment groups were not clearly reflected in viral titers (Figure 3.8D) and viral RNA levels (Figure 3.8E) in BAL samples collected at 3 dpi.

To improve the efficacy of the combination treatment against the H3N2 IAV strain used, we decided to prolong the treatment period from 5 to 10 days. Thus, mice were intranasally infected with the same lethal dose of the A/Hong Kong/8/1968 (H3N2) IAV strain and treated in the same ways as before between 2 and 12 dpi (10-day duration) (Figure 3.8F). Impressively, mice in both the AMT+OSCN$^-$ combination therapy and OSL treatment groups survived and regained their initial weight after completing the whole 21-day-long course of the experiment (Figures 3.8G, H). The monotherapies remained ineffective (Figures 3.8G, H).

BAL samples taken from surviving mice at 10 dpi (8 days posttreatment) revealed significantly lower viral titers (Figure 3.8I) and RNA levels (Figure 3.8J) in the combined therapy and OSL-treated groups compared to the placebo or the AMT or OSCN$^-$ monotherapy groups, further confirming the beneficial effects of the combined and OSL treatments.

Overall, AMT+OSCN$^-$ combination therapy and OSL monotherapy protected mice from lethal infections by both H1N1 and H3N2 IAV strains. Prolonging the treatment period proved to be successful in improving poor therapeutic effects.

Discussion

Several studies have reported that combining anti-influenza drugs can enhance the synergy in inhibiting viral replication *in vitro* or *in vivo* [289, 290, 291]. The rationale behind this study was to test whether OSCN$^-$alone has antiviral action against influenza *in vivo* or

can increase the efficacy of other antiviral drugs. Furthermore, knowing that the majority of influenza A strains have lower susceptibility to the current, Food and Drug Administration (FDA)-approved anti-influenza drugs, their possible combination with new antivirals such as $OSCN^-$ could synergistically improve their therapeutic action.

Combination treatment of AMT and $OSCN^-$ was highly efficacious in reducing weight loss and death in mice infected with A/PR/8/1934 and A/Hong Kong/8/1968 influenza viruses in our study. The therapeutic efficacy of the combined regimen was superior to that of treatment with a single drug, and the enhanced potency of AMT combined with $OSCN^-$ *in vivo* confirmed the synergy shown *in vitro*. The contribution of AMT to the therapeutic efficacy of a combined regimen in mice and *in vitro* indicates the synergistic antiviral effects of two independent therapeutic approaches. Furthermore, the therapeutic effect of TCAD treatment against A/WSN/1933 (AMT-resistant strain) and A/turkey/Kansas/4880/1980 (H1N1) (AMT-susceptible strain) was observed when OSL was added to the AMT+$OSCN^-$ combination. Generally, the dosing regimens used in our *in vitro* cell cultures and murine model were depicted to provide similar drug exposure to those carried out in humans and were all according to pharmacokinetic parameters achieved for used drugs in mice and humans.

Although the drug toxicity was not directly measured in this study, we have assessed potential drug toxicity by single agents and found that the anti-influenza drugs do not cause detectable toxicity *in vitro* (Figure 1C). Toxicity is unlikely to become a clinical issue when considering potential, future, human clinical tests, as AMT and OSL have been used in humans for years, and $OSCN^-$ is present in the human body at the concentrations used in this study. In addition, the drug concentrations of AMT and OSL

used in this study were 5- to >300-fold below the 50% lethal concentrations of each single treatment[10, 292 293]. The fact that the single treatment of AMT at its highest dose (46 mg/kg) cannot improve the survival rate in mice, while all mice survived in the combined group, and the fact that all mice in the combined group gained weight during treatment demonstrates that any toxic side effects did not affect our parameters of therapeutic efficacy (mortality and weight loss).

In our *in vitro* model, the triple combination treatment was effective against the AMT-susceptible [A/turkey/Kansas/4880/1980 (H1N1)] and AMT-resistant strain (A/WSN/1933) IAV strains as well. AMT, OSL, and $OSCN^-$ target different points of the virus replication cycle: M2 ion channel, neuraminidase, and hemagglutinin [potentially [178]], respectively. The advantage of any combination treatment is that there is not only one but also two or more targets increasing the chances to be clinically effective and decreasing the chances of emerging drug resistance. Furthermore, $OSCN^-$ (or SCN^- also added as part of the $OSCN^-$-generating solution) likely has an additional, beneficial anti-inflammatory effect too since it could diminish neutrophil-mediated, oxidative tissue damage that has been associated with IAV-induced lung injury[258, 294] (. Interactions among NA, M2, and hemagglutinin have been reported to affect susceptibilities to AMT and OSL, respectively[295, 296], and could represent one possible explanation for the synergistic effects of the tested antiviral drugs. Previous studies have reported that HA–M2 and HA–NA interactions can affect the susceptibility to AMT and OSL, respectively[297, 298]. The presence of the third compound is important for the synergistic antiviral efficacy of the combined treatment. In our previous study, $OSCN^-$demonstrated an inhibitory effect on influenza viral attachment and entry with several proposed mechanisms of action, which

remain to be explored[178] . These data indicate that the combined treatment may provide broad-spectrum antiviral activity against circulating IAVs, including strains that are resistant to either class of antivirals. Currently, most influenza A strains (99%) are resistant to either the adamantanes or OSL, but not to both[276], and therefore are expected to be susceptible to the combined treatment. At the present time, fast diagnostic tests are not available to evaluate the susceptibility profile of influenza viruses in patients in real time, and hence clinicians do not often have the needed information based on which to decide the use of the appropriate antiviral treatment. The accessibility of a broad-spectrum anti-influenza medication effective against most of the currently circulating strains would be of maximum clinical benefit. Since $OSCN^-$ has antimicrobial activities against a wide range of pathogens [reviewed by us here[32]] including respiratory viral and bacterial pathogens, results presented in this work also indicate that combining $OSCN^-$ with other drugs represents a potential therapeutic option for several additional infectious agents beyond IAVs.

This study focused on the combination of $OSCN^-$ with other antiviral drugs, although data in this manuscript also demonstrate that $OSCN^-$alone has beneficial effects against PR8 infection in mice. While mortality was not prevented by $OSCN^-$ alone, we also selected a relatively low dose of $OSCN^-$ (100 µl volume per oral gavage) for our experiments so that a potential synergistic effect by combining it with AMT could be observed. It remains to be determined whether $OSCN^-$alone, at doses higher than used here, can further improve the outcomes of lethal influenza A infection in mice.

While we have not performed an *in vivo* infection in mice with the AMT-resistant IAV strain A/WSN/1933 (H1N1), we expect that the $OSCN^-$+AMT combination treatment

would turn out to be less efficient than against the two viruses tested. In our view, this would be mainly due to the presence of only one, potentially efficient, antiviral drug, $OSCN^-$. Since the TCAD treatment further inhibited the *in vitro* proliferation of the A/WSN/1933 (H1N1) virus strain, we believe the TCAD treatment would further improve the outcomes of an *in vivo* infection beyond the double treatment.

Our results indicate that a combined anti-influenza regimen including AMT, $OSCN^-$, and OSL could represent an innovative therapeutic option for the treatment of severe outcomes of seasonal and pandemic influenza infections. We intentionally chose lethal doses of the influenza viruses tested *in vivo* because they represent an appropriate animal model for those, mainly immunocompromised, human patients who are hospitalized or even die following influenza infection worldwide. While influenza infections leading to death or admittance to the hospital make up only a minor portion of the total influenza cases, they represent the clinically most severe symptoms and need effective treatment options the most[299, 300, 301, 302]. Most of our outcomes in this study support the combined hypothesis, which declares that for any type of susceptible or resistant circulating influenza virus, at least two, and in some combinations all three, compounds in combined treatment will be effective. Moreover, the combined treatment seems to diminish drug resistance and hence could be a highly active antiviral therapy for seasonal and pandemic influenza. The pharmacokinetics, safety, hepatic metabolism, and plasma distribution of AMT and OSL as a monotherapy are well-acknowledged, and it is not predicted that co-administration of these compounds will cause harmful side effects to patients as compared to the administration of the single agent. Additionally, the AMT and OSL combination has been tested in humans without treatment complications [278].

In summary, we provide data for the successful use of the $OSCN^-$+AMT combination treatment to prevent lethal influenza A virus infection in mice. Future clinical trials would be needed to evaluate the efficacy and safety of the AMT and $OSCN^-$ combination against seasonal and pandemic influenza A virus strains.

Acknowledgments

We are thankful to UGA collaborators, Stephen Mark Tompkins, and Cheryl A. Jones for their help with viral propagation, assay establishment, and experimental troubleshooting.

Author contributions

NA and BR designed the experiments. NA conducted most of the experiments and performed data analysis. DS helped with performing mouse infection studies. TN performed histological analysis. NA wrote the original draft of the manuscript. NA, DS, TN, ZR, RAT, and BR revised and edited the manuscript. BR also performed data analysis. BR and RAT acquired funding and oversaw the project. All the authors read and approved the final version of the manuscript.

Figures and legends

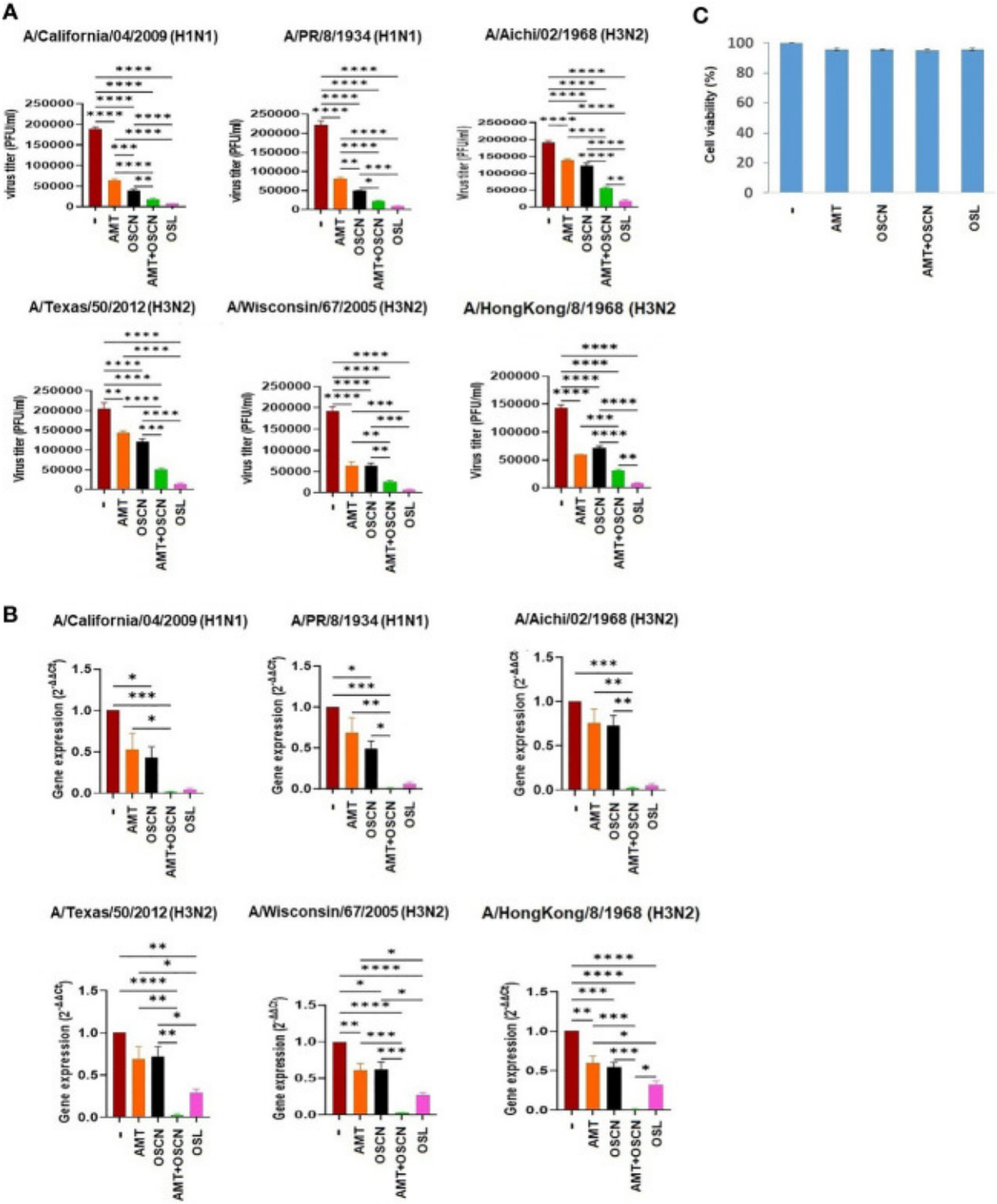

Figure 3.1 The AMT+OSCN$^-$ combination treatment significantly reduces the replication of several influenza A virus strains *in vitro*. (A) Confluent monolayers of MDCK cells were inoculated with 100 MOI of the indicated six H1N1 and H3N2 IAV strains individually. The overlay media were supplemented with the indicated antiviral compounds. Viral proliferation was measured by PFU assay. OSL phosphate was used as a control. Data are mean ± SEM of n = 6 (A/California/04/2009, A/PR/8/34, and A/Aichi/2/1968), n = 4 (A/Texas/50/12 and A/Hong Kong/8/68), and n = 5 (A/Wisconsin/67/2005) independent experiments. One-way ANOVA and Tukey's multiple comparisons tests. (B)Viral mRNA levels were measured under the exact same conditions and at the same time as in panel (A) by qRT-PCR for the indicated viral strains. All shown results were normalized and compared to housekeeping genes as control. OSL was used as a positive control. Mean ± SEM, n = 3. One-way ANOVA and Tukey's multiple comparisons test. (C) MDCK cells were exposed to the indicated treatment options without viral infection, and cell toxicity was measured by the MTT Cell Proliferation Kit (colorimetric assay). At 3 days after drug addition, the treatment was added at maximum dose: OSL at 5 μg/ml and AMT at 15 μg/ml. Untreated but infected cells were used as positive control for cell toxicity, while uninfected, untreated cells were used as negative control (n = 3). AMT, amantadine; MOI, the multiplicity of infection; OSCN$^-$, hypothiocyanite; OSL, oseltamivir; PFU, plaque-forming unit; MDCK, Madin–Darby canine kidney; IAV, influenza A virus. *, $p < 0.05$; **, $p < 0.01$; ***, $p < 0.001$; ****, $p < 0.0001$.

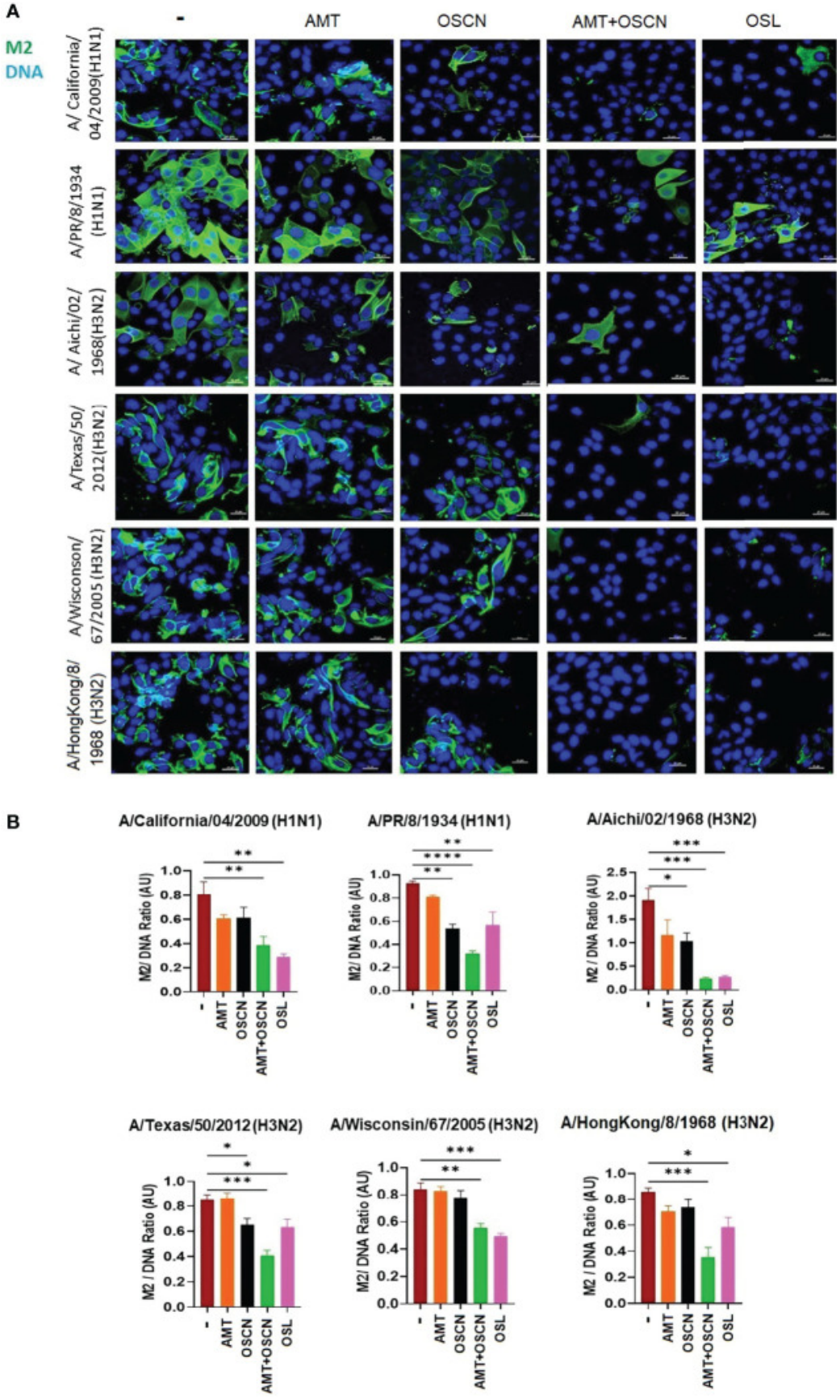
A
M2
DNA
-
AMT
OSCN
AMT+OSCN
OSL
A/ California/ 04/2009(H1N1)
A/PR/8/1934 (H1N1)
A/ Aichi/02/ 1968(H3N2)
A/Texas/50/ 2012(H3N2)
A/Wisconson/ 67/2005 (H3N2)
A/HongKong/8/ 1968 (H3N2)
B
A/California/04/2009 (H1N1)
A/PR/8/1934 (H1N1)
A/Aichi/02/1968 (H3N2)
A/Texas/50/2012 (H3N2)
A/Wisconsin/67/2005 (H3N2)
A/HongKong/8/1968 (H3N2)
M2/ DNA Ratio (AU)
AMT
OSCN
AMT+OSCN
OSL

Figure 3.2 The AMT+OSCN$^-$ combination treatment reduces influenza virus uptake into host cells. (A) MDCK cells were infected with 100 MOI of the indicated influenza A virus strains and incubated at 4°C for 1 h. Unbound virions were washed out, and MDCK cells were exposed to different treatment conditions for 1 h at 37°C as indicated. Cells were fixed, and the cellular localization of the viral M2 ion channel was detected by immunofluorescence at 3 hpi (green). Cellular DNA was labeled by DAPI (blue). OSL was used as a positive control. Merged images of the viral protein and DAPI-stained nuclei are shown. Images are representative of three independent experiments performed in duplicates (scale bars, 25 μm). The images were acquired at ×60 magnification using a confocal microscope. (B) Ratios of mean fluorescent intensities (MFI) of the M2 signal divided by the DAPI signal are shown (mean ± SEM). Ratios were measured for each strain using images from three independent experiments n = 3. One-way ANOVA and Tukey's multiple comparisons tests. AMT, amantadine; AU, arbitrary unit; MOI, the multiplicity of infection; M2, M2 ion channel; $OSCN^-$, hypothiocyanite; OSL, oseltamivir; MDCK, Madin–Darby canine kidney. *, $p < 0.05$; **, $p < 0.01$; ***, $p < 0.001$; ****, $p < 0.0001$.

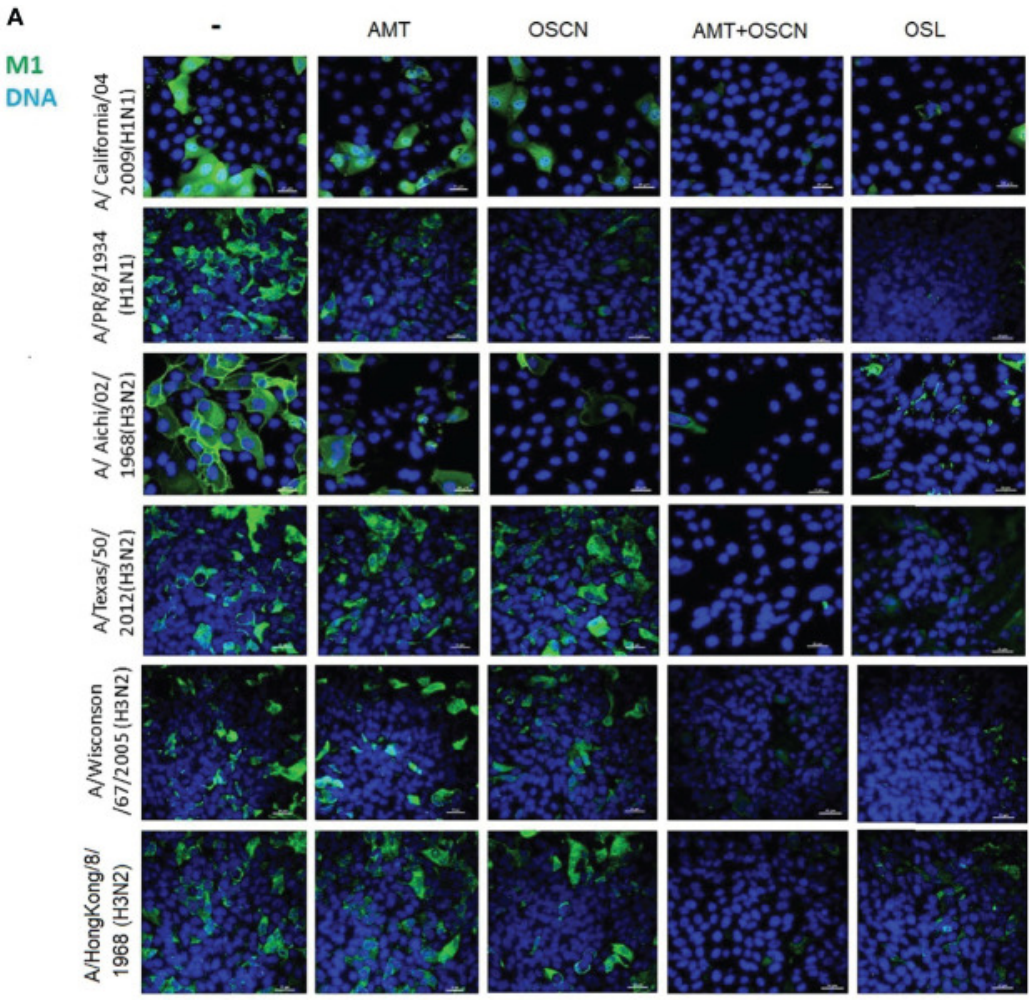
A
M1
DNA
-
AMT
OSCN
AMT+OSCN
OSL
A/ California/04 2009(H1N1)
A/PR/8/1934 (H1N1)
A/ Aichi/02/ 1968(H3N2)
A/Texas/50/ 2012(H3N2)
A/Wisconson /67/2005 (H3N2)
A/HongKong/8/ 1968 (H3N2)

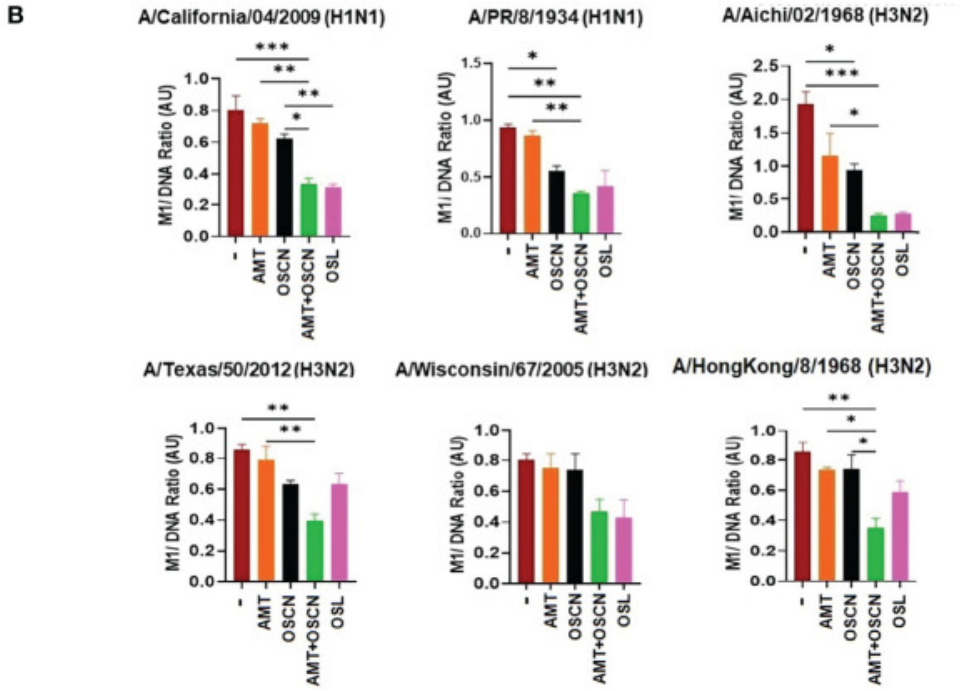
B
A/California/04/2009 (H1N1)
A/PR/8/1934 (H1N1)
A/Aichi/02/1968 (H3N2)
A/Texas/50/2012 (H3N2)
A/Wisconsin/67/2005 (H3N2)
A/HongKong/8/1968 (H3N2)
M1/ DNA Ratio (AU)
-
AMT
OSCN
AMT+OSCN
OSL

Figure 3.3 The AMT+OSCN$^-$ combination treatment reduces influenza virus uncoating in host cells. (A) MDCK cells were infected with 100 MOI of the indicated influenza A virus strains and incubated at 4°C for 1 h. Unbound virions were washed out, and MDCK cells were exposed to different treatment conditions for 1 h at 37°C, as indicated. Cells were fixed, and the cellular location of the viral M1 matrix protein was detected by immunofluorescence at 3 hpi (green). Cellular DNA was labeled by DAPI (blue). OSL was used as a positive control. Merged images of the M1 protein and DAPI-stained nuclei are shown. Images are representative of three independent experiments performed in duplicates (scale bars, 25 μm). The images were acquired at ×60 magnification using a confocal microscope. (B) Ratios of mean fluorescent intensities (MFI) of the M1 signal divided by the DAPI signal are shown (mean ± SEM). Ratios were measured for each strain using images from three independent experiments n = 3. One-way ANOVA and Tukey's multiple comparisons tests. AMT, amantadine; AU, arbitrary unit; M1, M1 matrix protein; MOI, the multiplicity of infection; OSCN$^-$, hypothiocyanite; OSL, oseltamivir; MDCK, Madin–Darby canine kidney. *, $p < 0.05$; **, $p < 0.01$; ***, $p < 0.001$.

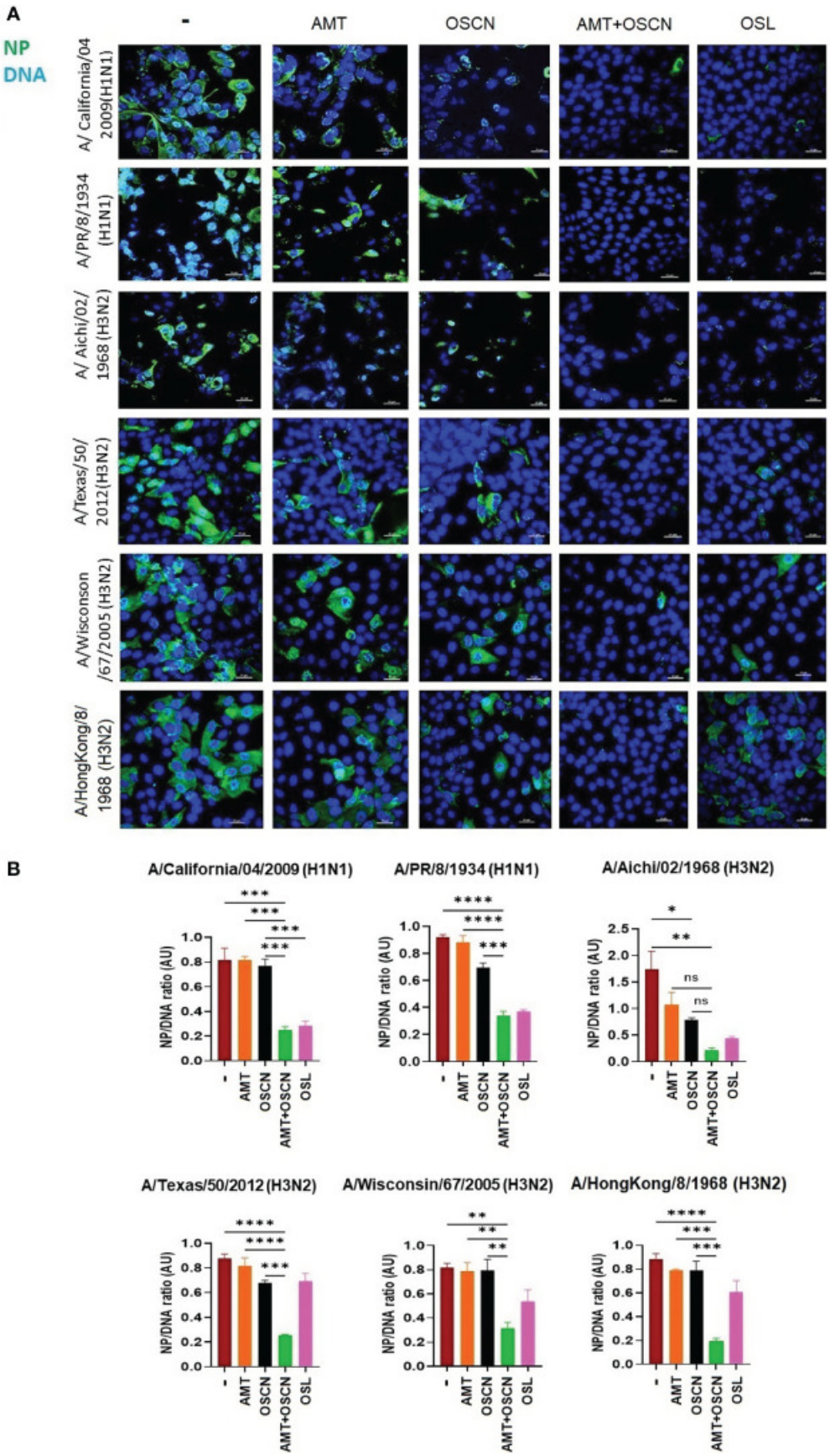
A
NP
DNA
-
AMT
OSCN
AMT+OSCN
OSL
A/ California/04 2009(H1N1)
A/PR/8/1934 (H1N1)
A/ Aichi/02/ 1968 (H3N2)
A/Texas/50/ 2012(H3N2)
A/Wisconson /67/2005 (H3N2)
A/HongKong/8/ 1968 (H3N2)
B
A/California/04/2009 (H1N1)
A/PR/8/1934 (H1N1)
A/Aichi/02/1968 (H3N2)
A/Texas/50/2012 (H3N2)
A/Wisconsin/67/2005 (H3N2)
A/HongKong/8/1968 (H3N2)
NP/DNA ratio (AU)
ns

Figure 3.4 The AMT+OSCN$^-$ combination treatment reduces nucleoprotein expression of influenza virus in host cells. (A) MDCK cells were infected with 100 MOI of the indicated influenza viral strains and incubated at 4°C for 1 h. Unbound virions were washed out, and MDCK cells were exposed to different treatment conditions for 1 h at 37°C as indicated. Cells were fixed, and the cellular location of the viral nucleoprotein (NP) was detected by immunofluorescence at 6 hpi (green). Cellular DNA was labeled by DAPI (blue). OSL was used as a positive control. Merged images of the viral protein and DAPI-stained nuclei are shown. Images are representative of three independent experiments performed in duplicates (scale bars, 25 μm). The images were acquired at ×60 magnification using a confocal microscope. **(B)** Ratios of mean fluorescent intensities (MFI) of the NP signal divided by the DAPI signal are shown (mean ± SEM). Ratios were measured for each strain using images from three independent experiments n = 3. One-way ANOVA and Tukey's multiple comparisons tests. AMT, amantadine; AU, arbitrary unit; MOI, multiplicity of infection; NP, nucleoprotein; OSCN$^-$, hypothiocyanite; OSL, oseltamivir; MDCK, Madin–Darby canine kidney. *, $p < 0.05$; **, $p < 0.01$; ***, $p < 0.001$; ****, $p < 0.0001$, ns, non-significant.

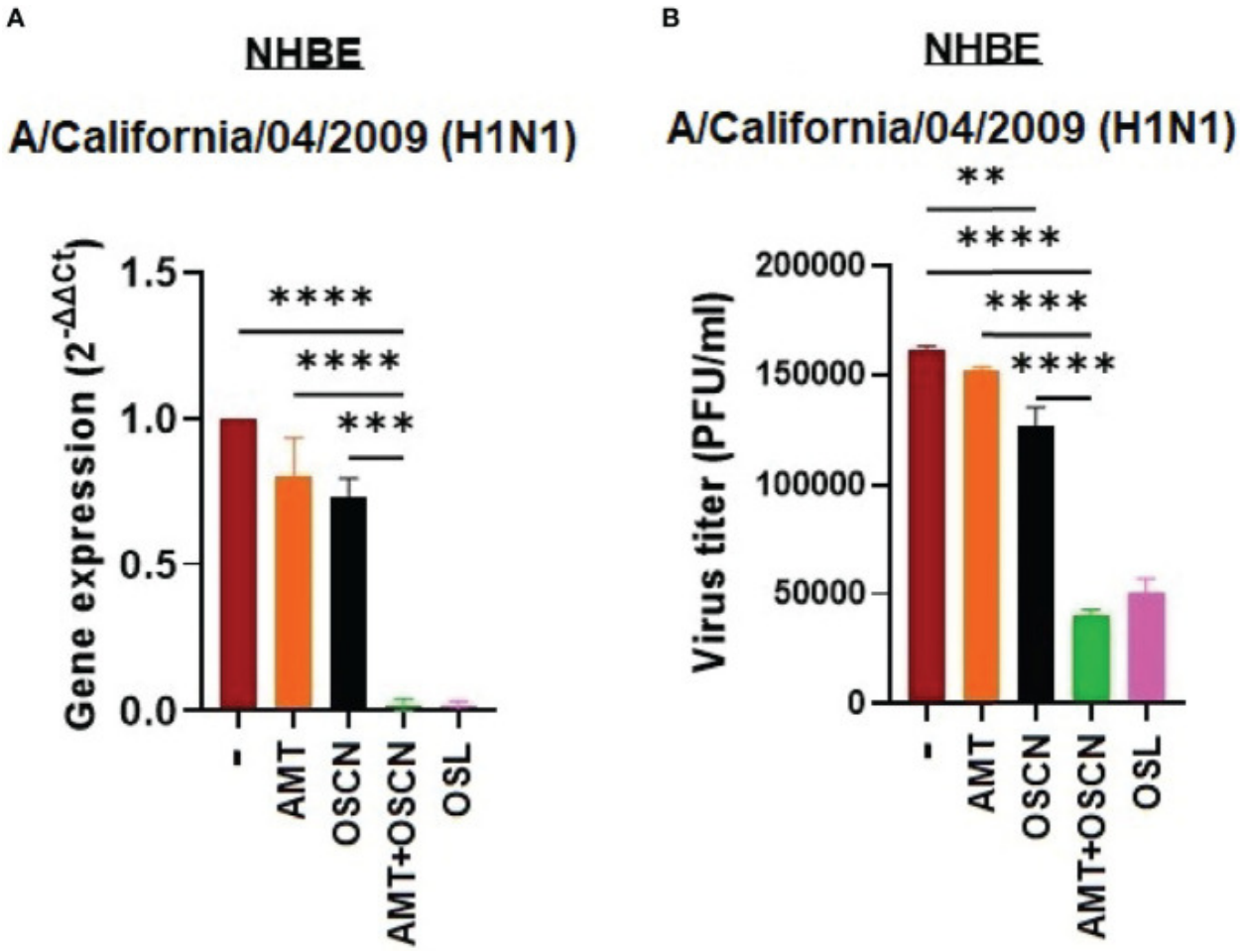

Figure 3.5 The AMT+OSCN$^-$ combination treatment restricts influenza virus replication in primary human bronchial epithelial cells. Primary normal human bronchial epithelial (NHBE) cells were infected with 100 MOI of the A/California/04/09 (H1N1) influenza A virus strain under the indicated conditions for 1 h. **(A)**mRNA expression was measured using real-time qPCR. β-Actin was used as a reference. OSL was used as a positive control. **(B)** Viral proliferation was assessed using PFU assay. Data are expressed as mean ± SEM of n = 3 independent experiments performed in triplicates. One-way ANOVA and Tukey's multiple comparisons tests. AMT, amantadine; MOI, the multiplicity of infection; NHBE, normal human tracheobronchial epithelial cells;

$OSCN^-$, hypothiocyanite; OSL, oseltamivir; PFU, plaque-forming unit. **, $p < 0.01$; ***, $p < 0.001$; ****, $p < 0.0001$.

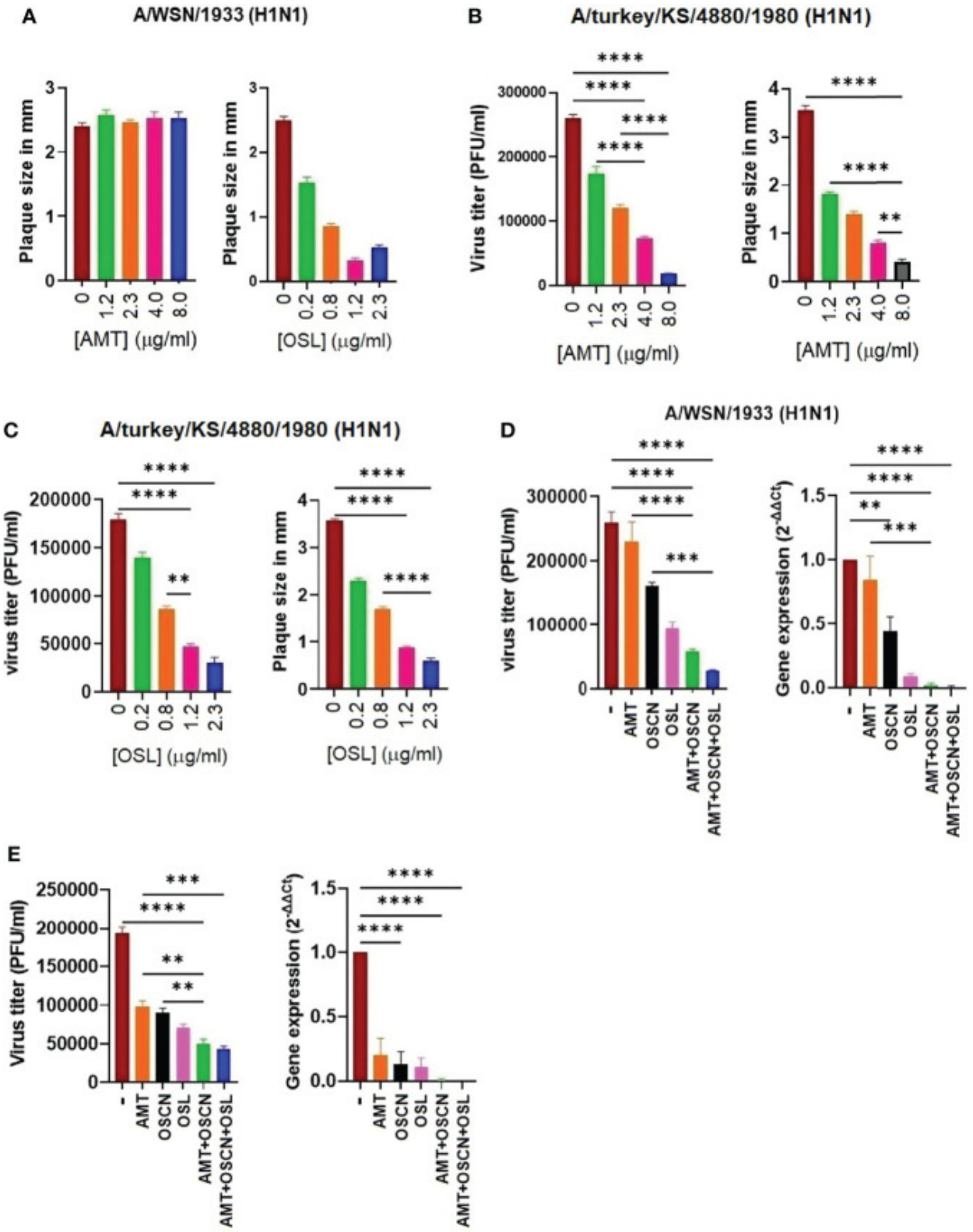
A
A/WSN/1933 (H1N1)
Plaque size in mm
[AMT] (μg/ml)
[OSL] (μg/ml)
B
A/turkey/KS/4880/1980 (H1N1)
Virus titer (PFU/ml)
C
virus titer (PFU/ml)
D
Gene expression ($2^{-\Delta\Delta Ct}$)
-
AMT
OSCN
OSL
AMT+OSCN
AMT+OSCN+OSL
E

Figure 3.6 A triple combination therapy including AMT, $OSCN^-$, and OSL, is superior to dual and single drug regimens against amantadine-sensitive and amantadine-resistant influenza A strains *in vitro*. Confluent MDCK cell monolayers in 6-well plates were infected with 100 MOI of the **(A)** A/turkey/Kansas/4880/1980 (H1N1) (AMT-susceptible strain) or **(B, C)** the A/WSN/1933 (H1N1) (AMT-resistant) IAV strains. Cells were incubated with overlay media containing the indicated antiviral drugs and their combinations. The plaque numbers or the average plaque sizes measured in diameter were determined at 3 dpi. Mean ± SEM, three independent experiments. The efficacy of the triple combination treatment consisting of $OSCN^-$, AMT, and OSL on viral replication (plaque assays) and viral gene expression (qPCR) is shown for **(D)** the A/WSN/1933 (H1N1) and **(E)** A/turkey/Kansas/4880/1980 (H1N1) IAV strains. [AMT] = 15 μg/ml, [OSL] = 5 μg/ml. β-Actin was used as a housekeeping gene. Data are presented from three individual experiments (n = 3). One-way ANOVA and Tukey's multiple comparisons tests. AMT, amantadine; IAV, influenza A virus; $OSCN^-$, hypothiocyanite; MOI, the multiplicity of infection; OSL, oseltamivir; PFU, plaque-forming unit; MDCK, Madin–Darby canine kidney. **, $p < 0.01$; ***, $p < 0.001$; ****, $p < 0.0001$.

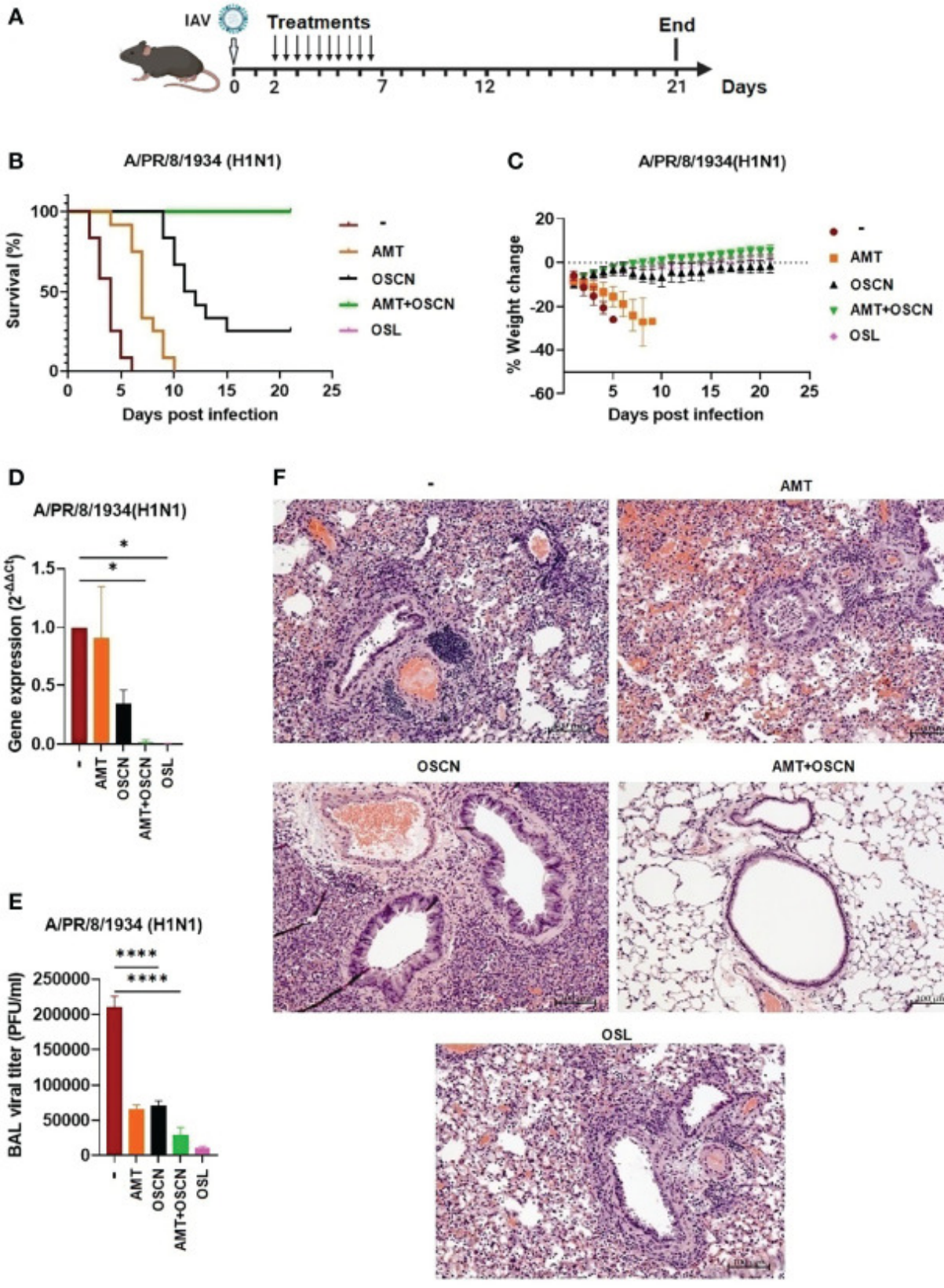
A
IAV
Treatments
End
0
2
7
12
21
Days
B
A/PR/8/1934 (H1N1)
Survival (%)
Days post infection
-
AMT
OSCN
AMT+OSCN
OSL
C
A/PR/8/1934(H1N1)
% Weight change
Days post infection
D
A/PR/8/1934(H1N1)
Gene expression (2-ΔΔCt)
E
A/PR/8/1934 (H1N1)
BAL viral titer (PFU/ml)
F
AMT
OSCN
AMT+OSCN
OSL

Figure 3.7 The AMT+OSCN$^-$ combination treatment cured mice from lethal H1N1 influenza A virus infection. C57BL/6 mice were infected intranasally with 150 PFU of A/PR/8/34 (H1N1). Mice were treated with the indicated antiviral drugs and their combinations for 5 days (2–7 dpi) by oral gavage (two doses daily). In the untreated "placebo" group, animals received the equivalent volume of distilled water. Animals were observed until 21 dpi. **(A)**Experimental scheme. **(B)** Mortality was measured and presented as Kaplan–Meier survival curves. **(C)** Weight changes are presented as percentages of the initial body weight of the animals (6 mice per group, two independent experiments). At 3 dpi, BAL from infected mice treated as indicated was collected, and BAL cells and cell-free supernatants were separated by centrifugation. **(D)** Viral gene expression in BAL cells was measured by qPCR and normalized on the values of the infected but untreated group. **(E)** Viral titers in cell-free BAL supernatants were determined by PFU assays. Data are expressed as mean ± SEM of n = 3 independent experiments that each used 3 animals per group. **(F)** Histopathological images of H&E-stained, fixed lung tissue sections of infected mice treated as indicated (3 dpi). Magnification, ×10; scale bars, 100 μm. AMT, amantadine; BALF, bronchoalveolar lavage fluid; OSCN$^-$, hypothiocyanite; OSL, oseltamivir; PFU, plaque-forming unit. *, $p < 0.05$; ****, $p < 0.0001$.

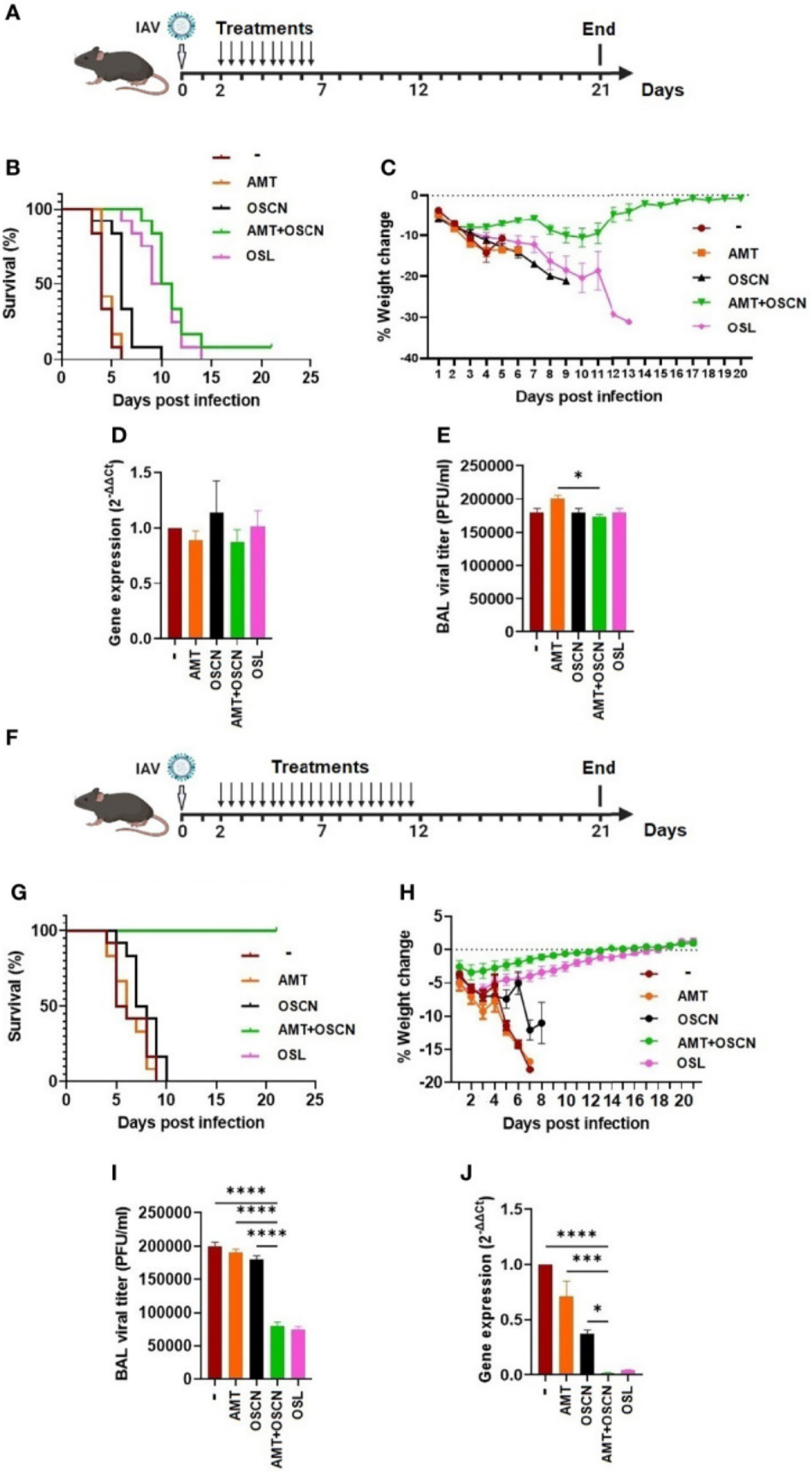
A
IAV
Treatments
End
0
2
7
12
21
Days
B
Survival (%)
Days post infection
-
AMT
OSCN
AMT+OSCN
OSL
C
% Weight change
Days post infection
D
Gene expression (2^-ΔΔCt)
E
BAL viral titer (PFU/ml)
*
F
G
H
I
****
J
***
*

Figure 3.8 The AMT+OSCN$^-$ combination treatment cured mice of lethal H3N2 influenza A virus challenge. (A–E) C57BL/6 mice were infected intranasally with 3,000 PFU of the A/Hong Kong/8/1968 (H3N2) IAV strain. Animals were treated with the indicated antiviral drugs and their combinations for 5 days (2–7 dpi) by oral gavage (two doses daily). In the untreated "placebo" group, animals received the equivalent volume of distilled water. Animals were observed until 21 dpi. **(A)** Experimental timeline for panels **(A–E)**. **(B)**Mortality was measured and presented as Kaplan–Meier survival curves, and **(C)** weight changes are presented as percentages of the initial body weight of the animals (6 mice per group, two independent experiments). At 3 dpi, BAL from infected mice treated as indicated was collected, and BAL cells and cell-free supernatants were separated by centrifugation. **(D)** Viral gene expression in BAL cells was measured by qPCR and normalized on the values of the infected but untreated group. **(E)** Viral titers in cell-free BAL supernatants were determined by PFU assays. Data are expressed as mean ± SEM of n = 3 independent experiments that each used 3 animals per group. **(F–J)** Similarly to panels A–E, C57BL/6 mice were infected intranasally with 3,000 PFU of A/HK/1968 (H3N2) IAV. Animals were, however, treated with the indicated antiviral drugs and their combinations for a longer period of time, 10 days (2–12 dpi), by oral gavage (two doses daily). In the untreated "placebo" group, animals received the equivalent volume of distilled water. Animals were observed until 21 dpi. **(F)** Experimental timeline for panels **(F–J)**. **(G)**Mortality, **(H)** weight changes, **(I)** BAL cell viral gene expression, and **(J)** BAL supernatant viral titers were determined as indicated previously. AMT, amantadine; BALF, bronchoalveolar lavage fluid; OSCN, hypothiocyanite; OSL, oseltamivir; PFU, plaque-forming unit. *, $p < 0.05$; ***, $p < 0.001$; ****, $p < 0.0001$.

CHAPTER 4

ORAL/INTRAVENOUS NEBULIZED THIOCYANATE DELIVERY RESCUES MICE FROM LETHAL INFLUENZA VIRUS INFECTIONS

Ashtiwi, Nuha. To be submitted to *Frontiers in immunology*.

ABSTRACT:

Aims: To determine and optimize SCN^- therapy against lethal flu infections.

Methods: C57BL/6J mice were infected intranasally with lethal doses of different flu and bacterial strains of IAV, IBV. Infected mice were treated orally, intravenously or nebulized with different doses of SCN^- repeatedly for different days. Weight changes and survivals were monitored up to two weeks. Mice were also euthanized at chosen endpoints to process their lungs for histopathology and lung viral titer determinations. Whether the therapeutic potential of SCN^- was influenced by Dual oxidase 1 (Duox1), an airway epithelial source of H_2O_2 driving $OSCN^-$ formation, mice lacking the *Duox1* gene were tested.

Results: A four-day oral administration of 400 μg/kg/day NaSCN between 2–7 days post-infection (dpi) significantly reduced mortality of lethal A/PR8/34 (IAV)- or B/Florida 04/06 (IBV)-infected WT mice by more than 90%. While oral administration preventing mortality started no later than 48 hours for IBV, the intravenous administration of 200 μg/kg/day started at one dpi for three days for lethal IBV and IAV. Nebulized SCN^- was given twice a day for five days and rescued all treated mice.

Post-treatment lung histopathology performed at 5 dpi revealed notable decrease in lung pathology in IAV-and IBV-infected mice. However, the therapeutic effect of oral SCN^- is independent of Duox1 as *Duox1*-deficient animals were also rescued by SCN^- to the same extent as WT mice.

Conclusion. The conventional recommended dose for oral SCN^- treatment in flu-infected mice is 400 μg/kg/day, twice daily for 5 days except for A/HK/68 (H3N2) is 10 days. The therapeutic outcome of the intravenous route provided the same therapeutic efficacy as

the oral route with less dosage, interval and duration. Nebulized SCN^- is shortest and fastest way to provide us with an effective therapeutic outcome. The first 48 hours of lethal influenza infection (symptom appearance) is the best therapeutic window for treatment. Additionally, lung pathology was drastically improved after SCN^- treatment.

Introduction

Influenza infection is an infectious disease of the respiratory system with a major burden on public health and challenges[303]. The disease is caused by influenza virus, a segmented, negative-sense RNA virus, that rapidly infects the respiratory epithelium of both humans and animals [304]. In human population for example, seasonal IAV and IBV infections cause more than 500,000 annual deaths with pandemic events occurring sporadically with wide-ranging impact[305]. The influenza morbidity and mortality rates are high in vulnerable patients such as immunocompromised patients and patients with comorbidities[306]. Mortality rates in the United States alone among [303] people with HIV/AIDS in the pre-HAART era were more than 200 times higher than the general population and fourfold greater among the elderly[307]. Many other factors contribute to the increased risk of influenza infection among healthy adults[306]. Health care professionals, individuals in close contact with animals such as birds and swine, obesity, the elderly, and pregnancy are associated with higher risk of influenza infection making the burden of human infection and disease caused by influenza viruses a continuing challenge requiring a combined effort of research, surveillance, and medicine[308]. Current prophylactic treatments and vaccinations are facing additional challenges associated with resistance and efficacy of the already accepted drugs and vaccines[308 309].

Our previous investigations have focused on the earliest stages of influenza virus infections. We have shown that Dual oxidase 1 (Duox1), a NADPH oxidase family member highly expressed in the apical membrane of the respiratory epithelium, promotes antiviral immunity in influenza A virus infection in mice[14]. These initial *in vivo* investigations have demonstrated that mice lacking the *Duox1* gene have enhanced morbidity and mortality upon IAV infection with impaired lung viral clearance suggesting that Duox1 is instrumental in the extracellular antimicrobial immunity against sublethal IAV infection. Duox1 generates hydrogen peroxide (H_2O_2) that is used by lactoperoxidase (LPO) for the conversion of thiocyanate (SCN^-) to the antimicrobial hypothiocyanite ($OSCN^-$)[36]. The respiratory epithelial lining is the first line of defense that encounters microbial invasion. Duox1 is expressed by the respiratory epithelial cells[310] and provides H_2O_2 for $OSCN^-$ generation, hence enhancing the innate immunity against influenza virus[178].

SCN^- itself is a natural compound presents in human body fluids and secretions such as saliva, plasma, serum, urine, gastric juice and milk[311]. SCN^- peroxidation to $OSCN^-$ is catalyzed by LPO[312]. Previously in human medicine, potassium thiocyanate had been used to treat hypertension and its complication[313]. In hypertension management, the suggested loading dose of potassium thiocyanate was 0.8 gram with daily 4-hourly interval for 3 doses. The maintenance dose was half of the loading dose (0.4 grams) daily[314].

In our previous study, $OSCN^-$ was combined with FDA-approved anti-influenza drugs such as Amantadine to combat lethal IAV infection[20]. In various bacterial infections including *Streptococcus pneumoniae* and *Pseudomonas aeruginosa*, SCN^- was able to inhibit bacterial growth[23, 194]. Due to the growing resistance against anti-influenza and

anti-bacterial agents, we investigated the therapeutic efficacy of SCN^- against different influenza astrains. Resistance against anti-influenza agents is increasing especially in vulnerable immunocompromised individuals and patients with co-morbidities[315, 316].

Since birth, the human body encounters several challenges from different microbial agents which enhances the innate and adaptive immune system maturation. Immune compromised patients who usually suffer from post infection complication administer high doses of oseltamivir for longer treatment duration[317]. Additionally, children who were treated with oseltamivir (Tamiflu) exhibited severe neurological and cutaneous complications[318]. Clinically, oseltamivir is not safe for influenza infection treatment underage of 12 months[319, 320]. Hence, a new anti-influenza agent is needed. SCN^- is crucial for forming HOSCN and SCN^-[180]. Several toxic complications might appear due to overdosing of SCN^-[321, 322].

Both influenza A virus (IAV) and influenza B virus (IBV) strains are inactivated *in vitro* by $OSCN^-$ generated by the combination of LPO, SCN^-, and H_2O_2 [178]. *In vitro*, H_2O_2 is derived from an enzymatic reaction between glucose and glucose oxidase in the cell-free system or from normal human broncho;epithelial cells (NHBE) cells, which express Duox1 [178]. We have also demonstrated that $OSCN^-$ in combination with Amantadine, an antiviral drug that disrupts the transmembrane domain of the M2 viral protein preventing infectious viral nucleic acid entry into the host cell, rescued lethal IAV infection in mice[20]. In previous studies, $OSCN^-$ was generated *in vitro* by combining glucose (G), glucose oxidase (GO), LPO, and SCN^- for the instant generation of $OSCN^-$, the final antimicrobial compound[20].

In the present study, we evaluated and optimized the therapeutic potential of SCN^- alone without the external addition of any of the compounds of the full system. We hypothesized that SCN^- given orally, intravenously, and nebulized will be absorbed and will reach the extracellular airways, where it will be combined with readily available compounds (H_2O_2 and LPO and even MPO) for the generation of the final antimicrobial compound $OSCN^-$ with more potency against IAV and IBV infection *in vivo*. Therefore, optimization of SCN^- dosing and regimen as well as route of administration is mandatory for a positive endpoint outcome. Moreover, knowing the loading and maintenance dose is required to maintain steady state concentration of SCN^- in the body and the adequate generation of $OSCN^-$. In this study, we determined the efficacy of SCN^- therapy against lethal IAV and IBV infections, the optimal dose of therapeutic SCN^-, the duration of treatment, and routes of SCN^- administration. We also assessed whether Duox1 plays any role in the therapeutic effects of SCN^- against lethal IAV and IBV.

2. Material and Methods.

All experimentations with mice were approved by the Institutional Animal Care and Use Committee (IACUC) of the University of Georgia (UGA; Protocol ID: AUP#: A2020 11-001-A15).

2.1. Viral Adaptation and Propagation

IBV. B/Florida/04/2006 was provided by Ralph Tripp at the University of Georgia. Stocks were initially authenticated by RNA sequencing and neutralization to confirm the strain as previously[323]. Briefly, the virus was passaged twice in Mardin-Darby Canine Kidney

(MDCK) cells (ATCC CCL-34) after propagation to 80% confluency in complete DMEM (Cat No: SH30126.01) i.e., containing 10% FBS (Cat No: FBS002). Cells were then washed with sterile 1X PBS (Cat No: 119-0690-101), replenished with DMEM containing penicillin-streptomycin (Cat No 400-109), and 4% BSA (Cat No 22114). MDCKs were then inoculated with B/Florida/04/2006 in the presence of TPCK-Trypsin (Cat No: T1426-250MG) and incubated for 3 days at 37ºC until CPE was observed as previously reported[323]. The supernatants were harvested and centrifuged at 4ºC to pellet the cellular debris and stored frozen at -80ºC.

IAV. A/Puerto Rico/8/1934 (H1N1; NR-3169, BEI Resources, managed by ATCC, Manassas VA, USA) was propagated in MDCK cells as previously[14, 20]. This virus was cultured in MDCK cells using the infection medium (DMEM/F12 supplemented with 1mM L-Glutamine and 1ug/ml of TPCK-trypsin as above. Viral particles were harvested 48 hours after and grown in the allantoic cavity of 9-to-10-day-old specific pathogen-free embryonated chicken eggs at 37ºC. Viral particles were harvested, ultracentrifuged to remove debris, and back-tittered on MDCKs to determine the concentration of viral particles in PFUs/ml as previously[14, 20].

2.2. Mouse infection. Male and female C57BL/6J mice (8-10 weeks old) were obtained from Jackson Laboratories (Bar Harbor, ME, USA). Male and female BALB/c mice were purchased from Jackson Laboratories as well. *Duox1 KO* and their controls (C57BL/6J) were bred in-house in the Coverdell Vivarium. The mice were given water and food ad libitum. In every experiment, an equal number of male and female mice were divided into

two groups (SCN-treated and Placebo-treated also referred to as treated and untreated). These two groups of mice were anesthetized using avertin (2,2,2-tribromoethanol; Sigma) and intranasally infected with lethal doses of the different strains of influenza A and B viruses used in this study: 150 plaque-forming units (PFU) of A/PR8/34 (H1N1), 3,000 PFUs of A/Hong Kong/1968 (H3N2), 30,000 PFUs of B/Florida/04/2006 or 10,000s PFU of B/Lee/1940. For both viruses, the inoculum dose per mouse was resuspended in 50µl sterile 1X PBS. Mice were treated orally or intravenously with different doses of SCN^- repeatedly for different days. SCN^- doses are as following 100, 200, 250, 300, 350, 400, 800, 1000 µg/kg/day. Treatment was administered orally from day 2 to day 5 post-infection, twelve hours of interval. The first dose of treatment was started at different time 48, 72, 94 and 120 hours. Intravenous treatment was given at the dose of 200 µg/kg/day, once a day for 3 days. Survival and weight changes were monitored for up to two weeks. Mice were also euthanized at chosen endpoints to process their lungs for histology, histopathological scoring, and lung viral titer determinations. Mice deficient in the gene *Dual oxidase 1* (*Duox1*), an airway epithelial source of H_2O_2 driving $OSCN^-$ formation were also tested.

Clinical assessment. All infected animals were weighed daily. Any mouse that exceeded 20% weight loss of its original weight or displayed severe clinical symptoms was euthanized. Mice were also scored based on clinical signs and euthanized if their clinical score reached 3 or higher. All procedures were performed in accordance with the UGA IACUC. A clinical sign-scoring system was used to determine the outcome of the infection. Lethargy (score 1), dyspnea (score 2), body weight loss between 15 and 20% of original

weight (score 1), and body weight loss more than 20% of the original weight (3) were determined. Mice that accumulated a clinical score of 3 were euthanized.

Determination of lung viral load post treatment. At least three mice per group were sacrificed on day 7 post-infection (the last day of SCN^- treatment). Lungs were harvested and transferred to gentle MACS tubes (Cat#130093237; Miltenyi Biotech, Westphalia, Germany) containing DMEM supplemented with PS. The gentle MACS™ is a benchtop mechanical dissociator that creates viable single-cell suspensions or homogenates. The lung tissues were homogenized in 2 ml DMEM without enzymes using the gentle MACS Dissociator with preset program for mouse lung tissues followed by centrifugation at 500g for 10 minutes at 4ºC. The supernatant was collected and frozen at -80ºC and plaqued at later days for PFU determination.

Histopathology. Mouse lungs after 5 days post-infection/treatment or uninfected were inflated with 1 ml of 10% neutral buffered formalin and harvested as previously[20, 32]. All collected mouse lungs were fixed overnight in neutral buffered formalin, they were processed, and sections were prepared by the Histology laboratory (Department of Pathology) of the College of Veterinary Medicine at the University of Georgia. Sections were either stained with H&E[178] or left unstained for further processing. H&E-stained histological sections were evaluated blindly by a board-certified veterinary pathologist. Peri bronchiolitis, perivasculitis, interstitial pneumonitis, and alveolitis were assessed in placebo-treated versus SCN^-- treated as previously[20, 32, 323, 324].

Statistics. The data are presented as mean ± SEM or mean ± SD, as indicated in the figure legends as appropriate. Statistical significance between experimental groups was determined with chi-Square, two-tailed Students' t-test, or Mann-Whitney U test as indicated. For each test, $p \leq 0.05$ was required for significance between variable tested.

Results

Oral SCN^- delivery rescued mice from lethal A/PR8 infection in mice. We have previously shown that oral administration of $OSCN^-$ improves the outcome of lethal flu infection[20] . Previous investigations have shown that SCN^- attenuated atherosclerotic plaque formation and improved endothelial regeneration in mice and oral pretreatment with SCN^- protected against myocardial ischemia-reperfusion injury in rats, supporting an anti-inflammatory role of SCN^- *in vivo*[152]. In the present study, we show in Figures 1A and B that oral administration of SCN^- rescues lethal influenza at the dose of 400 μg/kg/day. Lower amount of SCN^- only improved the duration of survival compared to Placebo but none of these lower doses of SCN^- rescued mice from lethal flu infection. Higher doses (800 μg/kg/day and 1000 μg/kg/day) show some signs of discomfort in infected-treated animals (mouse raffle hair). Weight monitoring showed that mice receiving the 400 μg/kg/day had optimal weight change over the course of 14 dpi. Untreated mice died all by 7 dpi. This data indicates that mice orally treated with SCN^- at the dose of 200 μg/kg/12 hours for 5 consecutive days survived lethal IAV (PR8) infection. It is important to note that treatment started 48 hours post infection. Overall, these results suggest that the SCN^- therapy leads to significant improvements in outcomes of lethal IAV infection in mice.

Oral SCN^- delivery rescued mice from lethal IBV (B/Florida/04/06) infection in mice. To further assess whether this improved effect of SCN^- in lethal IAV is also effective with lethal IBV, we infected C57BL/6J mice with lethal IBV (B/Florida/04/06) at the dose of 30,000 PFU/mouse (predetermined lethal dose). Several doses of SCN^- from 200 µg/kg/day to 400 µg/kg/day were also tested. Placebo-treated mice and SCN^--treated animals at doses between 200 and 350 µg/kg/day died all by 7 dpi. Only SCN^- treated mice with the dose of 400 µg/kg/day efficiently rescued mice from lethal IBV infection (Figure 2A). Weight monitoring also showed that only SCN^-- treated mice with the dose of 400 µg/kg/day regained weight. The other groups of SCN^- treated or Placebo treated animals were either found dead the next day or reached endpoints that required euthanasia (Figure 2B). Overall, this data indicates that oral SCN^- therapy also rescues mice from lethal IBV infection suggesting that the effectiveness of SCN^- therapy during lethal influenza infection is not restricted to a viral strain.

Oral SCN^- therapy at the dose of 400 µg/kg/day rescued IAV and IBV only if treatment started 48hours post infection.

To assess the timing at which SCN^- therapy is effective at saving mice from lethal IAV and IBV, several groups of mice were infected at day 0, and SCN^- therapy started either at 48hrs, 72hrs, 96hrs, and 120hrs post-infection. Only mice in which treatment was started at 48hrs were fully rescued from lethal IAV (A/PR8/34) (Figure 3A and 3B) and IBV (B/Florida/o4/06) (Figure 3C and 3D). While 40% of SCN^-- treated mice were rescued from lethal IAV (A/PR8/34), none of the IBV (B/Florida/04/06) infected and SCN^- treated was rescued when treatment started later than 48hours (Figure 3C). Likewise, none of

the IAV infected animals with therapy starting at 96hours survived the lethal flu infection (Figure 3A). Overall, this data indicates that efficient oral SCN^- therapy requires starting treatment within 48 hours post-infection. Treatment starting later during lethal infection fails to rescue mice from deadly flu infection.

Oral SCN^- therapy at the dose of 400 µg/kg/day rescued IBV when treatment is applied for a minimum of 4 consecutive days.

To further assess the lengthiness of oral SCN^-- delivery required for efficient treatment against lethal infection, we infected mice with lethal B/Florida/04/06 (IBV) and divided the mice into 5 groups. One group of mice was treated with oral SCN^- for two consecutive days starting at 48 hours post-infection. A second group received treatment starting at 48 hours for three consecutive days. A third group received treatment for four days starting at 48 hours post-infection. A fourth group consecutively received treatment for five days starting at 48 hours post-infection. It is important to indicate that both groups received the same treatment dose of 400 µg/kg/day. Our results only done with IBV (B/Florida/04/06) indicate that a full four-day treatment was required for total rescue of all lethally infected animals (Figure 4A and 4B). While 2 and 3 full consecutive days of treatment showed some improvements compared to Placebo-treated mice, these treatment regiments were unable to rescue mice from lethal IBV (B/Florida/04/06) suggesting that a minimum four-day treatment is required for total rescue of mice from lethal infection.

\

Intravenous SCN^- therapy at the dose of 200 µg/kg/day rescued lethal flu infection.

A medication administration route is often classified by the location at which the drug is

applied, such as oral intravenous, or intranasal (nebulized or aerosolized). The choice depends on not only convenience but also on the drug properties and pharmacokinetics. We have tested whether the intravenous delivery of SCN^- has the potential to rescue lethal IAV and IBV like the oral delivery route. To address this, we infected both male and female C57BL/6J mice with lethal A/PR8/34 and lethal B/Florida/04/06 and divided mice into two groups for each flu virus. One group received intravenous SCN^- at the concentration of 200 μg/kg/day once a day for three consecutive days and another group received the placebo. Mice were monitored for 14 days as above. In both cases, intravenous SCN^- at the indicated dose for three days starting at 24 hours post-infection rescued mice from lethal IAV (A/PR8/34) (Figure 5A and 5B) and from lethal IBV (B/Florida/06/04) (Figure 5C and D). In both scenarios, all placebo treated animals succumbed to lethal infection by 7 dpi supporting the conclusion that SCN^- treatment saved the animals. This data indicates that direct administration of SCN^- to the systemic circulation has the advantages of rapid onset of action, predictable way of action with almost complete bioavailability, the potential problems of oral administration are eliminated by avoiding the gastrointestinal tract, and potentially the best way of administration in very ill and lethargic conditions even though this was not tested in the present study.

Oral SCN^- therapy significantly reduced lung parenchymal and bronchiolar area pathology as well as lung viral load.

To further assess the effect of oral SCN^- treatment on lung histopathology, the lungs of IAV- and IBV-infected untreated and SCN^-- treated mice were harvested at 5 dpi after

formalin infiltration via the trachea as previously[20, 178, 323]. Control uninfected but PBS-exposed (intranasal) mouse lungs were included in this experiment (Figure 6A-D). Lethal flu-infected and untreated lungs (Figure 6A- D) developed severe disease characterized by bronchiolitis, alveolitis, vasculitis, and inflammation, while flu-infected SCN^- treated animals showed significantly reduced lung parenchyma, less bronchiolar destruction, less cellular infiltration, and less secretions in their intraluminal space. The lung histological features of SCN^- treated animals look more like the lung features of PBS-exposed uninfected animals irrespective to the flu virus used (Figure 6A-D). In addition, compared to infected untreated animals, the total lung viral titers were significantly lower in SCN^- treated animals at 5 dpi further confirming the beneficial effect of SCN^- therapy in lethally infected mice (Figure 6E and F). Overall, this data indicates that SCN^- therapy diminishes viral replication and lung pathology in mice lethally infected with IAV and IBV suggesting that SCN^- treatment dampens the immune response and inactivates, reduces or eliminates viral replication in the lung micro-environment.

Therapeutic SCN^- is independent of Duox1.

We have shown previously that Duox1, a NADPH oxidase family member highly expressed in the apical membrane of the respiratory epithelium, promotes antiviral immunity in IAV infection in mice [178]. These initial *in vivo* investigations have demonstrated that mice lacking the *Duox1* gene have enhanced morbidity and mortality upon IAV infection with impaired lung viral clearance, suggesting that Duox1 is instrumental in the extracellular antimicrobial immunity against influenza virus. Because Duox1 generates H_2O_2 used by LPO to oxidize SCN^- into $OSCN^-$ [36], we tested whether the anti-viral effects

of SCN^- *in vivo* is dependent on Duox1. Therefore, we infected *Duox1 KO* and control C57BL/6J with lethal IAV (PR8) and treated them with SCN^-, $OSCN^-$ as previously[20] or gave them water only (placebo). In addition to A/PR8/34, several other viruses were tested including A/Hong Kong/8/1968 H3N2 (IAV) and another influenza B (B/Lee/1940) (IBV). In both cases mice infected with lethal doses of these viruses died by 7 dpi (Figure 7A and B). Overall, this data indicates that the therapeutic effects of SCN^- on lethal flu infection is independent of Duox1 when SCN^- is delivered orally. Additionally, SCN^- and $OSCN^-$ oral admiinistration provided the same therapeutic efficacy in both DUOX1-deficient mice and wild type mice.

Nebulized SCN^- treatment at the dose of 400 µg/kg/day rescued mice from lethal IBV infection.

Nebulized medications are the drug of choice in acute respiratory infections[325, 326]. The oral route is not preferred in patients with critical conditions and nebulized treatment is the fastest way to deliver the medication locally in the respiratory infections[327]. To explore this, both male and female C57BL/6J mice were infected with lethal B/Florida/04/06. One group administered Nebulized SCN^- at the concentration of 400 µg/kg/day twice a day for five consecutive days and another group administered the Placebo. Mice were followed up for 14 days as above. In both groups, Nebulized SCN^- at the indicated dose for five days starting at 48 hours post-infection rescued mice from lethal IBV (B/Florida/06/04) (Figure 8A and B). All animals who received placebo died by 7 dpi indicating Nebulized SCN^- treatment saved all treated group from mortality. This observation shows that Nebulized SCN^- is the fastest effective treatment of lethal

influenza infection. Nebulization is the most effective treatment method to apply locally on the infected and inflamed respiratory epithelial cells. Further studies should explore the overdosing effects of Nebulized SCN^-.

Discussion

The burden of human influenza infection and disease caused by IAV and IBV is a continuing global challenge which must be met with a combined effort of research, surveillance, and medicine[328]. Numerous factors can lead to susceptibility to infection by healthy adults and children—many of whom can prevent virus transmission by effective treatment and/or vaccination. As research continues, more groups of individuals at high risk of influenza-related disease are being identified, vaccines are not universal, and the drugs used are not as efficient as we expect. We must continue the search for alternatives to the present drugs available in the market.

LPO uses Duox1-derived H_2O_2 to convert SCN^- to the antimicrobial $OSCN^-$[36]. $OSCN^-$ has therapeutic potential during influenza virus infection[20]. In the present study, we tested the therapeutic potentials of SCN^- and optimized its dose and route of administration, and assessed whether SCN^- has a broad spectrum on influenza virus strains. We also assessed the effects of SCN^- administration on inflammation and lung tissue damage during lethal IAV and IBV infection.

SCN^- has been used in human studies to treat hypertension early in the 20th century[262, 263, 264]. Nebulized SCN^- improves the clearance of *P. aeruginosa* in the murine lung[23]. However, SCN^- is a substrate for LPO and other mammalian peroxidases

including myeloperoxidase (MPO)[21]. In fact, MPO prioritizes SCN^- over Cl^- as a substrate and therefore diminishes HOCl formation by PMNs[21]. In addition, SCN^- also degrades MPO-generated HOCl by forming HOSCN[21]. These reactions represent the main mechanisms by which SCN^- decreases HOCl formation. Therefore, supplemental amounts of SCN^- administration will reduce inflammatory tissue damage caused by excess formation of HOCl, an oxidant much more harmful to mammalian cells than HOSCN. The protective effect of SCN^- on HOCl-mediated cell damage was already established *in vitro,* and HOSCN accumulation in PMNs is nontoxic[167, 329, 330].

We have demonstrated that therapeutic SCN^- administrated orally at 400 μg/kg/day rescues mice from lethal IAV and IBV infection in mice (Figure 1 & 2). We have also demonstrated that oral SCN^- administration must be administered 48 hours post-infection to save mice from lethal infection (Figure 3). Administration of the compound after 48 hours cannot successfully rescue mice from lethal flu irrespective of the virus used. Our data also shows that a treatment duration of 4 days minimum is required for effective SCN^- treatment (Figure 4). Intravenous administration of SCN^-, which delivers the drug in the systemic circulation, is also effective at rescuing mice from IAV and IBV lethal infections. However, a lower dose of treatment (200 μg/kg/day) once a day for only three days was enough to overcome deaths from lethal IAV and IBV infections (Figure 5). To further demonstrate the therapeutic and anti-inflammatory effects of SCN^-, we tested the potential effects of SCN^- on viral load/clearance as well as its effects on lung pathology. On both cases, SCN^- demonstrated an inhibitory effect on viral replication with significantly lower viral particles in SCN^- treated animals versus untreated or placebo treated mice (Figure 6A-D). Likewise, the anti-inflammatory effect of SCN^- was evident

with only sporadic, perivascular, and peribronchiolar infiltrates containing some mononuclear cells in the lung of 200μg/kg SCN^-- treated mice (data not shown) while there were no histological lesions or abnormalities in the lung (Figure 6), liver or kidney of 400 μg/kg SCN^- treated animals at 14 dpi (data not shown). These results suggest that SCN^- treatment of lethal influenza infection irrespective of the viral strains prevents mortality, lung immune-pathology and viral proliferation. Using the nebulized SCN^- was the safest and fastest way to save the lethally infected mice (Figure 7A and B). Our results demonstrate that oral or systemic delivery of SCN^- alone could represent an innovative therapeutic option for treating severe outcomes of seasonal and pandemic influenza infection. We chose the lethal doses of IAV and IBV as previously[20] because lethal infections represent a model for vulnerable individuals, mainly the immunocompromised who are hospitalized for severe influenza infection and have the highest risk of dying from severe flu A or B infection worldwide.

Limitations: Despite the positive effects demonstrated using either oral or systemic delivery of SCN^-, some aspects of our experimental approach were not addressed in this study and will be addressed in future studies. First, we don't know the role played by other peroxidases, such as MPO. Using MPO-deficient mice will help us address the possible implications of MPO in the therapeutic feature of SCN^-. Second, the timing of systemic delivery of SCN^- was not addressed in detail, and the helpful nature of systemic delivery of the drug in severely ill mice was also not addressed. Future investigations will assess whether lethargic/moribund mice upon lethal influenza infection can still be saved by systemic SCN^- delivery. In addition, a more detailed toxicity study of

SCN^- therapy in mice will also need to be addressed. We will need to explicitly identify the concentrations at which SCN^- therapy induces tissue damage in the infected animals' lung, liver, kidneys, spleen or other organs. These studies will be performed without influenza infections. Third, whether SCN^- significantly decreases BAL pro-inflammatory cytokines and chemokines is unknown. Finally, assessing other delivery methods such as aerosolized or nebulized delivery would also help expand the most convenient routes of delivery of the drug since influenza are primarily acute respiratory infections. Also, the study has not quantified the concentration of LPO, SCN^-, and $OSCN^-$ in uninfected (treated or not), and flu-infected SCN^- treated or placebo-treated. It would be informative and helpful to know the concentration of these compounds in the systemic circulation and in the bronchoalveolar lavage fluid when assessing the mechanisms by which SCN^- treatment rescues mice from lethal influenza infection.

Overall, we provide data for the successful use of SCN^- regimens for the prevention of lethal influenza A and B infections in animal mouse models of influenza. Future investigations will focus on the mechanisms by which SCN^- delivery is so powerful at clearing the virus, dampening the cellular inflammatory response associate with lethal infections, and how it helps overcome lung tissue damage associated with infections.

Figures and legends

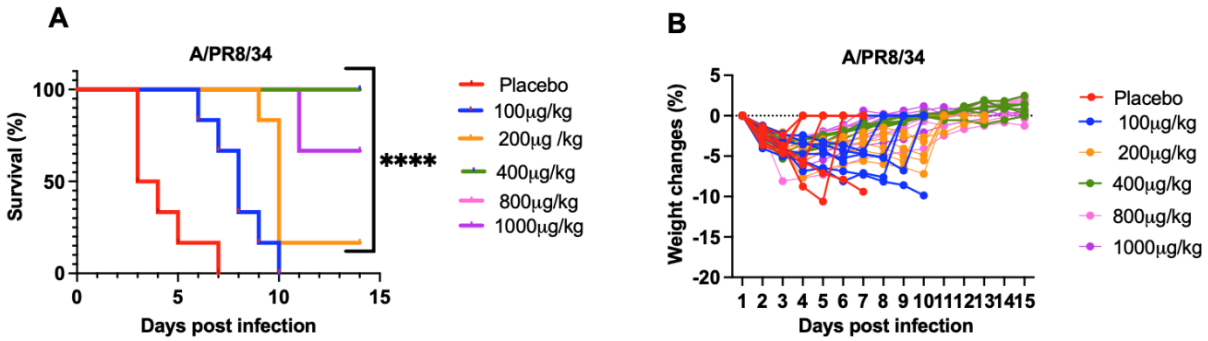

Figure 4.1: Oral administration of different doses ranging 100- 1000 µg/kg/day of SCN^- treatment cured mice from lethal H1N1 influenza A virus infection. C57BL/6 mice were infected intranasally with 150 PFU of A/PR/8/34 (H1N1). Mice were treated orally with SCN^- for 5 days (2-7 dpi) by oral gavage (each 12 hours). In the untreated ‘’placebo’’ group, animals received the equivalent distilled water. Mice were followed up until 14 dpi. **(A)** Mortality was measured and presented as Kaplan-Meier survival curves. 200,400,800 and 1000 µg/kg/day rescued mice from lethal A/PR8/34 infection **(B)** Weight changes are presented as percentages of the initial body weight of the animals (6 mice per group, two independent experiments).

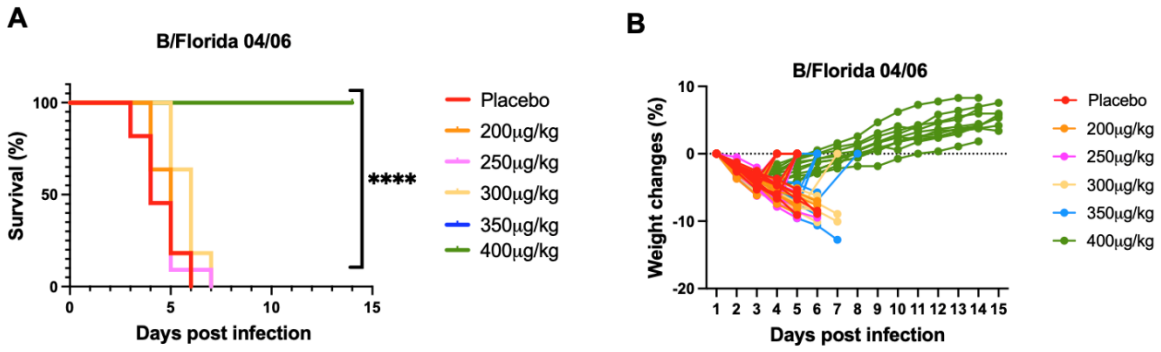

Figure 4.2: Oral administration of SCN^- 400 μg/kg/day 2-7 dpi rescued mice from mortality after lethal B/Florida/04/06 infection. **(A)** Mortality was measured and presented as Kaplan-Meier survival curves. Oral 400 μg/kg/day rescued mice from lethal B/Florida/04/06 infection. **(B)** Only mice who were treated with 400 μg/kg/day were able to maintain their weight changes positively compared to other treatment groups. (6 mice per each group) (Two independent experiments).

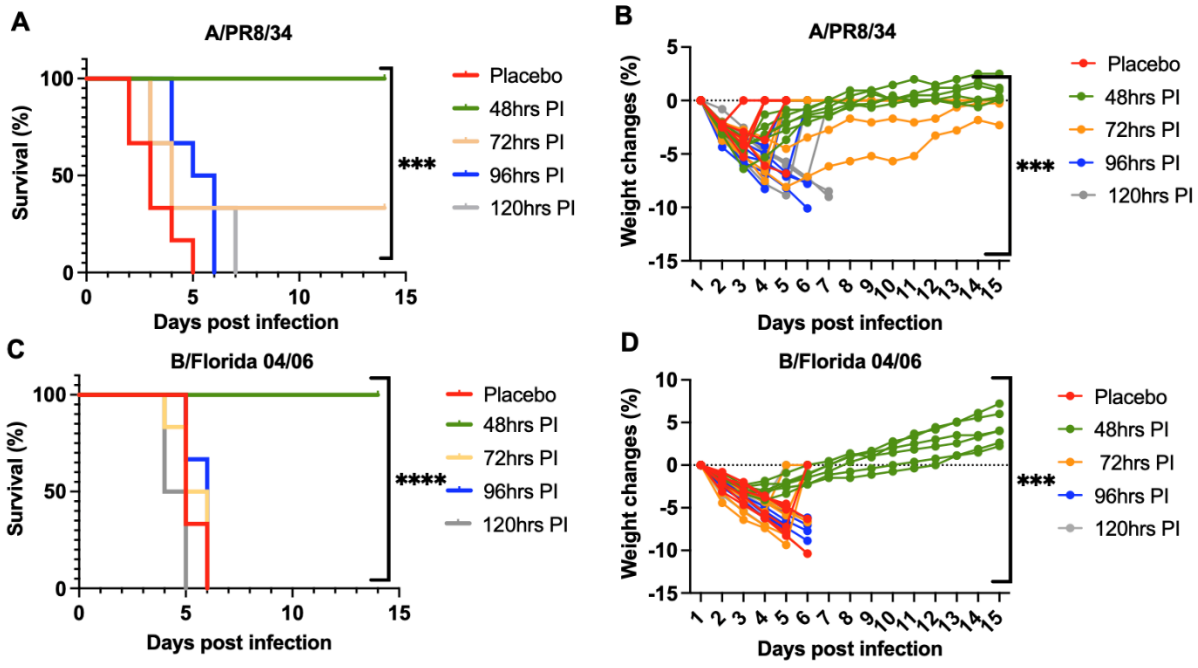

Figure 4.3: Oral SCN^- treatment was started different days post infection (48hrs, 72hrs, 96hrs and 120hrs post infection. **(A)** All mice were rescued when treatment started 48 hours after the lethal A/PR8/34 infection. **(B)** mice treated after 48 hours were more able to maintain their weight positively than the other groups. (6 mice per each group) (2 independent experiments). **(C and D)** Mice were infected with a lethal dose of B/ Florida/04/06, treated as previously stated in this figure.

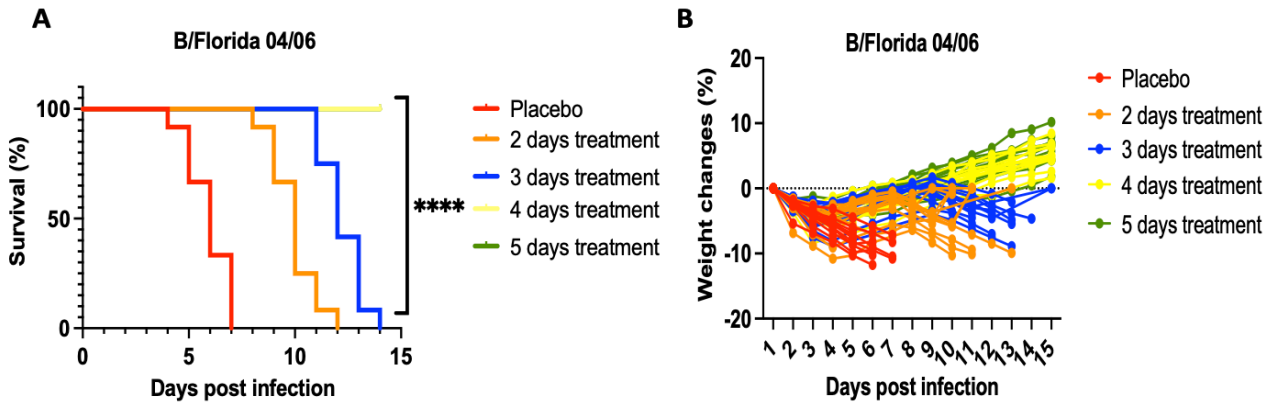

Figure 4.4: All Oral SCN^- treatment was continued for 2, 3, 4, 5 days after mice were infected with lethal dose of B/Florida 04/2006. (A) All mice were rescued when treatment continued for 4 to 5 days after lethal B/Florida infection. (B) Mice treated with 4 to 5 days regimen were more able to maintain their weight positively compared to the 2 and 3 treatment duration groups. (6 mice per each group) (2 independent experiments).

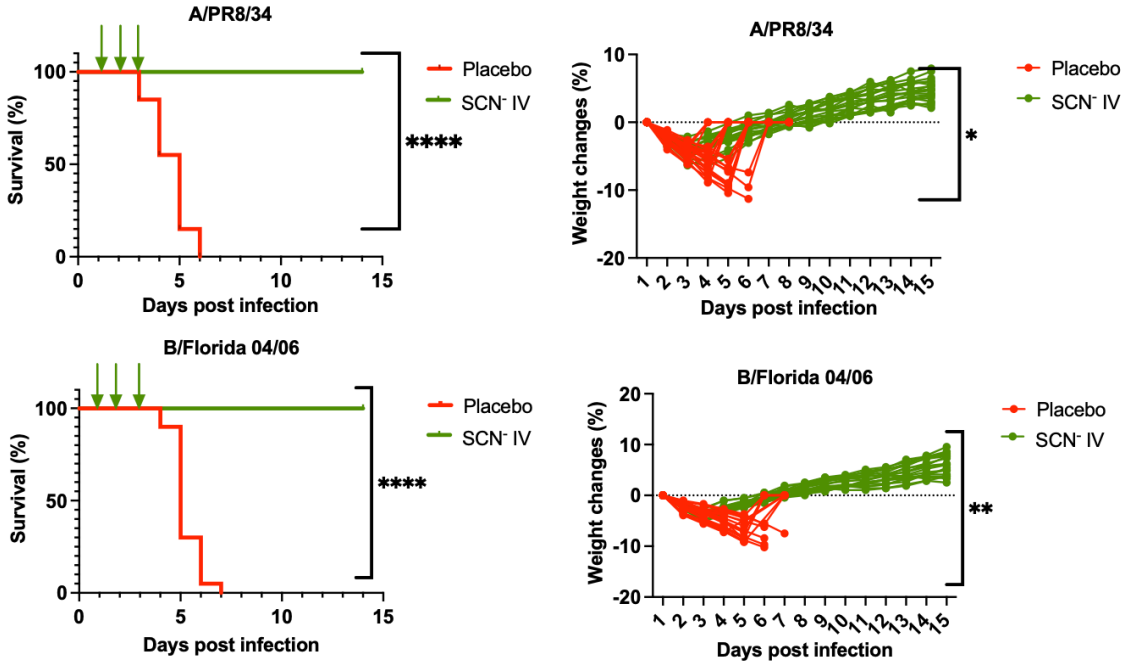

Figure 4.5: Intravenous administration of 200 µg/kg/day SCN^- (1-3 dpi) prevents mortality in C57BL/6J mice infected with lethal doses of A/PR8/34 (A and B), B/Florida 04/06 (C and D).

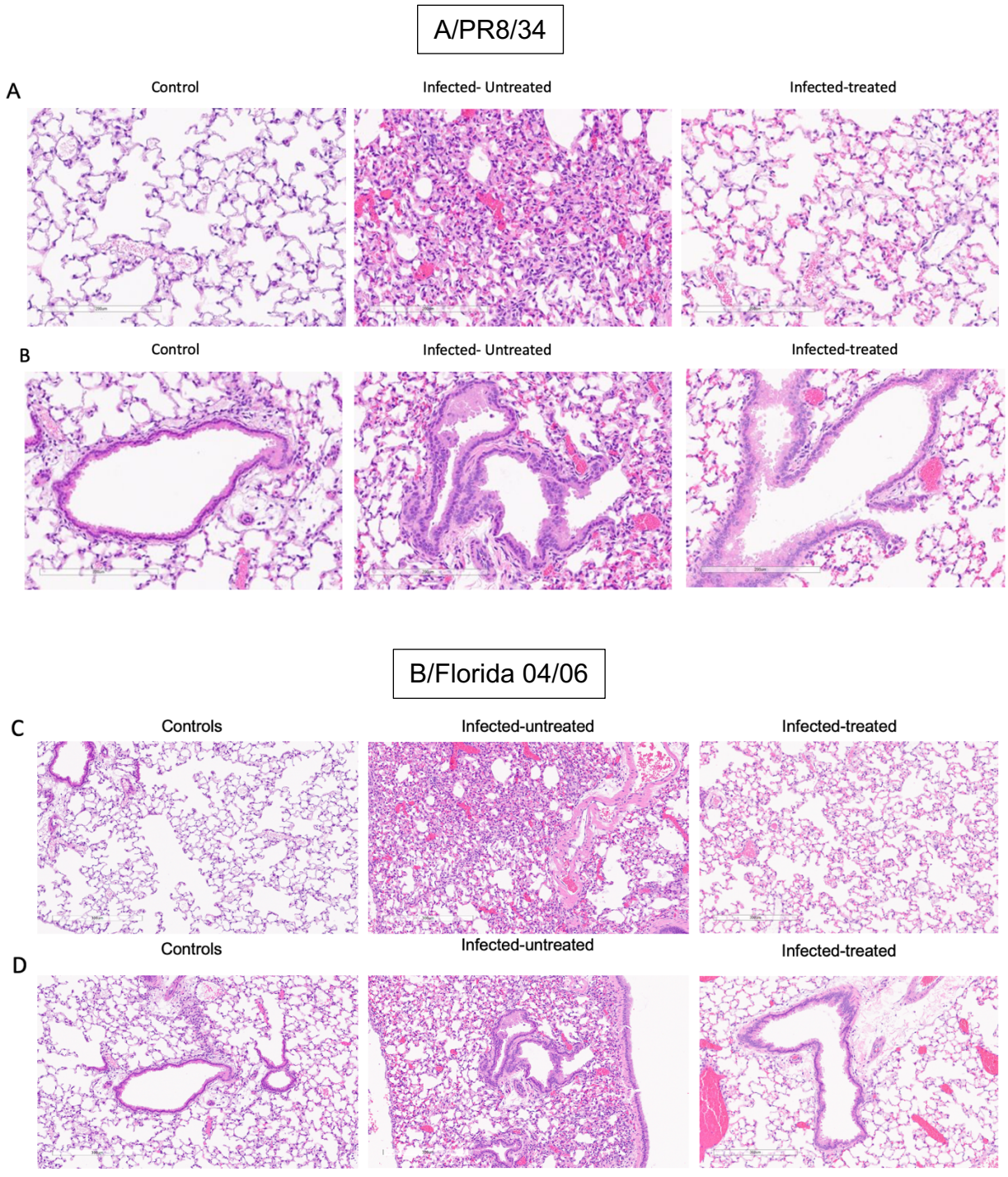
A/PR8/34
A
Control
Infected- Untreated
Infected-treated
B
Control
Infected- Untreated
Infected-treated
B/Florida 04/06
C
Controls
Infected-untreated
Infected-treated
D
Controls
Infected-untreated
Infected-treated

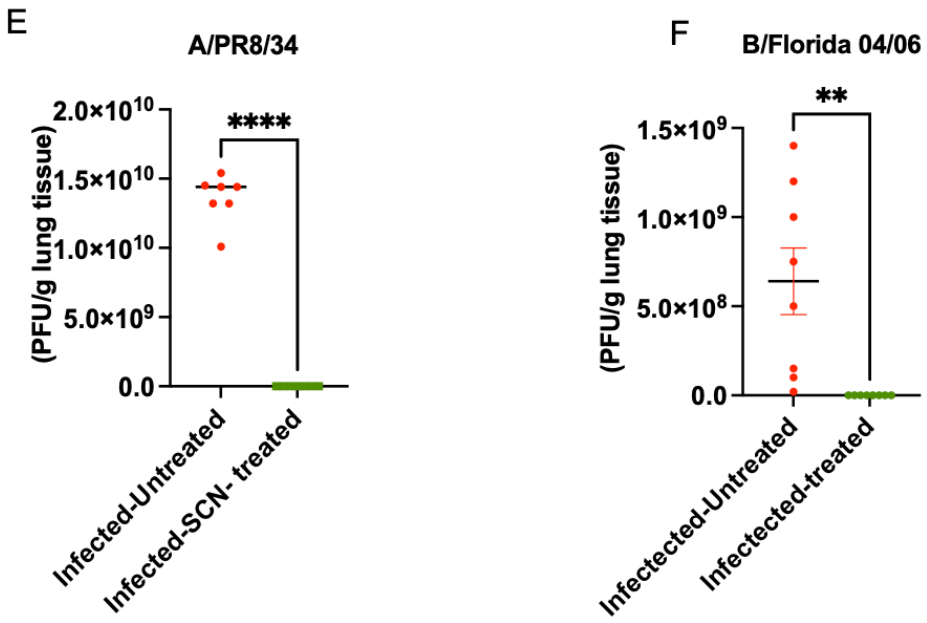

Figure 4.6: Lung histology performed at 5 dpi demonstrates robust lung pathology in A/PR8/34 and B/Florida- infected mice that were mainly prevented by oral SCN^- treatment (400 µg/kg/day, 2-7 dpi). (A and C) Show less hemorrhage, cellular infiltration, and bleeding in the parenchymal areas. (B and D) Treated bronchiolar area shows less bronchiolar destruction, cellular infiltration and less secretion in the intra-luminal space compared to the control and infected area. (E and F) Plaque forming units PFU titer shows that treated mice had less viral load in their lung homogenate than untreated ones.

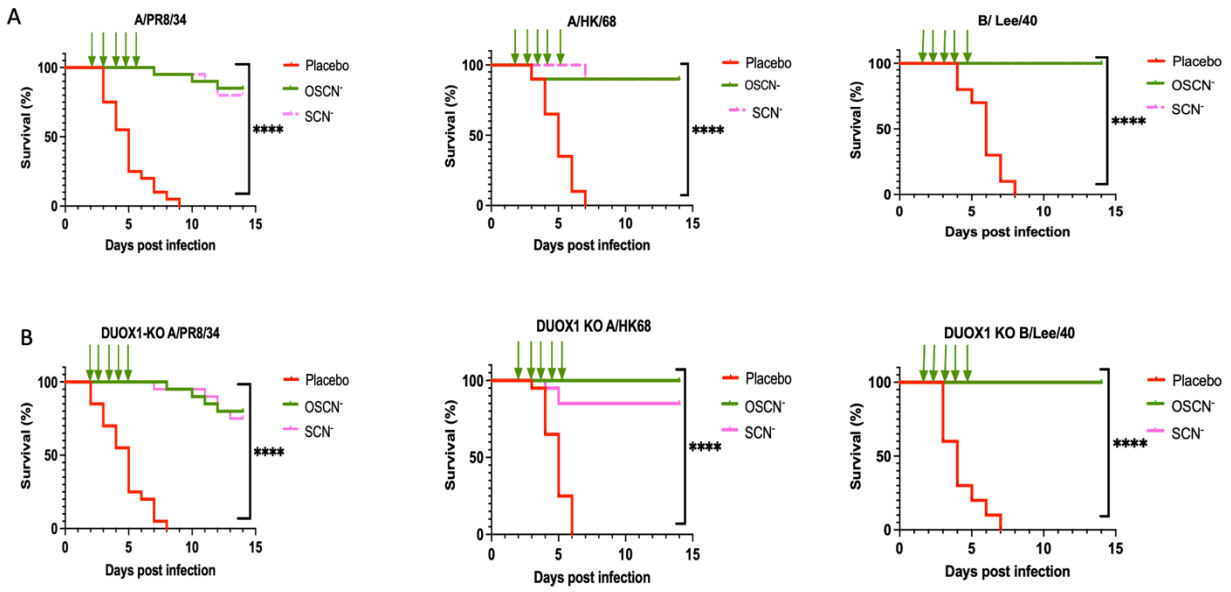

Figure 4.7: Oral SCN^- and $OSCN^-$ provided similar therapeutic efficacy regardless of DUOX1 presence. (A) Comparison of survivals among wild type mice infected with lethal influenza infection of A/PR8/34 (H1N1), A/HK/68 (H3N2) and B/Lee/40. (B) Comparison of survivals among DUOX1-deficient mice infected with lethal influenza infections of the same viruses.

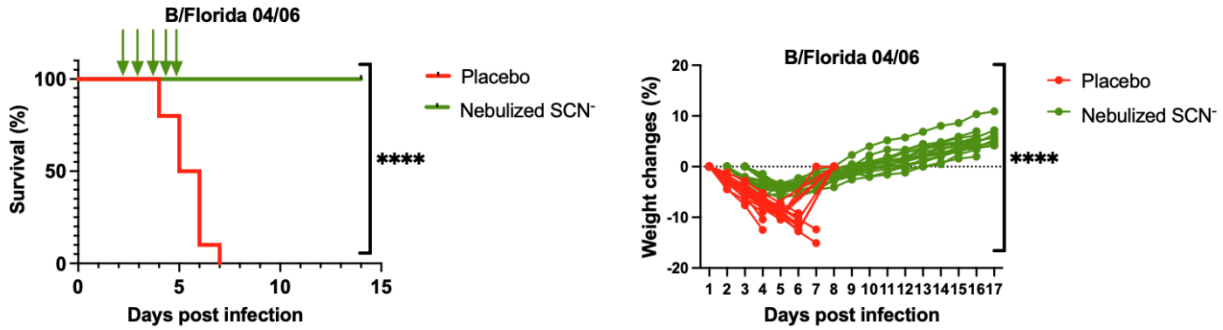

Figure 4.8: Nebulization of 400 µg/kg/day SCN^- (1-5 dpi), twice a day, prevents mortality in C57BL/6J mice infected with lethal doses of B/Florida 04/06 (A and B).

CHAPTER 5

CONCLUSIONS AND DISCUSSION

The respiratory system epithelium faces various microbial invasions during the process of inhalation. It is crucial to know natural body products produced by humans to combat microbial infections. In this work, we explored and determined the therapeutic efficacy of thiocyanate which acts as broad-spectrum antimicrobial agent. SCN^- treated different strains of influenza. Long time ago, SCN^- was explored to be used for hypertension treatment with controversial results, however, its therapeutic efficacy had not yet been discovered against lethal influenza infections in murine model[28]. In the infected-inflamed area, neutrophils accumulate which leads to massive HOCL production, hence extensive tissue damage. In addition to the therapeutic effect of SCN^- against various microbial infections, SCN^- treatment alleviated many inflammatory conditions such as myocardial infarction in rats and ulcerative colitis[26, 331]. Leukopenia is caused by several disease conditions such as rheumatoid arthritis, cancers and infections[332, 333]. Patients who diagnosed with leukopenia (neutropenia) are vulnerable to various infections[334]. At the site of infection and inflammation, neutrophils accumulate and activate their NOX2 to produce the superoxide[335]. The superoxide dismutates to H_2O_2, which is catalyzed by MPO to produce HOCL[335]. SCN^- shifts the HOCL cycle to reversible HOSCN production, hence works as antimicrobial and anti-inflammatory compound[163]. Net traps are released by neutrophils at the site of infection and inflammation as defense

mechanism against microbial and foreign bodies in human body[336]. The effect of $OSCN^-$ against neutrophile nets is still unexplored. Our main hypothesis was that SCN^- has a positive therapeutic efficacy to combat lethal influenza infections regardless of DUOX1 presence at certain dose, time and duration. Furthermore, we hypothesized that the therapeutic outcomes of $OSCN^-$ similar to SCN^- *in vivo*. To prove this hypothesis, we explored the following specific aims:

Specific Aim 1: To determine dosage regimen, dosing interval, treatment duration, and routes of SCN^- against lethal influenza infections in a murine model. The hypothesis conclusion is that systemic and nebulized SCN^- treatment can treat lethal influenza infections in a murine model. The results of chapter 4 revealed that intravenous SCN^- treatment had equal therapeutic efficacy as the oral treatment at lower dose and less duration (3 days instead of 4 or 5 days). Indicating that the intravenous route is crucial in critical cases of influenza infections to reach the maintenance level of dosing in the shortest time. Chapter 4 results showed also precise details related to the SCN^- treatment duration. At least 4 days of oral treatment is required for a positive therapeutic outcome. Systemic SCN^- treatment should be given at a certain dose regimen, time and duration for positive end point efficacy. Treatment with the intravenous route of 200 μg/kg/mouse SCN^- provided similar therapeutic efficacy to the oral treatment with less duration (3 days). We tested different doses of the oral SCN^- to prove that a dose of 400 μg/kg/mouse is the lowest and safest effective dose that can be used via the oral route. Additionally, post-treatment complications and toxicity started to appear at 1000 μg/kg/mouse. Hair loss was notified after a high dose of treatment, however toxic kinetics should be investigated

to prevent toxic side effects. Lung histology showed a robust reduction in lung pathology in A/PR8/34- or B/Florida/04/2006-infected mice that was mainly prevented by oral SCN^- treatment. After treatment, infected lung histology showed less parenchymal hemorrhage, less parenchymal infiltration, less intrabronchial bleeding, less epithelial line destruction, and less hyperplasia. We tested the SCN^- nebulization route and found that SCN^- nebulization is the shortest and fastest way to maximize the therapeutic efficacy and maintain the treatment loading plasma level. We also explored the function of myeloperoxidase enzyme MPO in the *in vitro* inhibition system and found a significant inhibitory effect against different strains of influenza A and B, leading us to conclude that MPO is essential for the $OSCN^-$ formation (Data not shown). These results were further supported by testing SCN^- - treatment in the MPO-deficient murine model whose data demonstrated a significant therapeutic efficacy in wild type B6 mice compared to the MPO KO mice (Data not shown). These results indicate that MPO is very crucial for the $OSCN^-$ formation in the *in vivo* model. This data shows also that SCN^- treatment has a broad-spectrum activity against different influenza virus strains. These results also suggest that MPO has an essential role in the H_2O_2 formation and patients with MPO dysfunction and leukopenia might confront more resistance to the SCN^- treatment compared to patients with normal MPO and leukocyte levels. Thus, higher doses should be administered in patients with MPO and leukocyte deficiency.

Specific Aim 2: To evaluate the therapeutic efficacy of hypothiocyanite ($OSCN^-$) when combined with FDA-approved drugs. The working hypothesis is that combining $OSCN^-$ with FDA-approved drugs such as amantadine and oseltamivir will reduce the

drug resistance against influenza virus. We tested the effectiveness of $OSCN^-$ single and combined treatment *in vitro* and *in vivo* C57BL/6J murine model. We infected WT mice with lethal doses of different strains of influenza A (H1N1 and H3N2) and evaluated mortality and morbidity. During treatment, we notified significant increase in mortality and morbidity in mice treated with single treatment of Amantadine or $OSCN^-$ compared to mice treated with combined treatment. We used oseltamivir as a positive treatment control. Moreover, we evaluated lung viral titer, gene expression and lung histology after treatment; mice treated with combined therapy had lower lung viral load and lower pathological features compared to mice treated with single treatment. These results demonstrate that combined therapy has more efficacy to combat lethal influenza A infection compared to Amantadine and $OSCN^-$ single treatment. Moreover, using combined treatment regimen reduces post-treatment side effects and increases treatment susceptibility.

Specific Aim 3: Examine the therapeutic efficacy of $OSCN^-$ versus thiocyanate SCN^- in WT and Duox1-deficient mice. The working hypothesis is that SCN^- *in vivo* treatment has the same therapeutic efficacy as $OSCN^-$ *in vivo* treatment in WT and Duox1-deficient mice. WT and Duox1-deficient mice were treated orally with $OSCN^-$ and SCN^-. Mice were infected with lethal dose of A/PR8/34 (H1N1), A/HK/68 (H3N2) and B/Lee/40. SCN^- endpoint treatment outcome was similar to $OSCN^-$ endpoint treatment outcome. The data demonstrated that the therapeutic effect of oral SCN^- is independent of Duox1 as Duox1-deficient animals were rescued by SCN^- to the same extent as WT mice. Additionally, we used mice deficient in MPO, a peroxidase that is abundantly expressed in neutrophils. The data indicates that neutrophils are the main source of H_2O_2

at the site of infection and inflammation. These results reveal for the first time that HOSCN is produced reversibly in the presence of MPO.

Generally, the data of these aims revealed that SCN^- treatment can be used as a single or combined treatment at lower doses. Additionally, our study revealed the broad-spectrum inhibitory effect of SCN^- against various types and strains of influenza virus. Our data was also the first to explore that SCN^- positively treats lethal flu infection in *Duox1*-deficient mice. Knowing the therapeutic aspects of SCN^- is very important to reduce or eliminate the antiviral resistance against influenza.

Furthermore, this study outcomes indicate that Neutrophils have an essential role in producing H_2O_2 that utilized for HOCL and HOSCN formation. Adding external SCN^- is needed for shifting the HOCL production cycle into reversible HOSCN formation. This work also further demonstrates the importance of NOX2 presence as it is the main player in producing H_2O_2 in neutrophils. Our study showed that MPO is very crucial for the HOSCN formation as all MPO-deficient mice were completely resistant to the oral SCN-treatment compared to the wild type mice with normal levels of MPO. Further testing the SCN^- treatment into LPO-deficient mice is mandatory to determine the extent of MPO function in HOSCN formation. In addition, testing SCN^- treatment in NOX2-deficient is preferred to explore the NOX2 function in H_2O_2 production in neutrophils. Taken all together, the results suggest that neutrophils have a great function in H_2O_2 production at the site of infection and inflammation.

Broad-spectrum anti-influenza prodrug is needed which can play a positive impact toward reducing influenza infection mortality rates every year. Even though the FDA-approved anti-influenza drugs have shown positive therapeutic effects against severe

influenza infections in clinical practice, their efficacy at decreasing mortality rates is limited. Oseltamivir, for example, cannot be administered in children less than 12 months[337]. Additionally, the FDA-approved anti-influenza drugs do not appear to b highly effective at preventing mortality in patients with co-morbidities[315, 338]. Thus, a novel mono or combined therapy is needed, optimized doses, different routes and duration must be examined.

The first direction is to precisely determine the effective doses to reach the loading and maintainace levels, Current doses of Oseltamivir, for instance, are mainly 75mg twice a day while in children older than 1 year, from 30-75mg once daily depending on nthe case severity[339]. For instance, oseltamivir can cause bradycardia in severly ill patients, hence, high doses should be used with caution in any drug usage[340]. Dose optimization is a crucial step to evaluate the pharmacokinetics and pharmacodynamic parameters. In addition, knowing the concentration- effect relationships must be clarified to maximize the therapeutic efficacy.

The second direction is to study the combination therapy that targets various mechanistic pathways to synergistically inhibit and decrease the frequency of tolerance. Our study obviously reveals that a single treatment of $OSCN^-$ or amantadine have a comparatively low therapeutic benefit compared to both combination in the treatment of lethal influenza infection in murine model[20]. For example, double combination (e.g., $OSCN^-$ and Amantadine) or triple combination (such as amantadine, OSCN-, and oseltamivir) treatment were shown to be more efficacious against amantadine-resistant influenza A *in vitro*. Clearly, combined drugs regimen is preferable and recommended to diminish treatment adverse effect.

The third approach for reducing mortality rates, is focusing on the mode of drug administration. In the clinical practice, severely ill patients would not be able to swallow oral medications such as tablets or syrup. Therefore, other options of administration should be available. Studies should focus on how SCN^- can be delivered to lungs in a short duration for the maximum efficacy. Treatment timing is critical in severely ill patients. In general, Nebulization and intravenous routes are always effective in providing the required loading dose[341]. A combination of intravenous and local aerosolized administration of SCN^- could be more beneficial than oral SCN^- administration when SCN^- is used to treat acute influenza infection. Thus, further studies are required to explore mode of SCN^- administration, which combined routes should provide th best outcome.

Fourth, exploring the anti-inflammatory effect of SCN^- and its effect on the neutrophils function, selectively, NOX2, MPO and neutrophil NETs against several influenza strains, while the exact mechanism of action is still unclear. There was clear evidence in our study that SCN^- can shift the HOCL formation cycle to HOSCN, hence may work as anti-inflammatory as well. Currently, a potent anti-influenza drug is urgently required to decrease hospital mortalities and morbidities. We believe that SCN^- can work as prodrug against influenza infection with different paths of action, such as optimized doses, different concentrations and combinations. Lastly, SCN- will prove to be beneficial for increasing the clinical effectiveness in influenza infection.

References

1. Ryu, S. & Cowling, B.J. Human Influenza Epidemiology. *Cold Spring Harb Perspect Med* **11** (2021).

2. Thompson, W.W. *et al.* Mortality associated with influenza and respiratory syncytial virus in the United States. *JAMA* **289**, 179-186 (2003).

3. de Vries, R.D., Altenburg, A.F. & Rimmelzwaan, G.F. Universal influenza vaccines, science fiction or soon reality? *Expert Rev Vaccines* **14**, 1299-1301 (2015).

4. Mousa, H.A. Prevention and Treatment of Influenza, Influenza-Like Illness, and Common Cold by Herbal, Complementary, and Natural Therapies. *J Evid Based Complementary Altern Med* **22**, 166-174 (2017).

5. Dong, G. *et al.* Adamantane-resistant influenza a viruses in the world (1902-2013): frequency and distribution of M2 gene mutations. *PLoS One* **10**, e0119115 (2015).

6. van der Vries, E., Schutten, M., Fraaij, P., Boucher, C. & Osterhaus, A. Influenza virus resistance to antiviral therapy. *Adv Pharmacol* **67**, 217-246 (2013).

7. Jefferson, T. *et al.* Neuraminidase inhibitors for preventing and treating influenza in adults and children. *Cochrane Database Syst Rev* **2014**, CD008965 (2014).

8. Jefferson, T. *et al.* Neuraminidase inhibitors for preventing and treating influenza in healthy adults. *Cochrane Database Syst Rev*, CD001265 (2010).

9. Ison, M.G. *et al.* Early treatment with baloxavir marboxil in high-risk adolescent and adult outpatients with uncomplicated influenza (CAPSTONE-2): a randomised, placebo-controlled, phase 3 trial. *Lancet Infect Dis* **20**, 1204-1214 (2020).

10. Tagarro, A. *et al.* [Oseltamivir for the treatment of influenza in children and adolescents]. *An Pediatr (Engl Ed)* **90**, 317 e311-317 e318 (2019).

11. Abed, Y., Pizzorno, A., Bouhy, X., Rheaume, C. & Boivin, G. Impact of potential permissive neuraminidase mutations on viral fitness of the H275Y oseltamivir-resistant influenza A(H1N1)pdm09 virus in vitro, in mice and in ferrets. *J Virol* **88**, 1652-1658 (2014).

12. Whitsett, J.A. Airway Epithelial Differentiation and Mucociliary Clearance. *Ann Am Thorac Soc* **15**, S143-S148 (2018).

13. Patel, U. *et al.* Susceptibility of influenza viruses to hypothiocyanite and hypoiodite produced by lactoperoxidase in a cell-free system. *PLoS One* **13**, e0199167 (2018).

14. Ashtiwi, N.M., Sarr, D. & Rada, B. DUOX1 in mammalian disease pathophysiology. *J Mol Med (Berl)* **99**, 743-754 (2021).

15. Strengert, M. *et al.* Mucosal reactive oxygen species are required for antiviral response: role of Duox in influenza a virus infection. *Antioxid Redox Signal* **20**, 2695-2709 (2014).

16. Chandler, J.D. & Day, B.J. Thiocyanate: a potentially useful therapeutic agent with host defense and antioxidant properties. *Biochem Pharmacol* **84**, 1381-1387 (2012).

17. Ngogang, J., Eben-Moussi, E. & Raisonnier, A. [Salivary, urinary and plasma thiocyanate in smokers and non-smokers]. *Pathol Biol (Paris)* **31**, 155-160 (1983).

18. Weuffen, W. *et al.* [The thiocyanate ion as a physiologically significant active substance in living nature]. *Pharmazie* **45**, 16-29 (1990).

19. Mikola, H., Waris, M. & Tenovuo, J. Inhibition of herpes simplex virus type 1, respiratory syncytial virus and echovirus type 11 by peroxidase-generated hypothiocyanite. *Antiviral Res* **26**, 161-171 (1995).

20. Ashtiwi, N.M. *et al.* The Hypothiocyanite and Amantadine Combination Treatment Prevents Lethal Influenza A Virus Infection in Mice. *Front Immunol* **13**, 859033 (2022).

21. Chandler, J.D. & Day, B.J. Biochemical mechanisms and therapeutic potential of pseudohalide thiocyanate in human health. *Free Radic Res* **49**, 695-710 (2015).

22. Day, B.J. *et al.* The thiocyanate analog selenocyanate is a more potent antimicrobial pro-drug that also is selectively detoxified by the host. *Free Radic Biol Med* **146**, 324-332 (2020).

23. Chandler, J.D., Min, E., Huang, J., Nichols, D.P. & Day, B.J. Nebulized thiocyanate improves lung infection outcomes in mice. *Br J Pharmacol* **169**, 1166-1177 (2013).

24. Gaitonde, B.B., Kulkarni, H.J., Kamat, R.A. & Vakil, B.J. Clinical evaluation of a new anthelmintic; phenylene di-iso thiocyanate (Bitoscanate) in hookworm and roundworm infestation. *J Trop Med Hyg* **72**, 253-258 (1969).

25. Mickelson, M.N. Effect of lactoperoxidase and thiocyanate on the growth of Streptococcus pyogenes and Streptococcus agalactiae in a chemically defined culture medium. *J Gen Microbiol* **43**, 31-43 (1966).

26. Hall, L. *et al.* Oral pre-treatment with thiocyanate (SCN(-)) protects against myocardial ischaemia-reperfusion injury in rats. *Sci Rep* **11**, 12712 (2021).

27. Zietzer, A. *et al.* Sodium thiocyanate treatment attenuates atherosclerotic plaque formation and improves endothelial regeneration in mice. *PLoS One* **14**, e0214476 (2019).

28. Siddle, S.G. & Mills, P.J. Thiocyanate for hypertension. *Lancet* **1**, 465 (1947).

29. San Gabriel, P.T., Liu, Y., Schroder, A.L., Zoellner, H. & Chami, B. The Role of Thiocyanate in Modulating Myeloperoxidase Activity during Disease. *Int J Mol Sci* **21** (2020).

30. Ohye, H. & Sugawara, M. Dual oxidase, hydrogen peroxide and thyroid diseases. *Exp Biol Med (Maywood)* **235**, 424-433 (2010).

31. Edens, W.A. *et al.* Tyrosine cross-linking of extracellular matrix is catalyzed by Duox, a multidomain oxidase/peroxidase with homology to the phagocyte oxidase subunit gp91phox. *J Cell Biol* **154**, 879-891 (2001).

32. Sarr, D., Toth, E., Gingerich, A. & Rada, B. Antimicrobial actions of dual oxidases and lactoperoxidase. *J Microbiol* **56**, 373-386 (2018).

33. Ling, Q. *et al.* Epigenetic silencing of dual oxidase 1 by promoter hypermethylation in human hepatocellular carcinoma. *Am J Cancer Res* **4**, 508-517 (2014).

34. Dupuy, C. *et al.* Purification of a novel flavoprotein involved in the thyroid NADPH oxidase. Cloning of the porcine and human cdnas. *J Biol Chem* **274**, 37265-37269 (1999).

35. Pachucki, J., Wang, D., Christophe, D. & Miot, F. Structural and functional characterization of the two human ThOX/Duox genes and their 5'-flanking regions. *Mol Cell Endocrinol* **214**, 53-62 (2004).

36. Geiszt, M., Witta, J., Baffi, J., Lekstrom, K. & Leto, T.L. Dual oxidases represent novel hydrogen peroxide sources supporting mucosal surface host defense. *FASEB J* **17**, 1502-1504 (2003).

37. Dupuy, C., Deme, D., Kaniewski, J., Pommier, J. & Virion, A. Ca2+ regulation of thyroid NADPH-dependent H2O2 generation. *FEBS Lett* **233**, 74-78 (1988).

38. Morand, S. *et al.* Targeting of the dual oxidase 2 N-terminal region to the plasma membrane. *J Biol Chem* **279**, 30244-30251 (2004).

39. Ameziane-El-Hassani, R. *et al.* Dual oxidase-2 has an intrinsic Ca2+-dependent H2O2-generating activity. *J Biol Chem* **280**, 30046-30054 (2005).

40. Grasberger, H. & Refetoff, S. Identification of the maturation factor for dual oxidase. Evolution of an eukaryotic operon equivalent. *J Biol Chem* **281**, 18269-18272 (2006).

41. Xu, C., Linderholm, A., Grasberger, H. & Harper, R.W. Dual oxidase 2 bidirectional promoter polymorphisms confer differential immune responses in airway epithelia. *Am J Respir Cell Mol Biol* **47**, 484-490 (2012).

42. Hirakawa, S., Saito, R., Ohara, H., Okuyama, R. & Aiba, S. Dual oxidase 1 induced by Th2 cytokines promotes STAT6 phosphorylation via oxidative inactivation of protein tyrosine phosphatase 1B in human epidermal keratinocytes. *J Immunol* **186**, 4762-4770 (2011).

43. Donko, A. *et al.* Urothelial cells produce hydrogen peroxide through the activation of Duox1. *Free Radic Biol Med* **49**, 2040-2048 (2010).

44. Habibovic, A. *et al.* DUOX1 mediates persistent epithelial EGFR activation, mucous cell metaplasia, and airway remodeling during allergic asthma. *JCI Insight* **1**, e88811 (2016).

45. Rada, B., Park, J.J., Sil, P., Geiszt, M. & Leto, T.L. NLRP3 inflammasome activation and interleukin-1beta release in macrophages require calcium but are independent of calcium-activated NADPH oxidases. *Inflamm Res* **63**, 821-830 (2014).

46. Meziani, L. *et al.* Dual oxidase 1 limits the IFNgamma-associated antitumor effect of macrophages. *J Immunother Cancer* **8** (2020).

47. Donko, A., Peterfi, Z., Sum, A., Leto, T. & Geiszt, M. Dual oxidases. *Philos Trans R Soc Lond B Biol Sci* **360**, 2301-2308 (2005).

48. Conner, G.E., Salathe, M. & Forteza, R. Lactoperoxidase and hydrogen peroxide metabolism in the airway. *Am J Respir Crit Care Med* **166**, S57-61 (2002).

49. Conner, G.E., Wijkstrom-Frei, C., Randell, S.H., Fernandez, V.E. & Salathe, M. The lactoperoxidase system links anion transport to host defense in cystic fibrosis. *FEBS Lett* **581**, 271-278 (2007).

50. Gerson, C. *et al.* The lactoperoxidase system functions in bacterial clearance of airways. *Am J Respir Cell Mol Biol* **22**, 665-671 (2000).

51. Wijkstrom-Frei, C. *et al.* Lactoperoxidase and human airway host defense. *Am J Respir Cell Mol Biol* **29**, 206-212 (2003).

52. Fragoso, M.A., Torbati, A., Fregien, N. & Conner, G.E. Molecular heterogeneity and alternative splicing of human lactoperoxidase. *Arch Biochem Biophys* **482**, 52-57 (2009).

53. Pedemonte, N. *et al.* Thiocyanate transport in resting and IL-4-stimulated human bronchial epithelial cells: role of pendrin and anion channels. *J Immunol* **178**, 5144-5153 (2007).

54. Moskwa, P. *et al.* A novel host defense system of airways is defective in cystic fibrosis. *Am J Respir Crit Care Med* **175**, 174-183 (2007).

55. De Deken, X. *et al.* Cloning of two human thyroid cDNAs encoding new members of the NADPH oxidase family. *J Biol Chem* **275**, 23227-23233 (2000).

56. Moreno, J.C. *et al.* Inactivating mutations in the gene for thyroid oxidase 2 (THOX2) and congenital hypothyroidism. *N Engl J Med* **347**, 95-102 (2002).

57. Weber, G., Rabbiosi, S., Zamproni, I. & Fugazzola, L. Genetic defects of hydrogen peroxide generation in the thyroid gland. *J Endocrinol Invest* **36**, 261-266 (2013).

58. Szinnai, G. Clinical genetics of congenital hypothyroidism. *Endocr Dev* **26**, 60-78 (2014).

59. Rada, B., Lekstrom, K., Damian, S., Dupuy, C. & Leto, T.L. The Pseudomonas toxin pyocyanin inhibits the dual oxidase-based antimicrobial system as it imposes oxidative stress on airway epithelial cells. *J Immunol* **181**, 4883-4893 (2008).

60. Rada, B., Boudreau, H.E., Park, J.J. & Leto, T.L. Histamine stimulates hydrogen peroxide production by bronchial epithelial cells via histamine H1 receptor and dual oxidase. *Am J Respir Cell Mol Biol* **50**, 125-134 (2014).

61. Forteza, R., Salathe, M., Miot, F., Forteza, R. & Conner, G.E. Regulated hydrogen peroxide production by Duox in human airway epithelial cells. *Am J Respir Cell Mol Biol* **32**, 462-469 (2005).

62. Gattas, M.V. *et al.* Oxidative epithelial host defense is regulated by infectious and inflammatory stimuli. *Free Radic Biol Med* **47**, 1450-1458 (2009).

63. Niethammer, P., Grabher, C., Look, A.T. & Mitchison, T.J. A tissue-scale gradient of hydrogen peroxide mediates rapid wound detection in zebrafish. *Nature* **459**, 996-999 (2009).

64. Chang, S. *et al.* Dual oxidase regulates neutrophil recruitment in allergic airways. *Free Radic Biol Med* **65**, 38-46 (2013).

65. Louzada, R.A. *et al.* NADPH oxidase DUOX1 sustains TGF-beta1 signalling and promotes lung fibrosis. *Eur Respir J* **57** (2021).

66. Faria, C.C. & Fortunato, R.S. The role of dual oxidases in physiology and cancer. *Genet Mol Biol* **43**, e20190096 (2020).

67. Buvelot, H., Posfay-Barbe, K.M., Linder, P., Schrenzel, J. & Krause, K.H. Staphylococcus aureus, phagocyte NADPH oxidase and chronic granulomatous disease. *FEMS Microbiol Rev* **41**, 139-157 (2017).

68. Sirokmany, G., Donko, A. & Geiszt, M. Nox/Duox Family of NADPH Oxidases: Lessons from Knockout Mouse Models. *Trends Pharmacol Sci* **37**, 318-327 (2016).

69. Little, A.C. *et al.* DUOX1 silencing in lung cancer promotes EMT, cancer stem cell characteristics and invasive properties. *Oncogenesis* **5**, e261 (2016).

70. Lu, C.L. *et al.* NADPH oxidase DUOX1 and DUOX2 but not NOX4 are independent predictors in hepatocellular carcinoma after hepatectomy. *Tumour Biol* **32**, 1173-1182 (2011).

71. Luxen, S. *et al.* Heterodimerization controls localization of Duox-DuoxA NADPH oxidases in airway cells. *J Cell Sci* **122**, 1238-1247 (2009).

72. Morand, S. *et al.* Duox maturation factors form cell surface complexes with Duox affecting the specificity of reactive oxygen species generation. *FASEB J* **23**, 1205-1218 (2009).

73. Carre, A. *et al.* When an Intramolecular Disulfide Bridge Governs the Interaction of DUOX2 with Its Partner DUOXA2. *Antioxid Redox Signal* **23**, 724-733 (2015).

74. Meitzler, J.L., Hinde, S., Banfi, B., Nauseef, W.M. & Ortiz de Montellano, P.R. Conserved cysteine residues provide a protein-protein interaction surface in dual oxidase (DUOX) proteins. *J Biol Chem* **288**, 7147-7157 (2013).

75. Ueyama, T. *et al.* The extracellular A-loop of dual oxidases affects the specificity of reactive oxygen species release. *J Biol Chem* **290**, 6495-6506 (2015).

76. Xie, X. *et al.* NIP/DuoxA is essential for Drosophila embryonic development and regulates oxidative stress response. *Int J Biol Sci* **6**, 252-267 (2010).

77. Qin, H. *et al.* A novel transmembrane protein recruits numb to the plasma membrane during asymmetric cell division. *J Biol Chem* **279**, 11304-11312 (2004).

78. Ostrakhovitch, E.A. Interplay between Numb and Notch in epithelial cancers: role for dual oxidase maturation factor. *Eur J Cancer* **45**, 2071-2076 (2009).

79. Huang, T. *et al.* NOTCH receptors in gastric and other gastrointestinal cancers: oncogenes or tumor suppressors? *Mol Cancer* **15**, 80 (2016).

80. Nowell, C.S. & Radtke, F. Notch as a tumour suppressor. *Nat Rev Cancer* **17**, 145-159 (2017).

81. Sandiford, S.D., Kennedy, K.A., Xie, X., Pickering, J.G. & Li, S.S. Dual oxidase maturation factor 1 (DUOXA1) overexpression increases reactive oxygen species production and inhibits murine muscle satellite cell differentiation. *Cell Commun Signal* **12**, 5 (2014).

82. Kennedy, K.A. *et al.* Mammalian numb-interacting protein 1/dual oxidase maturation factor 1 directs neuronal fate in stem cells. *J Biol Chem* **285**, 17974-17985 (2010).

83. Ostrakhovitch, E.A. & Li, S.S. NIP1/DUOXA1 expression in epithelial breast cancer cells: regulation of cell adhesion and actin dynamics. *Breast Cancer Res Treat* **119**, 773-786 (2010).

84. Juarez, M.T., Patterson, R.A., Sandoval-Guillen, E. & McGinnis, W. Duox, Flotillin-2, and Src42A are required to activate or delimit the spread of the transcriptional response to epidermal wounds in Drosophila. *PLoS Genet* **7**, e1002424 (2011).

85. van der Hoeven, R., Cruz, M.R., Chavez, V. & Garsin, D.A. Localization of the Dual Oxidase BLI-3 and Characterization of Its NADPH Oxidase Domain during Infection of Caenorhabditis elegans. *PLoS One* **10**, e0124091 (2015).

86. Hill, T., 3rd & Rice, R.H. DUOX expression in human keratinocytes and bronchial epithelial cells: Influence of vanadate. *Toxicol In Vitro* **46**, 257-264 (2018).

87. Choi, H. *et al.* Hydrogen peroxide generated by DUOX1 regulates the expression levels of specific differentiation markers in normal human keratinocytes. *J Dermatol Sci* **74**, 56-63 (2014).

88. Han, H., Roan, F. & Ziegler, S.F. The atopic march: current insights into skin barrier dysfunction and epithelial cell-derived cytokines. *Immunol Rev* **278**, 116-130 (2017).

89. Hamid, Q., Boguniewicz, M. & Leung, D.Y. Differential in situ cytokine gene expression in acute versus chronic atopic dermatitis. *J Clin Invest* **94**, 870-876 (1994).

90. Neis, M.M. *et al.* Enhanced expression levels of IL-31 correlate with IL-4 and IL-13 in atopic and allergic contact dermatitis. *J Allergy Clin Immunol* **118**, 930-937 (2006).

91. Candel, S. *et al.* Tnfa signaling through tnfr2 protects skin against oxidative stress-induced inflammation. *PLoS Biol* **12**, e1001855 (2014).

92. Hristova, M. *et al.* Identification of DUOX1-dependent redox signaling through protein S-glutathionylation in airway epithelial cells. *Redox Biol* **2**, 436-446 (2014).

93. Cho, D.Y. *et al.* Expression of dual oxidases and secreted cytokines in chronic rhinosinusitis. *Int Forum Allergy Rhinol* **3**, 376-383 (2013).

94. Svenningsen, S. & Nair, P. Asthma Endotypes and an Overview of Targeted Therapy for Asthma. *Front Med (Lausanne)* **4**, 158 (2017).

95. Harper, R.W. *et al.* Differential regulation of dual NADPH oxidases/peroxidases, Duox1 and Duox2, by Th1 and Th2 cytokines in respiratory tract epithelium. *FEBS Lett* **579**, 4911-4917 (2005).

96. Wynne, M., Atkinson, C., Schlosser, R.J. & Mulligan, J.K. Contribution of Epithelial Cell Dysfunction to the Pathogenesis of Chronic Rhinosinusitis with Nasal Polyps. *Am J Rhinol Allergy* **33**, 782-790 (2019).

97. Shao, M.X. & Nadel, J.A. Dual oxidase 1-dependent MUC5AC mucin expression in cultured human airway epithelial cells. *Proc Natl Acad Sci U S A* **102**, 767-772 (2005).

98. Arbiser, J.L. *et al.* Reactive oxygen generated by Nox1 triggers the angiogenic switch. *Proc Natl Acad Sci U S A* **99**, 715-720 (2002).

99. Suh, Y.A. *et al.* Cell transformation by the superoxide-generating oxidase Mox1. *Nature* **401**, 79-82 (1999).

100. Nagai, K. *et al.* Dual oxidase 1 and 2 expression in airway epithelium of smokers and patients with mild/moderate chronic obstructive pulmonary disease. *Antioxid Redox Signal* **10**, 705-714 (2008).

101. Stevens, W.W., Schleimer, R.P. & Kern, R.C. Chronic Rhinosinusitis with Nasal Polyps. *J Allergy Clin Immunol Pract* **4**, 565-572 (2016).

102. Fischer, H. Mechanisms and function of DUOX in epithelia of the lung. *Antioxid Redox Signal* **11**, 2453-2465 (2009).

103. Loukides, S., Bouros, D., Papatheodorou, G., Panagou, P. & Siafakas, N.M. The relationships among hydrogen peroxide in expired breath condensate, airway inflammation, and asthma severity. *Chest* **121**, 338-346 (2002).

104. Barnes, P.J. *et al.* Chronic obstructive pulmonary disease. *Nat Rev Dis Primers* **1**, 15076 (2015).

105. MacNee, W. Oxidants/antioxidants and COPD. *Chest* **117**, 303S-317S (2000).

106. Repine, J.E., Bast, A. & Lankhorst, I. Oxidative stress in chronic obstructive pulmonary disease. Oxidative Stress Study Group. *Am J Respir Crit Care Med* **156**, 341-357 (1997).

107. Tian, Z. *et al.* Cigarette Smoke Impairs A(2A) Adenosine Receptor Mediated Wound Repair through Up-regulation of Duox-1 Expression. *Sci Rep* **7**, 44405 (2017).

108. Schiffers, C. *et al.* Downregulation of epithelial DUOX1 in chronic obstructive pulmonary disease. *JCI Insight* **6** (2021).

109. Barratt, S.L., Creamer, A., Hayton, C. & Chaudhuri, N. Idiopathic Pulmonary Fibrosis (IPF): An Overview. *J Clin Med* **7** (2018).

110. Todaro, D.R., Augustus-Wallace, A.C., Klein, J.M. & Haas, A.L. Oligomerization of the HECT ubiquitin ligase NEDD4-2/NEDD4L is essential for polyubiquitin chain assembly. *J Biol Chem* **293**, 18192-18206 (2018).

111. Ballester, B., Milara, J. & Cortijo, J. Idiopathic Pulmonary Fibrosis and Lung Cancer: Mechanisms and Molecular Targets. *Int J Mol Sci* **20** (2019).

112. Little, A.C. *et al.* Paradoxical roles of dual oxidases in cancer biology. *Free Radic Biol Med* **110**, 117-132 (2017).

113. Roy, K. *et al.* NADPH oxidases and cancer. *Clin Sci (Lond)* **128**, 863-875 (2015).

114. Schmidt, M. *et al.* Regulation of G2/M Transition by Inhibition of WEE1 and PKMYT1 Kinases. *Molecules* **22** (2017).

115. Luxen, S., Belinsky, S.A. & Knaus, U.G. Silencing of DUOX NADPH oxidases by promoter hypermethylation in lung cancer. *Cancer Res* **68**, 1037-1045 (2008).

116. Chen, S. *et al.* Dual oxidase 1: A predictive tool for the prognosis of hepatocellular carcinoma patients. *Oncol Rep* **35**, 3198-3208 (2016).

117. Pulcrano, M. *et al.* Poorly differentiated follicular thyroid carcinoma: prognostic factors and relevance of histological classification. *Thyroid* **17**, 639-646 (2007).

118. Fortunato, R.S. *et al.* DUOX1 Silencing in Mammary Cell Alters the Response to Genotoxic Stress. *Oxid Med Cell Longev* **2018**, 3570526 (2018).

119. Greer, J.B. & Whitcomb, D.C. Inflammation and pancreatic cancer: an evidence-based review. *Curr Opin Pharmacol* **9**, 411-418 (2009).

120. Cho, S.Y. *et al.* Dual oxidase 1 and NADPH oxidase 2 exert favorable effects in cervical cancer patients by activating immune response. *BMC Cancer* **19**, 1078 (2019).

121. You, X., Ma, M., Hou, G., Hu, Y. & Shi, X. Gene expression and prognosis of NOX family members in gastric cancer. *Onco Targets Ther* **11**, 3065-3074 (2018).

122. Olusola, P., Banerjee, H.N., Philley, J.V. & Dasgupta, S. Human Papilloma Virus-Associated Cervical Cancer and Health Disparities. *Cells* **8** (2019).

123. McKay, C.J., Glen, P. & McMillan, D.C. Chronic inflammation and pancreatic cancer. *Best Pract Res Clin Gastroenterol* **22**, 65-73 (2008).

124. Taunk, N.K., Haffty, B.G., Kostis, J.B. & Goyal, S. Radiation-induced heart disease: pathologic abnormalities and putative mechanisms. *Front Oncol* **5**, 39 (2015).

125. Heo, G.S. *et al.* Molecular Imaging Visualizes Recruitment of Inflammatory Monocytes and Macrophages to the Injured Heart. *Circ Res* **124**, 881-890 (2019).

126. Peng, J.J., Xiong, S.Q., Ding, L.X., Peng, J. & Xia, X.B. Diabetic retinopathy: Focus on NADPH oxidase and its potential as therapeutic target. *Eur J Pharmacol* **853**, 381-387 (2019).

127. Filopei, J. & Frishman, W. Radiation-induced heart disease. *Cardiol Rev* **20**, 184-188 (2012).

128. Yahyapour, R. *et al.* Metformin Protects Against Radiation-Induced Heart Injury and Attenuates the Upregulation of Dual Oxidase Genes Following Rat's Chest Irradiation. *Int J Mol Cell Med* **7**, 193-202 (2018).

129. Kerner, W., Bruckel, J. & German Diabetes, A. Definition, classification and diagnosis of diabetes mellitus. *Exp Clin Endocrinol Diabetes* **122**, 384-386 (2014).

130. Aliasgharzadeh, A. *et al.* Melatonin Attenuates Upregulation of Duox1 and Duox2 and Protects against Lung Injury following Chest Irradiation in Rats. *Cell J* **21**, 236-242 (2019).

131. Pongnimitprasert, N. *et al.* Potential role of the "NADPH oxidases" (NOX/DUOX) family in cystic fibrosis. *Ann Biol Clin (Paris)* **66**, 621-629 (2008).

132. Donko, A. *et al.* Hypothyroidism-associated missense mutation impairs NADPH oxidase activity and intracellular trafficking of Duox2. *Free Radic Biol Med* **73**, 190-200 (2014).

133. Liu, S. *et al.* Genetic and functional analysis of two missense DUOX2 mutations in congenital hypothyroidism and goiter. *Oncotarget* **9**, 4366-4374 (2018).

134. Park, W. *et al.* Metabolic syndrome is an independent risk factor for synchronous colorectal neoplasm in patients with gastric neoplasm. *J Gastroenterol Hepatol* **27**, 1490-1497 (2012).

135. Mu, G. *et al.* Subclinical hypothyroidism as an independent risk factor for colorectal neoplasm. *Clin Res Hepatol Gastroenterol* **39**, 261-266 (2015).

136. Tseng, F.Y. *et al.* Subclinical hypothyroidism is associated with increased risk for cancer mortality in adult Taiwanese-a 10 years population-based cohort. *PLoS One* **10**, e0122955 (2015).

137. Lee, P.L., West, C., Crain, K. & Wang, L. Genetic polymorphisms and susceptibility to lung disease. *J Negat Results Biomed* **5**, 5 (2006).

138. Lozano, R. *et al.* Global and regional mortality from 235 causes of death for 20 age groups in 1990 and 2010: a systematic analysis for the Global Burden of Disease Study 2010. *Lancet* **380**, 2095-2128 (2012).

139. Bulla, A. & Hitze, K.L. Acute respiratory infections: a review. *Bull World Health Organ* **56**, 481-498 (1978).

140. Williams, B.G., Gouws, E., Boschi-Pinto, C., Bryce, J. & Dye, C. Estimates of world-wide distribution of child deaths from acute respiratory infections. *Lancet Infect Dis* **2**, 25-32 (2002).

141. Mohamed, G.A. *et al.* Etiology and Incidence of Viral Acute Respiratory Infections Among Refugees Aged 5 Years and Older in Hagadera Camp, Dadaab, Kenya. *Am J Trop Med Hyg* **93**, 1371-1376 (2015).

142. Li, Z.J. *et al.* Etiological and epidemiological features of acute respiratory infections in China. *Nat Commun* **12**, 5026 (2021).

143. Rudan, I., Boschi-Pinto, C., Biloglav, Z., Mulholland, K. & Campbell, H. Epidemiology and etiology of childhood pneumonia. *Bull World Health Organ* **86**, 408-416 (2008).

144. Chan, L. *et al.* Review of Influenza Virus Vaccines: The Qualitative Nature of Immune Responses to Infection and Vaccination Is a Critical Consideration. *Vaccines (Basel)* **9** (2021).

145. Mahla, R.S. & Dustin, L.B. Lessons from a large-scale COVID-19 vaccine trial. *J Clin Invest* **132** (2022).

146. Varghese, R., Jayaraman, R. & Veeraraghavan, B. Current challenges in the accurate identification of Streptococcus pneumoniae and its serogroups/serotypes in the vaccine era. *J Microbiol Methods* **141**, 48-54 (2017).

147. Zhao, Y. *et al.* Efficacy and safety of single-dose antiviral drugs for influenza treatment: A systematic review and network meta-analysis. *J Med Virol* **94**, 3270-3302 (2022).

148. Sheikh, B.A., Bhat, B.A. & Mir, M.A. Antimicrobial resistance: new insights and therapeutic implications. *Appl Microbiol Biotechnol* **106**, 6427-6440 (2022).

149. Venkatesan, P. 2022 post-ECCMID day on antimicrobial resistance. *Lancet Microbe* **3**, e565-e566 (2022).

150. Westley, J. Rhodanese. *Adv Enzymol Relat Areas Mol Biol* **39**, 327-368 (1973).

151. Schultz, C.P., Ahmed, M.K., Dawes, C. & Mantsch, H.H. Thiocyanate levels in human saliva: quantitation by Fourier transform infrared spectroscopy. *Anal Biochem* **240**, 7-12 (1996).

152. Nedoboy, P.E. *et al.* High plasma thiocyanate levels are associated with enhanced myeloperoxidase-induced thiol oxidation and long-term survival in subjects following a first myocardial infarction. *Free Radic Res* **48**, 1256-1266 (2014).

153. Madiyal, A. *et al.* Status of thiocyanate levels in the serum and saliva of non-smokers, ex-smokers and smokers. *Afr Health Sci* **18**, 727-736 (2018).

154. Fragoso, M.A. *et al.* Transcellular thiocyanate transport by human airway epithelia. *J Physiol* **561**, 183-194 (2004).

155. Lundquist, P., Kagedal, B. & Nilsson, L. An improved method for determination of thiocyanate in plasma and urine. *Eur J Clin Chem Clin Biochem* **33**, 343-349 (1995).

156. Klebanoff, S.J., Clem, W.H. & Luebke, R.G. The peroxidase-thiocyanate-hydrogen peroxide antimicrobial system. *Biochim Biophys Acta* **117**, 63-72 (1966).

157. Nagy, P., Jameson, G.N. & Winterbourn, C.C. Kinetics and mechanisms of the reaction of hypothiocyanous acid with 5-thio-2-nitrobenzoic acid and reduced glutathione. *Chem Res Toxicol* **22**, 1833-1840 (2009).

158. Hawkins, C.L. The role of hypothiocyanous acid (HOSCN) in biological systems. *Free Radic Res* **43**, 1147-1158 (2009).

159. Furtmuller, P.G. *et al.* Kinetics of interconversion of redox intermediates of lactoperoxidase, eosinophil peroxidase and myeloperoxidase. *Jpn J Infect Dis* **57**, S30-31 (2004).

160. Dull, T.J., Uyeda, C., Strosberg, A.D., Nedwin, G. & Seilhamer, J.J. Molecular cloning of cDNAs encoding bovine and human lactoperoxidase. *DNA Cell Biol* **9**, 499-509 (1990).

161. Koksal, Z. & Alim, Z. Lactoperoxidase, an antimicrobial enzyme, is inhibited by some indazoles. *Drug Chem Toxicol* **43**, 22-26 (2020).

162. van Dalen, C.J., Whitehouse, M.W., Winterbourn, C.C. & Kettle, A.J. Thiocyanate and chloride as competing substrates for myeloperoxidase. *Biochem J* **327 (Pt 2)**, 487-492 (1997).

163. Furtmuller, P.G., Burner, U. & Obinger, C. Reaction of myeloperoxidase compound I with chloride, bromide, iodide, and thiocyanate. *Biochemistry* **37**, 17923-17930 (1998).

164. Furtmuller, P.G. *et al.* Active site structure and catalytic mechanisms of human peroxidases. *Arch Biochem Biophys* **445**, 199-213 (2006).

165. Aratani, Y. Myeloperoxidase: Its role for host defense, inflammation, and neutrophil function. *Arch Biochem Biophys* **640**, 47-52 (2018).

166. Thomson, E. *et al.* Identifying peroxidases and their oxidants in the early pathology of cystic fibrosis. *Free Radic Biol Med* **49**, 1354-1360 (2010).

167. Thomas, E.L. & Fishman, M. Oxidation of chloride and thiocyanate by isolated leukocytes. *J Biol Chem* **261**, 9694-9702 (1986).

168. Ashby, M.T., Carlson, A.C. & Scott, M.J. Redox buffering of hypochlorous acid by thiocyanate in physiologic fluids. *J Am Chem Soc* **126**, 15976-15977 (2004).

169. Nagy, P., Beal, J.L. & Ashby, M.T. Thiocyanate is an efficient endogenous scavenger of the phagocytic killing agent hypobromous acid. *Chem Res Toxicol* **19**, 587-593 (2006).

170. van Dalen, C.J., Whitehouse, M.W., Winterbourn, C.C. & Kettle, A.J. Thiocyanate and chloride as competing substrates for myeloperoxidase. *Biochem J* **327 (Pt 2)**, 487-492 (1997).

171. Barrett, T.J. & Hawkins, C.L. Hypothiocyanous acid: benign or deadly? *Chem Res Toxicol* **25**, 263-273 (2012).

172. Pattison, D.I., Davies, M.J. & Hawkins, C.L. Reactions and reactivity of myeloperoxidase-derived oxidants: differential biological effects of hypochlorous and hypothiocyanous acids. *Free Radic Res* **46**, 975-995 (2012).

173. Babior, B.M. The respiratory burst oxidase. *Adv Enzymol Relat Areas Mol Biol* **65**, 49-95 (1992).

174. Winterbourn, C.C. & Kettle, A.J. Redox reactions and microbial killing in the neutrophil phagosome. *Antioxid Redox Signal* **18**, 642-660 (2013).

175. Lambeth, J.D. NOX enzymes and the biology of reactive oxygen. *Nat Rev Immunol* **4**, 181-189 (2004).

176. Rigutto, S. *et al.* Activation of dual oxidases Duox1 and Duox2: differential regulation mediated by camp-dependent protein kinase and protein kinase C-dependent phosphorylation. *J Biol Chem* **284**, 6725-6734 (2009).

177. Riedel, C., Dohan, O., De la Vieja, A., Ginter, C.S. & Carrasco, N. Journey of the iodide transporter NIS: from its molecular identification to its clinical role in cancer. *Trends Biochem Sci* **26**, 490-496 (2001).

178. Sarr, D. *et al.* Dual oxidase 1 promotes antiviral innate immunity. *Proc Natl Acad Sci U S A* **118** (2021).

179. Gupta, T. *et al.* Dual oxidase 1 is dispensable during Mycobacterium tuberculosis infection in mice. *Front Immunol* **14**, 1044703 (2023).

180. Meredith, J.D. & Gray, M.J. Hypothiocyanite and host-microbe interactions. *Mol Microbiol* **119**, 302-311 (2023).

181. Femling, J.K. *et al.* The antibacterial activity of human neutrophils and eosinophils requires proton channels but not BK channels. *J Gen Physiol* **127**, 659-672 (2006).

182. Courtois, P., van Beers, D., de Foor, M., Mandelbaum, I.M. & Pourtois, M. Abolition of herpes simplex cytopathic effect after treatment with peroxidase generated hypothiocyanite. *J Biol Buccale* **18**, 71-74 (1990).

183. Magacz, M., Kedziora, K., Sapa, J. & Krzysciak, W. The Significance of Lactoperoxidase System in Oral Health: Application and Efficacy in Oral Hygiene Products. *Int J Mol Sci* **20** (2019).

184. Ghodratnama, F., Riggio, M.P. & Wray, D. Search for human herpesvirus 6, human cytomegalovirus and varicella zoster virus DNA in recurrent aphthous stomatitis tissue. *J Oral Pathol Med* **26**, 192-197 (1997).

185. Pedersen, A., Madsen, H.O., Vestergaard, B.F. & Ryder, L.P. Varicella-zoster virus DNA in recurrent aphthous ulcers. *Scand J Dent Res* **101**, 311-313 (1993).

186. Hedner, U., Glazer, S. & Falch, J. Recombinant activated factor VII in the treatment of bleeding episodes in patients with inherited and acquired bleeding disorders. *Transfus Med Rev* **7**, 78-83 (1993).

187. Perides, G., Rahemtulla, F., Lane, W.S., Asher, R.A. & Bignami, A. Isolation of a large aggregating proteoglycan from human brain. *J Biol Chem* **267**, 23883-23887 (1992).

188. Tenovuo, J., Pruitt, K.M. & Thomas, E.L. Peroxidase antimicrobial system of human saliva: hypothiocyanite levels in resting and stimulated saliva. *J Dent Res* **61**, 982-985 (1982).

189. Sugita, C. *et al.* Antiviral activity of hypothiocyanite produced by lactoperoxidase against influenza A and B viruses and mode of its antiviral action. *Acta Virol* **62**, 401-408 (2018).

190. Gingerich, A. *et al.* Hypothiocyanite produced by human and rat respiratory epithelial cells inactivates extracellular H1N2 influenza A virus. *Inflamm Res* **65**, 71-80 (2016).

191. Cegolon, L. *et al.* In vitro antiviral activity of hypothiocyanite against A/H1N1/2009 pandemic influenza virus. *Int J Hyg Environ Health* **217**, 17-22 (2014).

192. Cegolon, L. *et al.* Hypothiocyanite and Hypothiocyanite/Lactoferrin Mixture Exhibit Virucidal Activity In Vitro against SARS-CoV-2. *Pathogens* **10** (2021).

193. Puthenveetil, R. *et al.* S-acylation of SARS-CoV-2 spike protein: Mechanistic dissection, in vitro reconstitution and role in viral infectivity. *J Biol Chem* **297**, 101112 (2021).

194. Gingerich, A.D. *et al.* Oxidative killing of encapsulated and nonencapsulated Streptococcus pneumoniae by lactoperoxidase-generated hypothiocyanite. *PLoS One* **15**, e0236389 (2020).

195. Yassine, E. & Rada, B. Microbicidal Activity of Hypothiocyanite against Pneumococcus. *Antibiotics (Basel)* **10** (2021).

196. Shearer, H.L. *et al.* Resistance of Streptococcus pneumoniae to Hypothiocyanous Acid Generated by Host Peroxidases. *Infect Immun* **90**, e0053021 (2022).

197. Moreau-Marquis, S., Coutermarsh, B. & Stanton, B.A. Combination of hypothiocyanite and lactoferrin (ALX-109) enhances the ability of tobramycin and aztreonam to eliminate Pseudomonas aeruginosa biofilms growing on cystic fibrosis airway epithelial cells. *J Antimicrob Chemother* **70**, 160-166 (2015).

198. Tunney, M.M. *et al.* Activity of hypothiocyanite and lactoferrin (ALX-009) against respiratory cystic fibrosis pathogens in sputum. *J Antimicrob Chemother* **73**, 3391-3397 (2018).

199. Huang, L., Xuan, W., Sarna, T. & Hamblin, M.R. Comparison of thiocyanate and selenocyanate for potentiation of antimicrobial photodynamic therapy. *J Biophotonics* **12**, e201800092 (2019).

200. Benoy, M.J., Essy, A.K., Sreekumar, B. & Haridas, M. Thiocyanate mediated antifungal and antibacterial property of goat milk lactoperoxidase. *Life Sci* **66**, 2433-2439 (2000).

201. Landis, L., Kley, D. & Ercoli, N. Antifungal activity of a series of thiocyanates. *J Am Pharm Assoc Am Pharm Assoc* **40**, 321-325 (1951).

202. Ahariz, M. & Courtois, P. Candida albicans susceptibility to lactoperoxidase-generated hypoiodite. *Clin Cosmet Investig Dent* **2**, 69-78 (2010).

203. Fernandes, K.E. & Carter, D.A. The Antifungal Activity of Lactoferrin and Its Derived Peptides: Mechanisms of Action and Synergy with Drugs against Fungal Pathogens. *Front Microbiol* **8**, 2 (2017).

204. Welk, A. *et al.* Effect of lactoperoxidase on the antimicrobial effectiveness of the thiocyanate hydrogen peroxide combination in a quantitative suspension test. *BMC Microbiol* **9**, 134 (2009).

205. Bafort, F., Parisi, O., Perraudin, J.P. & Jijakli, M.H. Mode of action of lactoperoxidase as related to its antimicrobial activity: a review. *Enzyme Res* **2014**, 517164 (2014).

206. Thomas, E.L. & Aune, T.M. Susceptibility of Escherichia coli to bactericidal action of lactoperoxidase, peroxide, and iodide or thiocyanate. *Antimicrob Agents Chemother* **13**, 261-265 (1978).

207. Nakano, M. *et al.* Synergistic anti-candida activities of lactoferrin and the lactoperoxidase system. *Drug Discov Ther* **13**, 28-33 (2019).

208. Popper, L. & Knorr, D. Inactivation of yeast and filamentous fungi by the lactoperoxidase-hydrogen peroxide-thiocyanate-system. *Nahrung* **41**, 29-33 (1997).

209. Doyle, M.P. & Marth, E.H. Degradation of aflatoxin by lactoperoxidase. *Z Lebensm Unters Forsch* **166**, 271-273 (1978).

210. Morris, P.W., Kelley, K.M. & Logas, W.G. alpha-Amanitin: inactivation by bovine lactoperoxidase. *Experientia* **35**, 589-591 (1979).

211. Zheleva, A., Michelot, D. & Zhelev, Z.D. Sensitivity of alpha-amanitin to oxidation by a lactoperoxidase-hydrogen peroxide system. *Toxicon* **38**, 1055-1063 (2000).

212. Mickelson, M.N. Glucose transport in Streptococcus agalactiae and its inhibition by lactoperoxidase-thiocyanate-hydrogen peroxide. *J Bacteriol* **132**, 541-548 (1977).

213. Loimaranta, V., Tenovuo, J. & Korhonen, H. Combined inhibitory effect of bovine immune whey and peroxidase-generated hypothiocyanite against glucose uptake by Streptococcus mutans. *Oral Microbiol Immunol* **13**, 378-381 (1998).

214. Hamon, C.B. & Klebanoff, S.J. A peroxidase-mediated, streptococcus mitis-dependent antimicrobial system in saliva. *J Exp Med* **137**, 438-450 (1973).

215. Oram, J.D. & Reiter, B. The inhibition of streptococci by lactoperoxidase, thiocyanate and hydrogen peroxide. The effect of the inhibitory system on susceptible and resistant strains of group N streptococci. *Biochem J* **100**, 373-381 (1966).

216. Carlsson, J., Iwami, Y. & Yamada, T. Hydrogen peroxide excretion by oral streptococci and effect of lactoperoxidase-thiocyanate-hydrogen peroxide. *Infect Immun* **40**, 70-80 (1983).

217. Thomas, E.L. & Aune, T.M. Lactoperoxidase, peroxide, thiocyanate antimicrobial system: correlation of sulfhydryl oxidation with antimicrobial action. *Infect Immun* **20**, 456-463 (1978).

218. Shin, K., Yamauchi, K., Teraguchi, S., Hayasawa, H. & Imoto, I. Susceptibility of Helicobacter pylori and its urease activity to the peroxidase-hydrogen peroxide-thiocyanate antimicrobial system. *J Med Microbiol* **51**, 231-237 (2002).

219. Shearer, H.L. *et al.* Identification of Streptococcus pneumoniae genes associated with hypothiocyanous acid tolerance through genome-wide screening. *J Bacteriol*, e0020823 (2023).

220. Kim, S.N., Bae, Y.G. & Rhee, D.K. Dual regulation of dnaK and groE operons by HrcA and Ca++ in Streptococcus pneumoniae. *Arch Pharm Res* **31**, 462-467 (2008).

221. Derre, I., Rapoport, G. & Msadek, T. CtsR, a novel regulator of stress and heat shock response, controls clp and molecular chaperone gene expression in gram-positive bacteria. *Mol Microbiol* **31**, 117-131 (1999).

222. Kwon, H.Y., Kim, E.H., Tran, T.D., Pyo, S.N. & Rhee, D.K. Reduction-sensitive and cysteine residue-mediated Streptococcus pneumoniae HrcA oligomerization in vitro. *Mol Cells* **27**, 149-157 (2009).

223. Yang, J. & Liu, S. Influenza Virus Entry inhibitors. *Adv Exp Med Biol* **1366**, 123-135 (2022).

224. Davies, M.J., Hawkins, C.L., Pattison, D.I. & Rees, M.D. Mammalian heme peroxidases: from molecular mechanisms to health implications. *Antioxid Redox Signal* **10**, 1199-1234 (2008).

225. Chandler, J.D., Nichols, D.P., Nick, J.A., Hondal, R.J. & Day, B.J. Selective metabolism of hypothiocyanous acid by mammalian thioredoxin reductase promotes lung innate immunity and antioxidant defense. *J Biol Chem* **288**, 18421-18428 (2013).

226. Skaff, O., Pattison, D.I. & Davies, M.J. Hypothiocyanous acid reactivity with low-molecular-mass and protein thiols: absolute rate constants and assessment of biological relevance. *Biochem J* **422**, 111-117 (2009).

227. Aune, T.M. & Thomas, E.L. Oxidation of protein sulfhydryls by products of peroxidase-catalyzed oxidation of thiocyanate ion. *Biochemistry* **17**, 1005-1010 (1978).

228. Hawkins, C.L., Pattison, D.I., Stanley, N.R. & Davies, M.J. Tryptophan residues are targets in hypothiocyanous acid-mediated protein oxidation. *Biochem J* **416**, 441-452 (2008).

229. Ashby, M.T. & Aneetha, H. Reactive sulfur species: aqueous chemistry of sulfenyl thiocyanates. *J Am Chem Soc* **126**, 10216-10217 (2004).

230. Janssen-Heininger, Y.M. *et al.* Redox-based regulation of signal transduction: principles, pitfalls, and promises. *Free Radic Biol Med* **45**, 1-17 (2008).

231. Aune, T.M., Thomas, E.L. & Morrison, M. Lactoperoxidase-catalyzed incorporation of thiocyanate ion into a protein substrate. *Biochemistry* **16**, 4611-4615 (1977).

232. Thomas, E.L. Lactoperoxidase-catalyzed oxidation of thiocyanate: equilibria between oxidized forms of thiocyanate. *Biochemistry* **20**, 3273-3280 (1981).

233. Ashfaq, S. *et al.* The relationship between plasma levels of oxidized and reduced thiols and early atherosclerosis in healthy adults. *J Am Coll Cardiol* **47**, 1005-1011 (2006).

234. Schutte, R. *et al.* Blood glutathione and subclinical atherosclerosis in African men: the SABPA Study. *Am J Hypertens* **22**, 1154-1159 (2009).

235. Talib, J., Pattison, D.I., Harmer, J.A., Celermajer, D.S. & Davies, M.J. High plasma thiocyanate levels modulate protein damage induced by myeloperoxidase and perturb measurement of 3-chlorotyrosine. *Free Radic Biol Med* **53**, 20-29 (2012).

236. Pattison, D.I. & Davies, M.J. Reactions of myeloperoxidase-derived oxidants with biological substrates: gaining chemical insight into human inflammatory diseases. *Curr Med Chem* **13**, 3271-3290 (2006).

237. Aune, E., Roislien, J., Mathisen, M., Thelle, D.S. & Otterstad, J.E. The "smoker's paradox" in patients with acute coronary syndrome: a systematic review. *BMC Med* **9**, 97 (2011).

238. Ndrepepa, G. Myeloperoxidase - A bridge linking inflammation and oxidative stress with cardiovascular disease. *Clin Chim Acta* **493**, 36-51 (2019).

239. Zhang, R., Shen, Z., Nauseef, W.M. & Hazen, S.L. Defects in leukocyte-mediated initiation of lipid peroxidation in plasma as studied in myeloperoxidase-deficient subjects:

systematic identification of multiple endogenous diffusible substrates for myeloperoxidase in plasma. *Blood* **99**, 1802-1810 (2002).

240. Exner, M. *et al.* Thiocyanate catalyzes myeloperoxidase-initiated lipid oxidation in LDL. *Free Radic Biol Med* **37**, 146-155 (2004).

241. Bryant, J.C. *et al.* Pyruvate oxidase of Streptococcus pneumoniae contributes to pneumolysin release. *BMC Microbiol* **16**, 271 (2016).

242. Shearer, H.L., Paton, J.C., Hampton, M.B. & Dickerhof, N. Glutathione utilization protects Streptococcus pneumoniae against lactoperoxidase-derived hypothiocyanous acid. *Free Radic Biol Med* **179**, 24-33 (2022).

243. Shearer, H.L., Pace, P.E., Paton, J.C., Hampton, M.B. & Dickerhof, N. A newly identified flavoprotein disulfide reductase Har protects Streptococcus pneumoniae against hypothiocyanous acid. *J Biol Chem* **298**, 102359 (2022).

244. Mostertz, J., Hochgrafe, F., Jurgen, B., Schweder, T. & Hecker, M. The role of thioredoxin TrxA in Bacillus subtilis: a proteomics and transcriptomics approach. *Proteomics* **8**, 2676-2690 (2008).

245. Yesilkaya, H. *et al.* Role of manganese-containing superoxide dismutase in oxidative stress and virulence of Streptococcus pneumoniae. *Infect Immun* **68**, 2819-2826 (2000).

246. Shearer, H.L. *et al.* MerA functions as a hypothiocyanous acid reductase and defense mechanism in Staphylococcus aureus. *Mol Microbiol* **119**, 456-470 (2023).

247. Meredith, J.D. *et al.* Escherichia coli RclA is a highly active hypothiocyanite reductase. *Proc Natl Acad Sci U S A* **119**, e2119368119 (2022).

248. Derke, R.M. *et al.* The Cu(II) Reductase RclA Protects Escherichia coli against the Combination of Hypochlorous Acid and Intracellular Copper. *mBio* **11** (2020).

249. Sermon, J. *et al.* Unique stress response to the lactoperoxidase-thiocyanate enzyme system in Escherichia coli. *Res Microbiol* **156**, 225-232 (2005).

250. Farrant, K.V., Spiga, L., Davies, J.C. & Williams, H.D. Response of Pseudomonas aeruginosa to the Innate Immune System-Derived Oxidants Hypochlorous Acid and Hypothiocyanous Acid. *J Bacteriol* **203** (2020).

251. Groitl, B., Dahl, J.U., Schroeder, J.W. & Jakob, U. Pseudomonas aeruginosa defense systems against microbicidal oxidants. *Mol Microbiol* **106**, 335-350 (2017).

252. Rada, B., Gardina, P., Myers, T.G. & Leto, T.L. Reactive oxygen species mediate inflammatory cytokine release and EGFR-dependent mucin secretion in airway epithelial cells exposed to Pseudomonas pyocyanin. *Mucosal Immunol* **4**, 158-171 (2011).

253. Rada, B. & Leto, T.L. Pyocyanin effects on respiratory epithelium: relevance in Pseudomonas aeruginosa airway infections. *Trends Microbiol* **21**, 73-81 (2013).

254. Rada, B. & Leto, T.L. Redox warfare between airway epithelial cells and Pseudomonas: dual oxidase versus pyocyanin. *Immunol Res* **43**, 198-209 (2009).

255. Lorentzen, D. *et al.* Concentration of the antibacterial precursor thiocyanate in cystic fibrosis airway secretions. *Free Radic Biol Med* **50**, 1144-1150 (2011).

256. Akiba, Y. *et al.* Excess iodine exposure acutely increases salivary iodide and antimicrobial hypoiodous acid concentrations in humans. *Sci Rep* **12**, 20935 (2022).

257. Derscheid, R.J. *et al.* Increased concentration of iodide in airway secretions is associated with reduced respiratory syncytial virus disease severity. *Am J Respir Cell Mol Biol* **50**, 389-397 (2014).

258. Chandler, J.D. *et al.* Antiinflammatory and Antimicrobial Effects of Thiocyanate in a Cystic Fibrosis Mouse Model. *Am J Respir Cell Mol Biol* **53**, 193-205 (2015).

259. Delporte, C. *et al.* Myeloperoxidase-catalyzed oxidation of cyanide to cyanate: A potential carbamylation route involved in the formation of atherosclerotic plaques? *J Biol Chem* **293**, 6374-6386 (2018).

260. Hall, R.A., Massicotte, G., Kessler, M., Baudry, M. & Lynch, G. Thiocyanate equally increases affinity for two DL-alpha-amino-3-hydroxy-5-methylisoxazolepropionic acid (AMPA) receptor states. *Mol Pharmacol* **43**, 459-464 (1993).

261. Okamura, T. *et al.* (11)C-Labeled Radiotracer for Noninvasive and Quantitative Assessment of the Thiocyanate Efflux System in the Brain. *Bioconjug Chem* **33**, 1654-1662 (2022).

262. Aas, K. & Thingstad, R. Thiocyanate therapy of hypertension; further experiences. *Acta Med Scand* **139**, 229-241 (1951).

263. Domzalski, C.A., Kolb, L.C. & Hines, E.A., Jr. Delirious reactions secondary to thiocyanate therapy of hypertension. *Proc Staff Meet Mayo Clin* **28**, 272-280 (1953).

264. Kessler, D.L. & Hines, L.E. Hazards of thiocyanate therapy in hypertension. *J Am Med Assoc* **138**, 549-551 (1948).

265. Shearer, H.L. *et al.* Identification of Streptococcus pneumoniae genes associated with hypothiocyanous acid tolerance through genome-wide screening. *J Bacteriol* **205**, e0020823 (2023).

266. Tan, C.K. *et al.* Coinfection with Mycobacterium tuberculosis and pandemic H1N1 influenza A virus in a patient with lung cancer. *J Microbiol Immunol Infect* **44**, 316-318 (2011).

267. Lai, C.C. *et al.* Pneumonia due to pandemic (H1N1) 2009 influenza virus and Klebsiella pneumoniae capsular serotype K16 in a patient with nasopharyngeal cancer. *J Microbiol Immunol Infect* **45**, 382-384 (2012).

268. Gomez-Gomez, A., Sanchez-Ramos, E.L. & Noyola, D.E. Diabetes is a major cause of influenza-associated mortality in Mexico. *Rev Epidemiol Sante Publique* **69**, 205-213 (2021).

269. Sheth, A.N., Patel, P. & Peters, P.J. Influenza and HIV: lessons from the 2009 H1N1 influenza pandemic. *Curr HIV/AIDS Rep* **8**, 181-191 (2011).

270. Aoki, F.Y. *et al.* Early administration of oral oseltamivir increases the benefits of influenza treatment. *J Antimicrob Chemother* **51**, 123-129 (2003).

271. Kandun, I.N. *et al.* Factors associated with case fatality of human H5N1 virus infections in Indonesia: a case series. *Lancet* **372**, 744-749 (2008).

272. Gooskens, J., Jonges, M., Claas, E.C., Meijer, A. & Kroes, A.C. Prolonged influenza virus infection during lymphocytopenia and frequent detection of drug-resistant viruses. *J Infect Dis* **199**, 1435-1441 (2009).

273. Renaud, C. *et al.* H275Y mutant pandemic (H1N1) 2009 virus in immunocompromised patients. *Emerg Infect Dis* **17**, 653-660; quiz 765 (2011).

274. Nguyen, J.T. *et al.* Triple combination of amantadine, ribavirin, and oseltamivir is highly active and synergistic against drug resistant influenza virus strains in vitro. *PLoS One* **5**, e9332 (2010).

275. de Jong, M.D. *et al.* Fatal outcome of human influenza A (H5N1) is associated with high viral load and hypercytokinemia. *Nat Med* **12**, 1203-1207 (2006).

276. Nguyen, J.T. *et al.* Triple combination of oseltamivir, amantadine, and ribavirin displays synergistic activity against multiple influenza virus strains in vitro. *Antimicrob Agents Chemother* **53**, 4115-4126 (2009).

277. Ramakrishnan, M.A. Determination of 50% endpoint titer using a simple formula. *World J Virol* **5**, 85-86 (2016).

278. Seo, S. *et al.* Combination therapy with amantadine, oseltamivir and ribavirin for influenza A infection: safety and pharmacokinetics. *Antivir Ther* **18**, 377-386 (2013).

279. Nguyen, J.T. *et al.* Efficacy of combined therapy with amantadine, oseltamivir, and ribavirin in vivo against susceptible and amantadine-resistant influenza A viruses. *PLoS One* **7**, e31006 (2012).

280. Dawson, A.R., Wilson, G.M., Coon, J.J. & Mehle, A. Post-Translation Regulation of Influenza Virus Replication. *Annu Rev Virol* **7**, 167-187 (2020).

281. Liu, J., Wang, H., Fang, M., Chen, X. & Zeng, X. A human cell polarity protein Lgl2 regulates influenza A virus nucleoprotein exportation from nucleus in MDCK cells. *J Biosci* **45** (2020).

282. Krammer, F. The human antibody response to influenza A virus infection and vaccination. *Nat Rev Immunol* **19**, 383-397 (2019).

283. Suzuki, H. *et al.* Emergence of amantadine-resistant influenza A viruses: epidemiological study. *J Infect Chemother* **9**, 195-200 (2003).

284. Masihi, K.N., Schweiger, B., Finsterbusch, T. & Hengel, H. Low dose oral combination chemoprophylaxis with oseltamivir and amantadine for influenza A virus infections in mice. *J Chemother* **19**, 295-303 (2007).

285. Lehners, N. *et al.* Long-Term Shedding of Influenza Virus, Parainfluenza Virus, Respiratory Syncytial Virus and Nosocomial Epidemiology in Patients with Hematological Disorders. *PLoS One* **11**, e0148258 (2016).

286. Anjorin, A.A. & Adepoju, B.A. Serologic evidence of seasonal influenza A and B in HIV patients on combined antiretroviral therapy in Lagos, Nigeria. *Afr J Lab Med* **9**, 1048 (2020).

287. Agrati, C. *et al.* Cellular and humoral cross-immunity against two H3N2v influenza strains in presumably unexposed healthy and HIV-infected subjects. *PLoS One* **9**, e105651 (2014).

288. Elting, L.S. *et al.* Epidemiology of influenza A virus infection in patients with acute or chronic leukemia. *Support Care Cancer* **3**, 198-202 (1995).

289. Hayden, F.G. Combinations of antiviral agents for treatment of influenza virus infections. *J Antimicrob Chemother* **18 Suppl B**, 177-183 (1986).

290. Smee, D.F., Bailey, K.W., Morrison, A.C. & Sidwell, R.W. Combination treatment of influenza A virus infections in cell culture and in mice with the cyclopentane neuraminidase inhibitor RWJ-270201 and ribavirin. *Chemotherapy* **48**, 88-93 (2002).

291. Ghezzi, P. & Ungheri, D. Synergistic combination of N-acetylcysteine and ribavirin to protect from lethal influenza viral infection in a mouse model. *Int J Immunopathol Pharmacol* **17**, 99-102 (2004).

292. Vernier, V.G. *et al.* The toxicologic and pharmacologic properties of amantadine hydrochloride. *Toxicol Appl Pharmacol* **15**, 642-665 (1969).

293. Esposito, S. & Principi, N. Oseltamivir for influenza infection in children: risks and benefits. *Expert Rev Respir Med* **10**, 79-87 (2016).

294. Camp, J.V. & Jonsson, C.B. A Role for Neutrophils in Viral Respiratory Disease. *Front Immunol* **8**, 550 (2017).

295. Ilyushina, N.A., Govorkova, E.A., Russell, C.J., Hoffmann, E. & Webster, R.G. Contribution of H7 haemagglutinin to amantadine resistance and infectivity of influenza virus. *J Gen Virol* **88**, 1266-1274 (2007).

296. Matrosovich, M., Matrosovich, T., Carr, J., Roberts, N.A. & Klenk, H.D. Overexpression of the alpha-2,6-sialyltransferase in MDCK cells increases influenza virus sensitivity to neuraminidase inhibitors. *J Virol* **77**, 8418-8425 (2003).

297. Daniels, R.S. *et al.* Fusion mutants of the influenza virus hemagglutinin glycoprotein. *Cell* **40**, 431-439 (1985).

298. Steinhauer, D.A., Wharton, S.A., Skehel, J.J., Wiley, D.C. & Hay, A.J. Amantadine selection of a mutant influenza virus containing an acid-stable hemagglutinin glycoprotein: evidence for virus-specific regulation of the pH of glycoprotein transport vesicles. *Proc Natl Acad Sci U S A* **88**, 11525-11529 (1991).

299. Arrieta, E. *et al.* Influenza A-Associated In-Hospital Mortality in Very Older People: Does Inflammation Also Play a Role? *Gerontology* **68**, 780-788 (2022).

300. Muscatello, D.J., Nazareno, A.L., Turner, R.M. & Newall, A.T. Influenza-associated mortality in Australia, 2010 through 2019: High modelled estimates in 2017. *Vaccine* **39**, 7578-7583 (2021).

301. Aziz, F. *et al.* Impact of comorbidities on mortality in hospitalized influenza patients with diabetes - Analysis of the Austrian Health Insurance. *Diabetes Res Clin Pract* **174**, 108758 (2021).

302. Acosta, E. *et al.* Determinants of Influenza Mortality Trends: Age-Period-Cohort Analysis of Influenza Mortality in the United States, 1959-2016. *Demography* **56**, 1723-1746 (2019).

303. Alvarez, F., Froes, F., Rojas, A.G., Moreno-Perez, D. & Martinon-Torres, F. The challenges of influenza for public health. *Future Microbiol* **14**, 1429-1436 (2019).

304. Bouvier, N.M. & Palese, P. The biology of influenza viruses. *Vaccine* **26 Suppl 4**, D49-53 (2008).

305. Ahmed, M., Roguski, K., Tempia, S. & Iuliano, A.D. Reply to Alonso et al. "Bangladesh and Rwanda: Cases of high burden of influenza in tropical countries?". *Influenza Other Respir Viruses* **12**, 669-671 (2018).

306. Mettelman, R.C. & Thomas, P.G. Human Susceptibility to Influenza Infection and Severe Disease. *Cold Spring Harb Perspect Med* **11** (2021).

307. McHugh, M.L. Interrater reliability: the kappa statistic. *Biochem Med (Zagreb)* **22**, 276-282 (2012).

308. Smyk, J.M., Szydlowska, N., Szulc, W. & Majewska, A. Evolution of Influenza Viruses-Drug Resistance, Treatment Options, and Prospects. *Int J Mol Sci* **23** (2022).

309. Nowak, G.J., Sheedy, K., Bursey, K., Smith, T.M. & Basket, M. Promoting influenza vaccination: insights from a qualitative meta-analysis of 14 years of influenza-related communications research by U.S. Centers for Disease Control and Prevention (CDC). *Vaccine* **33**, 2741-2756 (2015).

310. Fischer, H. *et al.* Developmental regulation of DUOX1 expression and function in human fetal lung epithelial cells. *Am J Physiol Lung Cell Mol Physiol* **292**, L1506-1514 (2007).

311. Boxer, G.E. & Rickards, J.C. Determination of thiocyanate in body fluids. *Arch Biochem Biophys* **39**, 292-300 (1952).

312. Wever, R., Kast, W.M., Kasinoedin, J.H. & Boelens, R. The peroxidation of thiocyanate catalysed by myeloperoxidase and lactoperoxidase. *Biochim Biophys Acta* **709**, 212-219 (1982).

313. Watkinson, G. & Evans, G. Potassium thiocyanate in the treatment of hypertension. *Br Med J* **1**, 595-598 (1947).

314. Connell, W.F., Wharton, G.K. & Robinson, C.E. Thiocyanate therapy. *Can Med Assoc J* **62**, 20-27 (1950).

315. Lampejo, T. Influenza and antiviral resistance: an overview. *Eur J Clin Microbiol Infect Dis* **39**, 1201-1208 (2020).

316. McManus, M.C. Mechanisms of bacterial resistance to antimicrobial agents. *Am J Health Syst Pharm* **54**, 1420-1433; quiz 1444-1426 (1997).

317. Casper, C., Englund, J. & Boeckh, M. How I treat influenza in patients with hematologic malignancies. *Blood* **115**, 1331-1342 (2010).

318. Oseltamivir: cutaneous and neurological adverse effects in children. *Prescrire Int* **15**, 182-183 (2006).

319. Dixit, R. *et al.* Pharmacokinetics of oseltamivir in infants under the age of 1 year. *Clin Transl Med* **5**, 37 (2016).

320. Oo, C. *et al.* Pharmacokinetics of anti-influenza prodrug oseltamivir in children aged 1-5 years. *Eur J Clin Pharmacol* **59**, 411-415 (2003).

321. Japp, H., Wissler, U. & Baumann, P.C. [Toxicity and blood concentration of thiocyanate during sodium nitroprusside treatment]. *Schweiz Med Wochenschr* **108**, 1987-1991 (1978).

322. Watson, C.J. *et al.* Thiocyanate toxicity: a teaching case. *Clin Toxicol (Phila)* **60**, 876-881 (2022).

323. Bergeron, H.C. & Tripp, R.A. RSV Replication, Transmission, and Disease Are Influenced by the RSV G Protein. *Viruses* **14** (2022).

324. Yim, G., Wang, H.H. & Davies, J. Antibiotics as signalling molecules. *Philos Trans R Soc Lond B Biol Sci* **362**, 1195-1200 (2007).

325. Rau, J.L. The inhalation of drugs: advantages and problems. *Respir Care* **50**, 367-382 (2005).

326. Hickey, A.J. & Stewart, I.E. Inhaled antibodies: Quality and performance considerations. *Hum Vaccin Immunother* **18**, 1940650 (2022).

327. Luyt, C.E., Hekimian, G., Brechot, N. & Chastre, J. Aerosol Therapy for Pneumonia in the Intensive Care Unit. *Clin Chest Med* **39**, 823-836 (2018).

328. Macias, A.E. *et al.* The disease burden of influenza beyond respiratory illness. *Vaccine* **39 Suppl 1**, A6-A14 (2021).

329. Wagner, B.A. *et al.* Role of thiocyanate, bromide and hypobromous acid in hydrogen peroxide-induced apoptosis. *Free Radic Res* **38**, 167-175 (2004).

330. Rees, M.D. *et al.* Targeted subendothelial matrix oxidation by myeloperoxidase triggers myosin II-dependent de-adhesion and alters signaling in endothelial cells. *Free Radic Biol Med* **53**, 2344-2356 (2012).

331. Liu, Y. *et al.* The role of sodium thiocyanate supplementation during dextran sodium sulphate-stimulated experimental colitis. *Arch Biochem Biophys* **692**, 108490 (2020).

332. Arpas, T. & Doubek, M. Differential diagnosis of leukocytosis and leukopenia. *Vnitr Lek* **68**, 28-35 (2022).

333. Bargetzi, M.J. [Leukopenia/neutropenia]. *Ther Umsch* **63**, 78-82 (2006).

334. Sinko, J. [Treatment and prevention of infections in cancer patients with neutropenia]. *Magy Onkol* **55**, 155-163 (2011).

335. Winterbourn, C.C., Kettle, A.J. & Hampton, M.B. Reactive Oxygen Species and Neutrophil Function. *Annu Rev Biochem* **85**, 765-792 (2016).

336. Domer, D., Walther, T., Moller, S., Behnen, M. & Laskay, T. Neutrophil Extracellular Traps Activate Proinflammatory Functions of Human Neutrophils. *Front Immunol* **12**, 636954 (2021).

337. Kimberlin, D.W. *et al.* Safety of oseltamivir compared with the adamantanes in children less than 12 months of age. *Pediatr Infect Dis J* **29**, 195-198 (2010).

338. Pizzorno, A., Abed, Y. & Boivin, G. Influenza drug resistance. *Semin Respir Crit Care Med* **32**, 409-422 (2011).

339. Oseltamivir. *Drugs and Lactation Database (LactMed(R))*: Bethesda (MD), 2006.

340. MacLaren, R. *et al.* Oseltamivir-Associated Bradycardia in Critically Ill Patients. *Ann Pharmacother* **55**, 1318-1325 (2021).

341. Miniaci, A. & Gupta, V. Loading Dose. *StatPearls*: Treasure Island (FL), 2024.